

**GREEN TEA LEAVES AND PEANUT SHELLS AS BIOSORBENTS
FOR REMOVAL OF CHROMIUM (VI) AND NICKEL (II) IONS
FROM AQUEOUS SOLUTION**

DHIVESH A/L M B RAMESH KUMAR

**A project report submitted in partial fulfilment of the
requirements for the award of Bachelor of Engineering
(Honours) Chemical Engineering**

**Lee Kong Chian Faculty of Engineering and Science
Universiti Tunku Abdul Rahman**

April 2020

DECLARATION

I hereby declare that this project report is based on my original work except for citations and quotations which have been duly acknowledged. I also declare that it has not been previously and concurrently submitted for any other degree or award at UTAR or other institutions.

Signature : 

Name : Dhivesh A/L M B Ramesh Kumar

ID No. : 1502288

Date : 17/05/2020

APPROVAL FOR SUBMISSION

I certify that this project report entitled “**GREEN TEA LEAVES AND PEANUT SHELLS AS BIOSORBENT FOR REMOVAL OF CHROMIUM (VI) AND NICKEL (II) IONS FROM AQUEOUS SOLUTION**” was prepared by **DHIVESH A/L M B RAMESH KUMAR** has met the required standard for submission in partial fulfilment of the requirements for the award of Bachelor of Engineering (Honours) Chemical Engineering at Universiti Tunku Abdul Rahman.

Approved by,

Signature : 

Supervisor : Dr Sim Jia Huey

Date : 17/05/2020

Signature : _____

Co-Supervisor : _____

Date : _____

The copyright of this report belongs to the author under the terms of the copyright Act 1987 as qualified by Intellectual Property Policy of Universiti Tunku Abdul Rahman. Due acknowledgement shall always be made of the use of any material contained in, or derived from, this report.

© 2020, Dhivesh A/L M B Ramesh Kumar. All right reserved.

ACKNOWLEDGEMENT

I would like to thank everyone who has helped me to successfully complete this project. I would like to show my upmost gratitude to my supervisor Dr Sim Jia Huey for the guidance, advice and her tolerance in any difficulty faced during the project.

I also would like to express my gratitude and acknowledgement on the assistance provided by Universiti Tunku Abdul Rahman (UTAR) Laboratory staffs and LKC FES faculty staffs who had continuously helped me in carrying out the experiment and guide through the relative procedures.

On top of all, I would like to thank my loving parents and friends who had continuously stood be me during this project and provided me with the required information and emotional support.

ABSTRACT

This study was aimed to compare the relative removal efficiency of biosorbents (jasmine green tea leaves, genmaicha green tea leaves, salted peanut shells and unsalted peanut shells) on Nickel (II) and Chromium (VI) ions, to study the effects of initial biosorbent dosage and pH on heavy metal removal and to optimize the biosorption condition via Design Expert Software. The pre-screening stage proved that jasmine green tea leaves was the most effective biosorbent in removing 90.98% of Chromium (VI) and 96.13 % of Nickel (II) ions. Next, five level full factorial experimental design was used in batch biosorption process to investigate the individual and interactive effects of initial biosorbent dosage and biosorption system pH on the removal of heavy metal ions. According to the ANOVA of the design, initial biosorbent dosage and pH were considered as the significant factor in the removal of Chromium (VI) and Nickel (II) ions by jasmine green tea leaves. The numerical optimization tool provided that 100 % removal of Cr (VI) can be obtained using 2.011 g of jasmine green tea leaf with system pH 3, while, 92.42 % removal of Ni (II) can be obtained using 2.000 g of jasmine green tea leaf with system pH 7. Characterisation study on the biosorbent of before biosorption and after biosorption were performed using SEM-EDX, FTIR and XRD to detect the presence of heavy metals and changes in physical and chemical properties of the biosorbents. The SEM-EDX showed the large porous structure of the virgin jasmine green tea leaves and confirms the presence of Chromium and Nickel at 00.35 % and 02.02 % after adsorption, respectively. FTIR spectrum showed that hydroxyl, carbonyl and ether group were involved in the uptake of Ni (II), while, hydroxyl, alkene, carbonyl, aliphatic group, carboxyl and ether contributed in the uptake of Cr (VI). Finally, the analysis from XRD depicts that the adsorption of hexavalent chromium and nickel ions transformed amorphous surface of virgin jasmine green tea leaves into crystalline structure along with the increase in crystallite size from 2.1109 nm to 13.7927 nm and 58.8390, respectively. Higher removal efficiency of jasmine green tea leaves was strongly promoted by its large porous structure, high carbonaceous composition and oxygenated functional groups. The initial biosorbent dosage and pH of solution significantly influence the biosorption of Nickel and Chromium.

TABLE OF CONTENTS

TABLE OF CONTENTS	i
LIST OF TABLES	iv
LIST OF FIGURES	vii
LIST OF SYMBOLS / ABBREVIATIONS	ix
LIST OF APPENDICES	xi
CHAPTER	
1 INTRODUCTION	1
1.1 Background	1
1.2 Importance of the study	1
1.3 Conventional approaches and new technologies on heavy metal removal	3
1.4 Problem Statement	5
1.5 Aims and Objectives	7
1.6 Scope and Limitation of the Study	7
2 LITERATURE REVIEW	9
2.1 Introduction	9
2.2 Biosorption Mechanism	10
2.3 Selection of Biosorbent	12
2.3.1 Agricultural Waste as Biosorbent	13
2.4 Selection of Heavy Metals for the Study	15
2.5 Pre-treatment of Biosorbents	15
2.6 Parameters Affecting Biosorption Efficiencies	20
2.6.1 Influence of pH	20
2.6.2 Influence of Contact Time	23
2.6.3 Influence of Agitation Speed	25
2.6.4 Influence of Initial Biosorbent Dosage	26
2.6.5 Influence of Initial Concentration of Heavy Metal Ions	28

2.7	Optimum Operating Conditions for Biosorption Process	32
3	METHODOLOGY AND WORK PLAN	34
3.1	Introduction	34
3.1.1	Material Preparation	35
3.2	Overview of Project Methodology	36
3.2.1	Biosorbent Preparation	39
3.2.2	Biosorbate Preparation	39
3.3	Batch Adsorption Experiment	40
3.3.1	Pre-screening of the Most Effective Biosorbent	40
3.3.2	Optimization Study via Full Factorial Experimental Design	41
3.3.2.1	Effect of Biosorbent Dosage and pH of Aqueous Solution	42
3.4	Analysis of Experimental Data	46
3.4.1	Percentage Removal of Heavy Metal Ions	46
3.4.2	Statistical Analysis of Experimental Data and Optimizing Factors	46
3.5	Instrumental Analysis of Heavy Metal Ion Concentration and Characterisation Study of Biosorbent	49
3.5.1	Inductively Coupled Plasma Optical Emission Spectrometry (ICP-OES)	49
3.5.2	Scanning Electron Microscopy with Energy Dispersive X-ray Spectroscopy (SEM-EDX)	51
3.5.3	Fourier Transform Infrared Spectroscopy (FTIR)	52
3.5.4	X-ray Diffraction (XRD)	52
4	RESULTS AND DISCUSSION	54
4.1	Pre-screening of the Most Efficient Biosorbents (Green tea leaves and Peanut shells)	54
4.2	Influence of Initial Biosorbent Dosage and pH of Aqueous Solution on Percentage Removal of Cr (VI) and Ni (II) ions	57

4.2.1	Influence of Initial Biosorbent Dosage	60
4.2.2	Influence of pH of Aqueous Solution	64
4.3	Statistical Analysis in Design Expert Software	68
4.3.1	Analysis of Variance (ANOVA)	71
4.3.2	Diagnostic Plots	75
4.3.3	Box-Cox Plot for Power Transformation	76
4.3.4	Model Graphs	78
4.4	Optimization of Operating Condition using Design Expert	82
4.5	Characterisation of Green Tea Leaves	86
4.5.1	Scanning Electron Microscopy- Energy Dispersive X-ray Spectroscopy (SEM-EDX)	86
4.5.2	Fourier Transform Infrared Spectroscopy (FTIR)	89
4.5.3	X-ray Diffraction (XRD)	93
5	CONCLUSION AND RECOMMENDATIONS	98
5.1	Conclusion	98
5.2	Recommendations for Future Work	99
	REFERENCES	101
	APPENDICES	106

LIST OF TABLES

TABLE	TITLE	PAGE
Table 2.1	Experimental Results of Maximum Removal of Cr (VI) and Ni (II) by Various Agricultural Adsorbent.	14
Table 2.2	Maximum Contaminant Level (MCL) Drinking Water Standards for Hazardous Heavy Metals.	15
Table 2.3	Pre-treatment of Various Biosorbent Before Adsorption Process.	17
Table 2.4	Optimum pH of Various Biosorbent on Maximum Removal of Cr (VI) and Ni (II) ions.	21
Table 2.5	Optimum Contact Time of Various Biosorbent on Reaching Adsorption Equilibrium.	24
Table 2.6	Optimum Initial Biosorbent Dosage for Maximum Removal of Cr (VI) and Ni (II) ions.	27
Table 2.7	Optimum Initial concentration of heavy metal ions for Maximum Removal of Cr (VI) and Ni (II) ions.	30
Table 2.8	Summary of the Optimum Condition for Maximum Removal of Cr (VI) and Ni (II) ions.	33
Table 3.1	List of Materials used.	35
Table 3.2	List of Equipment used.	35
Table 3.3	Summary of Pre-screening Test Runs for the Removal of Cr (VI) and Ni (II) using Jasmine Green Tea Leaves, Genmaicha Green Tea Leaves, Salted Peanut Shells and Unsalted Peanut Shells.	41
Table 3.4	High and Low Levels of Factors	43
Table 3.5	Summary of Test Runs for the Removal of Cr ⁶⁺ using the most efficient biosorbent Leaves as Biosorbents.	44
Table 3.6	Summary of Test Runs for the Removal of Ni ²⁺ using the most efficient biosorbent Leaves as Biosorbents.	45
Table 3.7	Numerical Optimization Criteria	47
Table 3.8	Operating conditions of Inductively Coupled Plasma Optical Emission Spectrometry (ICP-OES).	50

Table 3.9	Operating conditions of Scanning Electron Microscopy with Energy Dispersive X-ray Spectroscopy (SEM-EDX)	51
Table 3.10	Operating conditions of Fourier Transform Infrared Spectroscopy (FTIR)	52
Table 3.11	Operating conditions of X-ray Diffractometer (XRD)	53
Table 4.1	Pre-screening Results for Jasmine Green Tea, Genmaicha Green Tea, Salted Peanut Shell and Unsalted Peanut Shell	56
Table 4.2	Experimental Design Matrix with Response for Adsorption of Cr (VI) ion	58
Table 4.3	Experimental Design Matrix with Response for Adsorption of Ni (II) ion	59
Table 4.4	Analysis of Variance (ANOVA) for removal of Cr (VI)	69
Table 4.5	Analysis of Variance (ANOVA) for removal of Ni (II)	70
Table 4.6	Summary of Analysis of Variance (ANOVA) for removal of Cr (VI)	72
Table 4.7	Summary of Analysis of Variance (ANOVA) for removal of Ni (II)	72
Table 4.8	Empirical Equation in Terms of Coded and Actual Factors for removal of Cr (VI)	73
Table 4.9	Empirical Equation in Terms of Coded and Actual Factors for removal of Ni (II)	74
Table 4.10	Constraints and Goals of Numerical Optimization of Cr (VI) Removal	74
Table 4.11	Constraints and Goals of Numerical Optimization of Ni (II) Removal	75
Table 4.12	Solution of Numerical Optimization of Cr (VI) Removal	83

Table 4.13	Solution of Numerical Optimization of Ni (II) Removal	83
Table 4.14	Summary of Optimized Condition Generated from Design Expert for the Removal of Cr (VI) and Ni (II)	84
Table 4.15	Energy Dispersive X-ray (EDX) Microanalysis Report of Virgin Jasmine Green Tea Leaves	84
Table 4.16	Energy Dispersive X-ray (EDX) Microanalysis Report of Jasmine Green Tea Leaves After Adsorption of Cr (VI)	85
Table 4.17	Energy Dispersive X-ray (EDX) Microanalysis Report of Virgin Jasmine Green Tea Leaves	88
Table 4.18	Energy Dispersive X-ray (EDX) Microanalysis Report of Jasmine Green Tea Leaves After Adsorption of Cr (VI)	88
Table 4.19	Energy Dispersive X-ray (EDX) Microanalysis Report of Jasmine Green Tea Leaves After Adsorption of Ni (II)	88
Table 4.20	Fourier Transformed Infrared (FTIR) Peak Wavelengths with Respective Functional Groups	92
Table 4.21	Crystallite Size of Virgin Jasmine Green Tea	97
Table 4.22	Crystallite Size of Jasmine Green Tea After Adsorption of Cr (VI)	97
Table 4.23	Crystallite Size of Jasmine Green Tea After Adsorption of Ni (II)	97

LIST OF FIGURES

FIGURE	TITLE	PAGE
Figure 2.1	Classification of Biosorption Mechanism.	10
Figure 2.2	Representation of Biosorption Mechanisms of Lead onto Biochar.	11
Figure 2.3	Adsorption mechanism of Chromium hexavalent on lignin-based adsorbent.	12
Figure 3.1	Experimental Flow Diagram	36
Figure 3.2	Gantt Chart	38
Figure 3.3	Overview of Full Factorial Design on Optimization Strategy.	48
Figure 4.1	Pre-screening of Different Biosorbents on Removal Percentage, R (%).	56
Figure 4.2	Percentage Removal, R (%) of Heavy Metal Ions at Different pH and at Different Initial Biosorbent Dosage of Jasmine Green Tea Leave on the Removal of (a) Cr (VI) and (b) Ni (II) ions.	63
Figure 4.3	Figure 4.3: Percentage Removal, R (%) of Heavy Metal Ions with 3g, 3.5g and 4g Dosage of Jasmine Green Tea Leave on the Adsorption of (a) Cr (VI) and (b) Ni (II) ions.	67
Figure 4.4	Predicted vs Actual Plot for Removal Percentage of Cr (VI).	76
Figure 4.5	Predicted vs Actual Plot for Removal Percentage of Ni (II).	76
Figure 4.6	Box-Cox Plot for Power Transform for removal of Cr (VI).	77
Figure 4.7	Box-Cox Plot for Power Transform for removal of Ni (II).	77
Figure 4.8	Contour Plot for Interaction between Initial Biosorbent Dosage (g) and pH of on Removal Percentage of Cr (VI).	79

Figure 4.9	3D Surface Plot for Interaction between Initial Biosorbent Dosage (g) and pH of on Removal Percentage of Cr (VI).	80
Figure 4.10	Contour Plot for Interaction between Initial Biosorbent Dosage (g) and pH of on Removal Percentage of Ni (II).	81
Figure 4.11	3D Surface Plot for Interaction between Initial Biosorbent Dosage (g), pH and Removal Percentage of Ni (II).	82
Figure 4.12	SEM Images of Jasmine Green Tea Leaves Before Adsorption at a) 1000x and b) 2000x Magnification.	86
Figure 4.13	SEM Images of Jasmine Green Tea Leaves After Adsorption of Cr (VI) ions at a) 1800x and b) 2700x Magnification.	87
Figure 4.14	SEM Images of Jasmine Green Tea Leaves After Adsorption of Ni (II) ions at a) 1300x and b) 2700x Magnification.	87
Figure 4.15	Fourier Transformed Infrared (FTIR) Spectra of Jasmine Green Tea Leaves Before and After Adsorption (a)Raw, (b) After adsorption of Ni (II) and (c) After adsorption of Cr (VI).	91
Figure 4.16	XRD Spectra of Raw Jasmine Green Tea Leaves.	94
Figure 4.17	XRD Spectra of Jasmine Green Tea Leaves After Adsorption of Cr (VI) ions.	94
Figure 4.18	XRD Spectra of Jasmine Green Tea Leaves After Adsorption of Ni (II) ions.	95

LIST OF SYMBOLS / ABBREVIATIONS

%	Percentage
°C	Degree Celsius
<i>mm</i>	millimeter
μm	micro-meter
<i>rpm</i>	revolution per meter
<i>ppm</i>	Parts per million
C_e	Concentration of the molecules at equilibrium, mg/L
C_f	Final concentration of the molecules, mg/L
Q_e	Equilibrium adsorption capacity, mg/g
q_m	Maximum adsorption capacity, mg/g
C'_0	Highest initial concentration of molecules examined, mg/L
C_0	Initial metal concentration, mg/L
R^2	Correlation coefficient
V	Volume of metal ion solution, L
m	Weight of adsorbents, g
$Q_{e,cal}$	Calculated equilibrium adsorption capacity, mg/g
$Q_{e,exp}$	Experimental value of equilibrium biosorption capacity, mg/g
$\bar{Q}_{e,exp}$	Average experimental value of equilibrium biosorption capacity, mg/g
Cr (VI)	Chromium (hexavalent) ion
Cr (III)	Chromium (trivalent) ion
Ni (II)	Nickel (II) ion
Na (I)	Sodium ion
Ca (II)	Calcium (II) ion
Cu (II)	Copper (II) ion
Zn (II)	Zinc (II) ion
Pb	Lead
Fe	Iron
MCL	Maximum Contamination Limit
DOE	Department of Environment

XRD	X-ray Diffraction
SEM-EDX	Scanning Electron Microscopy with Energy Dispersive X-ray Spectroscopy
FTIR	Fourier Transform Infrared Spectroscopy
XRD	X-ray Diffraction
ICP-OES	Inductively Coupled Plasma Optical Emission Spectrometry
$\text{NiSO}_4(\text{H}_2\text{O})_6$	Nickel (II) sulfate hexahydrate
$\text{K}_2\text{Cr}_2\text{O}_7$	Potassium dichromate
NaOH	Sodium hydroxide
HCl	Hydrochloric acid
L	Litre
RSM	Response Surface Methodology

LIST OF APPENDICES

- Appendix A Preparation of Heavy Metal Ion Solution
- Appendix B Preparation of 0.1 M of 37 % HCl
- Appendix C Preparation of 0.1 M of NaOH
- Appendix D Calibration Curve of Ni (II) Standard Solution
- Appendix E Calibration Curve of Cr (VI) Standard Solution
- Appendix F Sample Calculation of Removal Percentage, R (%) of Heavy Metal Ions
- Appendix G Spreadsheets of ICP-OES Results
- Appendix H EDX Results
- Appendix I XRD Raw Data
- Appendix J Sample Calculation of Crystallite Size, d_x (nm)

CHAPTER 1

INTRODUCTION

1.1 Background

In general, heavy metals are naturally occurring materials on the Earth's crust. As the industrial revolution began, the amount of heavy metals that are being handled by various industries around the globe has risen significantly. The more the amount of heavy metals are being utilized in industrial sectors, larger volume of heavy metal by-products are being discharged into the environment as potential contaminants. Heavy metals pollution has risen to be a major environmental problem due to the discharge of metal or metal-bearing waste in water bodies. Commonly, heavy metals in the environment are influenced by the human activities such as mining, electrolysis deposition, electroplating, metal finishing industry, energy and fuel production, wood processing, electrical appliance manufacturing and metalliferous smelting discharge a large volume of sludges and wastewaters containing metal residues causing serious environmental pollution, degradation of water quality and health effects on consumers (Wang and Chen, 2006). Heavy metals are hard to be degraded naturally which makes them to be persistent in the environment for a long period. If this condition persists, there is a high possibility of water and soil contamination causing chronic and acute effects, especially towards consumers. Hence, it is important to remove these heavy metal ions that are dissolved in water bodies via water treatment.

1.2 Importance of the study

Heavy metals generally refer to any metals or metalloid ions that have a high relative atomic density ranging from 3.5 - 7 g/cm³ (Gautam, et al., 2014). Most of the metal ions fall into this category are highly soluble in water, carcinogenic and have high toxicity at low concentrations. Since these metals are proven to be non-degradable and have the tendency to persist in the environment, the metalloids can be absorbed by plants, later entering the animal and human body via consumption and adversely affecting their body activity and health. The effects on humans can be chronic or acute where chronic effects are caused by

long-term exposure and acute effects are caused by short-term exposure to heavy metals. It is highly dependent on the toxicity of the heavy metals that has been exposed.

Even though, a certain group of metals are essential to human body such as Iron , Zinc , Chromium and Copper, it becomes immensely toxic at a concentration above safe level (Daneshfozoun, Abdullah and Abdullah, 2017). These metals are acknowledged to be highly toxic that require immediate and effective removal from wastewater streams to avoid any long-term exposure to humans. Toxic metals as such can cause serious damage to target organs, nervous system, even death at an extreme level (Gunatilake, 2015). On the contrary, many regulations were established to minimize heavy metal exposure to human and environment.

Toxic metals such as chromium is commonly used in paper and pulp production, rubber manufacturing, leather and tanning industries. Based on Table 2.2, the allowable limit of chromium (hexavalent) in industrial effluent has a maximum concentration limit (MCL) of 0.05 mg/L. Long term exposure to chromium can cause liver, kidney, central nervous system damage and skin ulceration. While, exposure to aquatic life can cause decrease in the rate of photosynthesis, immune response and hematological problems in freshwater fish (Gautam, et al.,2014).

Meanwhile, exposure to nickel significantly affects the synthesis of red blood cells along with damage to liver and heart. Nickel are considered toxic when the dosage reaches (>0.2 mg/L) where it could result in nickel poisoning. Consequently, it could cause reduction in cell growth and even cancer (Gautam, et al., 2014). Chromium (VI) and nickel (II) as highly hazardous heavy metals that needs to be removed from the environment in an eco-friendly way with minimum waste generation.

1.3 Conventional approaches and new technologies on heavy metal removal

Currently, there are various approaches in practice to remove metals from aqueous solution which includes biological, physical and chemical treatments. The conventional approaches can be divided into ion exchange, adsorption using activated carbon and biological materials (biomass), chemical precipitation, ultra-filtration, reverse osmosis, phytoremediation, chemical coagulation-flocculation and electrochemical treatment. All these approaches have their respective advantages and limitations in metal ion removal from solutions.

Ultra-filtration approach is peer pressure-driven membrane operation where the heavy metals are removed through porous membranes.

On the other hand, ion exchange focuses on metal ion removal from aqueous solutions through the exchange of ions by electrostatic forces between the heavy metal ions and the surface charge of resins (Gunatilake, 2015). However, this method becomes ineffective for large numbers of competing monovalent and divalent ions such as Na^+ and Ca^{2+} .

Reverse osmosis approach focuses on separating heavy metal ions via semi-permeable membrane. The separation is performed by the dissolved solids in the aqueous solutions causing the pressure to be larger than the osmotic pressure. Both of these methods are enormously expensive when treating at a large scale (Gunatilake, 2015).

Chemical precipitation approach is performed through utilization of coagulants such as alum, lime, organic polymers and iron salts that are used to extract metals ions from solutions. The major drawback is that it is ineffective when removing metal ions with concentration of 1-100 mg/L (Volesky, 2001).

Chemical coagulation-flocculation process begins with coagulation of colloidal particles where the net surface charge of the particles will be reduced by the addition of coagulant. The coagulant extensively reduces the electrostatic repulsion forces between the colloidal particles, resulting in formation of lumps. Consequently, the remaining discrete particles are forced into flocculation process where the colloids are interacted with organic polymers, forming large flocs due to additional collisions. Followingly, the large flocs are removed from

the water collection by straining, filtration or floatation means (Gunatilake, 2015).

Moving on, electrochemical process is used to eliminate heavy metals from wastewater by precipitation means through the addition of weak acid or neutralized catholyte such as hydroperoxide. Through destabilizing and electrolytic oxidation, heavy metals are precipitated out through formation of flocs. Though, this approach shows incompetent metal precipitation, low aggregation of metal precipitates and poor settling in separation chamber. One common drawback that these treatments share is the production of large volume of toxic containing sludge upon treatment and the long-term environmental impact arising due to the sludge disposal (Gunatilake, 2015).

Phytoremediation technique is the use of certain plants such as aquatic plants in freshwater, marine and estuarine systems that act as a receptor for metal contaminants in water. The major disadvantage for this technique is the long treatment period for metal removal and difficulty in regenerating the plants for further biosorption (Joshi, 2017).

On top of all, the adsorption approach is currently considered as the rapid phenomenon of passive metal sequestration method. This is mainly due to its huge benefits on the basis of both efficiency and environment. In general, activated carbon is declared as the most widely accepted and utilized adsorbent in the adsorption of highly toxic and diverse form of pollutants all around the world. Commercially available activated carbons are widely employed in vast heavy metal ion removal process from wastewater effluent. It is made of crude graphite with highly porous and amorphous structure with crevices to molecular dimensions and visible cracks. Activated carbon are highly recommended due to its large pore size, vast surface area, microporous structure, high adsorption capacity, regeneration ability and renewable origin (Raval, Shah and Shah, 2016).

However, as a developing alternative, biosorbents are being vastly studied to be a potential replacement for activated carbon due to its various benefits. Various groups of biomaterials such as microbial biomass, agricultural waste, aquatic biomass, terrestrial biomass, soil and mineral deposits are considered as potential biosorbents to adsorb heavy metal ions from polluted water streams (Joseph, et al., 2019). These biomaterials' high metal sequestering

characteristic and availability at cheaper rate makes them the ideal choice for metal removal processes, specifically in wastewater treatment. Biosorption is relatively cheap, less prone to sludge production, able to be regenerated and has high efficiency of metal recovery (Laboy-Nieves, Goosen and Emmanuel, 2010). Though, only those with adequately high adsorption capacity and affinity towards heavy metals are suitable to be used in a large-scale metal recovery process.

1.4 Problem Statement

Heavy metal contamination in wastewater streams has caused immense negative impacts on the environment and on human health. It tends to persist in the environment and prone to bioaccumulate in an organism once it has been consumed. This is mainly due to its non-biodegradable properties. Once heavy metal ions are consumed, the elements have a tendency to accumulate in the consumer's organs and eventually causing death. This occurrence is termed as heavy metal poisoning. Thus, it becomes extremely important to remove these heavy metal contents before human contact.

Activated carbon being the widely utilized adsorbent also accompanied by few disadvantages which creates a need to search for other alternative treatment methods. Activated carbon's use becomes restricted due to its costly supply chains. Eventually, the operation cost of treating wastewater in removing heavy metal ions will be increased due to the elevated cost of adsorbent. In addition, every adsorbent including activated carbon is said to reach a saturation state where the adsorbent will be exhausted after the active binding sites are completely filled with pollutants. Thus, regeneration is required before reusing the activated carbon. Generally, the activated carbon is regenerated via oxidation, chemical, electrochemical and thermal processes. Despite bearing the regeneration cost, activated carbon is said to face a reduction in adsorption capacity upon regeneration (Raval, Shah and Shah, 2016). Therefore, activated carbon is considered to be costly when treating large volume wastewater effluent. Therefore, it is required to develop cost-efficient and easily available material that has higher affinity towards heavy metal adsorption. As a potential substitute, low-cost adsorbents are generally preferred over activated carbon.

Low-cost adsorbents are commonly referred to any adsorbent that require lower processing cost prior to adsorption.

Various low-cost adsorbents, originated from natural biological materials, agricultural waste and terrestrial sources have been studied and applied in the extraction of heavy metals. In the past, many alternatives were studied based on their adsorption capacity towards various heavy metals. In this study, two kinds of green tea leaves (Jasmine and Genmaicha) and two kinds of peanut shells (Salted and Unsalted) were selected as biosorbents to adsorb heavy metals of Chromium (VI) and Nickel (II).

Green tea is one of the most consumed beverage worldwide with the average of billions of cups daily, and hence liberating considerable waste (Cherdchoo, Nithettham and Charoenpanich, 2019). Currently, there is various productions of green tea derived foods such as traditional medicine, matcha and beverages. The higher the consumption, the higher the waste produced. Hence, to handle such huge amount of waste, the environmentally friendly approach was to recycle these wastes as secondary useful materials. Taking into account of the fact that waste tea contains oxidizing organic chemicals mainly rich in oxygen. Most importantly, it consists of functional groups including amino carboxyl, phenolic, hydroxyl, and sulfonic functional groups that makes green tea to emerge as an efficient biosorbent. Green tea mainly composed of oxygenated functional groups could immensely contribute to the uptake of heavy metal ions either through ion exchange or complexation (Cherdchoo, Nithettham and Charoenpanich, 2019). Used green tea leaves have the potential to be cheap and efficient biosorbents for removing heavy metal ions from contaminated wastewater. Besides, there is not many researches have been conducted on the study of biosorption of green tea leaves and affinity towards Ni (II) and Cr (VI) ions.

Based on literature review taken from scientific thesis, there was no published report on the comparison between peanut shells and green tea leaves being a potential cost-effective adsorbent to remove Nickel and Chromium ions. Therefore, series of investigation had been carried out to search and develop an easily accessible biosorbent with low of cost for effective removal of hexavalent chromium and nickel ions from aqueous solution.

1.5 Aims and Objectives

The primary focus of this study is to optimize the operating condition of biosorbent process by using green tea leaves or peanut shells to adsorb Chromium (VI) and Nickel (II) ions at the maximum efficiency.

The objective of this study is:

- I. To screen for the most effective biosorbent (jasmine green tea leaves, genmaicha green tea leaves, salted peanut shells and unsalted peanut shells) for the adsorption of heavy metals (Cr (VI) and Ni (II)) in aqueous solution.
- II. To study the effects of initial biosorbent dosage and pH in affecting the percentage removal of Cr (VI) and Ni (II) ions from aqueous solution.
- III. To optimize the operating condition (Biosorption parameters: initial biosorbent dosage and pH of aqueous solution) of the batch biosorption process by using response surface methodology.
- IV. To perform characterisation study on the most effective biosorbent before and after adsorption process by using XRD, SEM-EDX and FTIR.

1.6 Scope and Limitation of the Study

In this study, jasmine green tea leaves, genmaicha green tea leaves, salted peanut shells and unsalted peanut shells are used as biosorbents for the removal of chromium (VI) and nickel (II) ions from aqueous solution. The effectiveness of the biosorbent is determined based on the removal efficiency of biosorbents.

As a preliminary study, jasmine green tea leaves, genmaicha green tea leaves, salted peanut shells and unsalted peanut shells was studied on their affinity towards Ni (II) and Cr (VI) ions. While, only the best biosorbent was be chosen to be used in further optimization of biosorption study and characterisation study. In addition, the adsorption of heavy metals onto a biosorbent can be majorly affected by initial concentration of metal ion in the aqueous solution, initial biosorbent dose and the pH of the solution. The influence of these factors on the percentage removal of heavy metal ions are further studied in this research. The parameters are selected on the basis of the most dominant effect provided on the removal efficiency of heavy metal ions.

The experimental runs were carried out based on the design in accordance with the Full Factorial Experimental design from Design Expert @ Software

Version 12. The independent variable of initial biosorbent dosage and pH was optimized as numerical factors to obtain the maximum value of the response variable which is the percentage removal of the heavy metal ions.

As for the characterisation study, XRD and SEM-EDX were employed before and after the batch biosorption to identify the physical and chemical changes incurred by the biosorbent due to adsorption. XRD explores the crystallinity and elemental composition on the biosorbent surface while SEM-EDX provides the physical changes in the adsorbent surface morphology along with elemental identification (Abdolali, et al., 2016).

The major limitation of the study is the influence of other contributing factors on the removal efficiency. Biosorption of heavy metal ions might be affected by several physical and chemical factors such as contact time, particle size, initial concentration of heavy metal ions and temperature of the solution. When investigating the effect of one parameter, it is necessary to maintain the other parameters of the adsorption process at constant state to avoid any contradiction of results. Although, they are several influencing parameters, only the majorly affecting condition such as initial biosorbent dosage and initial pH of aqueous solution are studied. Furthermore, due to time constraint and insufficient samples, the most frequently studied scope of maximum biosorption capacity based on equilibrium behaviours described by isotherm models and thermodynamic parameters of the adsorption operation will not be included in this study.

CHAPTER 2

LITERATURE REVIEW

2.1 Introduction

In recent years, eliminating heavy metal ions from water bodies via adsorption using biomass has attracted much attention. It has become a hot topic among researchers due to the problems and shortcomings faced by the conventional methods in adsorbing heavy metal ions. It significantly reduces the elements of heavy metals in the solution, even when it is in the least concentration. This is achieved through binding of metal ions onto the vastly available active binding sites present on the surface of the biosorbent. Several biosorbents that were studied previously had proven to have high sequestering properties of dissolved metal ions in dilute complex solution, significantly reducing the metal concentration. However, this high metal sequestering properties are not found in all biosorbents. Thus, detail study is required to determine the ideal biosorbent that have a higher affinity towards the desired heavy metal ions.

Biosorption refers to the adsorption of metal ions, elements or compound in an adsorbate onto a solid biological based adsorbent (Gadd, 1993). The process is driven by the high affinity of the biosorbent towards the adsorbate (heavy metal ions). The adsorption continues till the amount of metal ions adsorbed onto the biosorbent surface and its portion remaining in the solution reaches equilibrium (Ahalya, Ramachandra, and Kanamad, 2005).

This chapter aims to review the studies that are conducted previously on the efficiency of various potential biosorbents towards heavy metal adsorption. The study is performed to review the types of biosorbents and its efficiency in removing heavy metal ions under different conditions. The effects of the operating parameters such as agitation speed, temperature, pH, initial biosorbent dosage and initial concentration of metal ions on the removal efficiency of the heavy metal ions are studied thoroughly.

2.2 Biosorption Mechanism

The biosorption of metal ions onto solid biosorbent can be described qualitatively and quantitatively with several complex mechanism, depending on the nature and origin of the biosorbent species and the parameters of adsorption process. Complex mechanisms such as physical adsorption, ion exchange, chelation and entrapment of ions in the polysaccharide, are commonly described more specifically in the intra and inter fibrillar spaces of structural network (Volesky and Holan, 1995). These mechanisms and their respective adsorption pathway are well described in Figure 2.1.

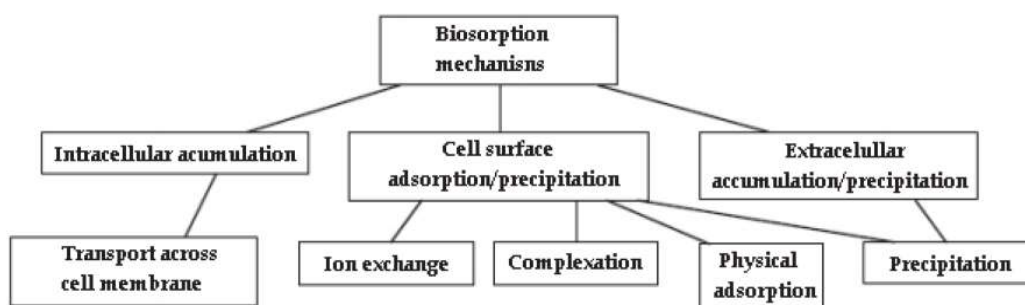


Figure 2.1: Classification of Biosorption Mechanism (Pieper and Reineke, 2000).

As mentioned earlier, surface adsorption depicts an interaction between an adsorbent and adsorbate molecule. The high affinity of the adsorbent towards the adsorbate (heavy metal ions) will cause the attraction and binding of the elements by several process mechanisms. The mechanisms of biosorption can be classified into adsorption on pores and surface, chemisorption, chelation, ion exchange, surface complexation which can be well seen in Figure 2.1 (Sud, Mahajan and Kaur, 2008). Figure 2.2 represents the various category of biosorption mechanisms that could describe the behaviour of the biosorption.

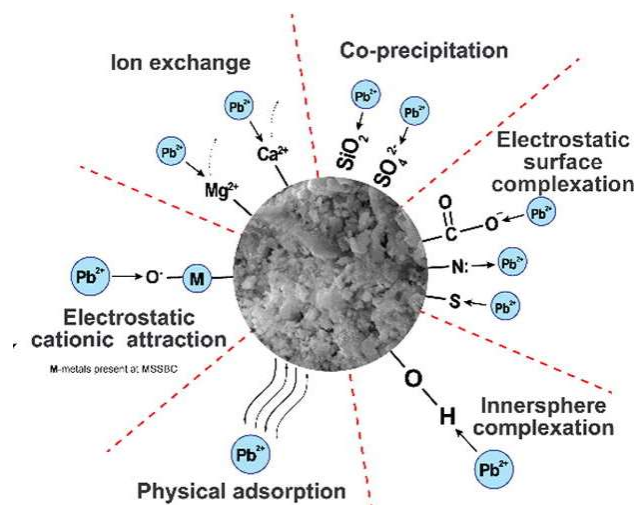


Figure 2.2: Representation of Biosorption Mechanisms of Lead onto Biochar (Ifthikar, et al., 2017).

Figure 2.2 shows various pathways of biosorption, depending on the nature of the biosorbents. Agricultural waste used as biosorbents are composed of lignin and cellulose as major constituents and hemicellulose, proteins, lipids, extractives, simple sugars, starches, hydrocarbons, water and ash as minor constituents. These constituents are known to contain variety of functional groups that plays major part in the adsorption process which could attract and sequester metal ions. On the contrary, functional groups such as carbonyl, phenolic, hydroxyl, carboxyl, amino, amido, acetamido groups of chitins, esters, phosphate group in nucleic acids, structural polysaccharides and sulphhydryl are largely involved in the adsorption process. The presence of various functional groups shows high affinity towards metal complexation (Volesky and Holan, 1995). Most importantly, the efficiency of a waste materials is evaluated based on the affinity, specificity, physio-chemical nature and biosorption capacity and heavy metal removal efficiency of the adsorbent.

The adsorption mechanism of heavy metal adsorbate on agricultural biosorbents can be expressed with surface adsorption followed by interstitial adsorption. The adsorption mechanism across the boundary layer of an adsorbent is well represented in Figure 2.3.

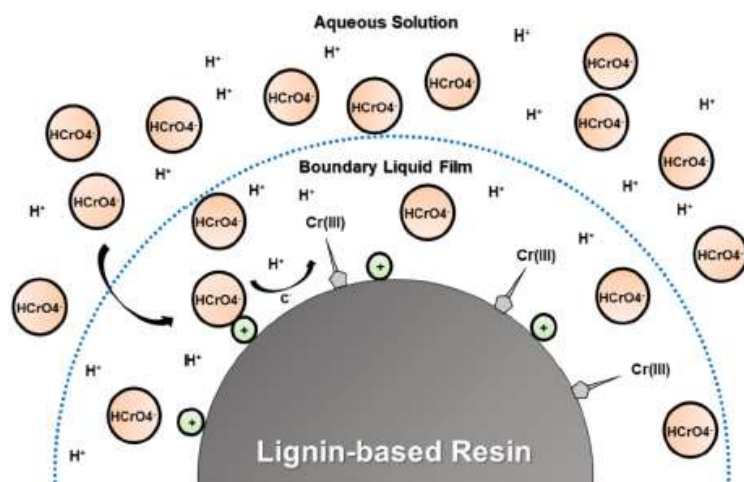


Figure 2.3: Adsorption mechanism of chromium hexavalent on lignin-based adsorbent (Liang, et al., 2013).

Figure 2.3 illustrates the diffusion of chromium hexavalent, Cr^{6+} ions across the aqueous boundary layer and into the biosorbent external boundary layer. First of all, surface adsorption occurs when the metal ions travel through the bulk solution and diffuse across the liquid film boundary layer surrounding the biosorbent surface. The biosorbent offers numerous active adsorption binding sites for metals. Later, the diffused ions are attached onto the surface of the biosorbent due to the presence of opposite charges on the biosorbent surface. This phenomenon is strongly promoted by strong forces such as hydrogen bonding or weak Van Der Waals forces and dipole interactions (Joseph, et al., 2019).

This occurrence is followed by interstitial adsorption where the heavy metal ions are further diffused into the pores of the adsorbent and gets attached to the interior portion of the pores (Joseph, et al., 2019). This can be widely observed in microporous materials.

2.3 Selection of Biosorbent

In the past, various research has been conducted on the study of the metal uptake capacity and metal ion removal efficiency of agricultural waste. Besides, the optimum biosorbent that has higher affinity towards heavy metal ions in aqueous solution was determined. Different biosorbent shows different adsorption efficiency towards heavy metal ions as they are highly dependent on its physio-chemical characteristics and the micro-environment of the targeted

metal ion solution (Naskar, et al., 2016). On practical basis, selecting the most optimum biosorbent depends on the availability, application and economical value of the biomass. Meanwhile, a predominant factor that has to be taken into account on scientific basis for determining a suitable sorbent is the equilibrium isotherm (Wang and Chen, 2009).

2.3.1 Agricultural Waste as Biosorbent

Agricultural wastes and by-products such as rice bran, coffee grounds and tea waste had been studied widely on the uptake of heavy metal ions from wastewater. Since these materials are not being reused after end of its life cycle, they could potentially be recycled as low-cost biosorbents. As mentioned earlier, biomass is mainly composed of cellulose, lignin and hemicellulose. In relation to functional groups, lignin is composed of alcohols, carboxylic, phenolic, ketones and aldehyde functional groups. These functional groups plays a major in promoting adsorption process due to their ability to bind heavy metals via donating electrons pairs to the metal ions in bulk solution, forming complexes (Abdel Ghani and El Chaghaby, 2014). Hemicellulose and pectin found in biomaterials have a general ability to bind toxic metals such as Cr (VI). Thus, different agro-waste shows different biosorption capacity due to the presence of different functional groups and surface characteristics on its biosorbent surface (Taşar, Kaya and Özer, 2014).

Table 2.1 summarizes various past researches that has been successfully proven that agro-waste as an effective biosorbent on adsorbing Ni (II) and Cr (VI) (heavy metal ions) from aqueous solution.

Table 2.1: Experimental Results of Maximum Removal of Cr (VI) and Ni (II) by Various Agricultural Adsorbent.

Biosorbent	Metal ion	Maximum heavy metal removal (%)	Reference
Camellia sinensis tea leaves	Ni (II)	100.00	(Malkoc and Nuhoglu, 2005)
Sugarcane bagasse	Cr (VI)	92.00	(Garg, et al., 2007)
Wheat bran	Cr (VI)	51.00	(Kaya, et al., 2014)
Orange peel	Ni (II)	32.00	(Gonen and Serin, 2012)
Cashew nut shell	Ni (II)	73.89	(Senthil Kumar, et al., 2011)
Almond shell	Cr (VI)	55.00	(Pehlivan and Altun, 2008)
Walnut shell	Cr (VI)	85.32	
Hazelnut shell	Cr (VI)	88.46	
Coffee grounds	Cr (VI)	85.25	(Cherdchoo, Nithettham and Charoenpanich, 2019)
Mixed tea waste	Cr (VI)	95.08	
Rice bran	Ni (II)	57.00	(Zafar, et al., 2007)

Table 2.1 clearly depicts the removal percentage of various agricultural waste towards Ni (II) and Cr (VI) ions. Every study has been conducted with different operating conditions. Based on the displayed results, camellia sinensis tea leaves, mixed waste tea, sugarcane bagasse and hazelnut shell showed the utmost removal efficiency of 100.00 %, 95.08 %, 92.00 % and 88.46 %, respectively. On contrary, the optimum operating condition required by each biosorbent to achieve maximum heavy metal removal are not similar. Thus, it strongly depends on its composition and surface properties of the biosorbent.

2.4 Selection of Heavy Metals for the Study

There is a wide range of toxic heavy metals in water streams mainly caused by the discharge of metal containing effluents. They are considered as one of the critical environmental issues since it can be toxic to organisms and humans even at lower concentration. Therefore, strict regulation is set by the governmental bodies by limiting the contaminant limit of the toxic metals in water. Hexavalent chromium and nickel are highly toxic even at lower concentration. Thus, to control excessive exposure of hexavalent chromium and nickel to aquatic life and humans, the Maximum Contaminant Limit (MCL) is determined. The MCL recognized by the Department of Environment Malaysia (DOE) is shown in Table 2.2.

Table 2.2: Maximum Contaminant Level (MCL) Drinking Water Standards for Hazardous Heavy Metals.

Heavy metals	MCL (mg/L)	Reference
Chromium (hexavalent)	0.05	(Department of Environment, 2010)
Nickel	0.20	(Department of Environment, 2010)

The MCL of hexavalent chromium and nickel in wastewater streams are determined by the Department of Environment under the command of Ministry of Natural Resources and Environment. An increase the concentration level above the limits shown in Table 2.2 is considered as hazardous to the humans when exposed.

2.5 Pre-treatment of Biosorbents

In this study, raw biosorbents are planned to be used for the biosorption of Ni (II) and Cr (VI) ions. Since, biosorbents are generally obtained from external parties, it is essential to undergo pre-treatment to remove contaminants and prepare it for adsorption. Pre-treatment of adsorbents can immensely enhance its biosorption capacity as not all biomass holds a good biosorption capacity. It requires additional treatment to boost the adsorption efficiency of the biosorbent

Pre-treatment includes chemical treatment where the chemical treatment includes acid or alkali washing and physical treatment which involves drying, cutting, grinding, thermal heating and steam activation. However, the treatment varies with biosorbent type and the targeted metal ions.

Chemical treatment had also shown significant increase in adsorption capacity. Chemical treatment is usually performed to enhance the affinity of biosorbent towards the selected metal ion of interest. It involves alteration of chemical composition and modification of binding groups of biosorbents. For instance, acidic pre-treatment is one of the widely used methods to clean up biomass by leaching out light metal ions, odour-causing substances and other impurities. Other chemical treatments includes alkali, ethanol, formaldehyde treatment have proved successful improvements in biosorption capacity of adsorbents (Vijayaraghavan and Balasubramanian, 2015). Some of the pre-treatment approaches to treat various biosorbents are shown in Table 2.3.

Agricultural waste used as biosorbent are generally grounded into small particles to increase the contact area between adsorbate in solution and biosorbent surface. In order to remove any presence of dust or soluble material, deionized water is used to thoroughly wash the sample. (Senthil Kumar, et al., 2011).

Table 2.3: Pre-treatment of Various Biosorbents Before Adsorption Process.

Biosorbent	Heavy Metal	Pre-treatment	Reference
Camellia sinensis tea leaves	Ni (II)	Camellia sinensis are high quality tea leaves that are harvested from tea plantations. The collected leaves were washed with distilled water until a colourless solution is observed at room temperature. The decolourised washed tea leaves are dried in an oven for few days.	(Malkoc and Nuhoglu, 2005)
Wheat bran	Cr (VI)	The wheat bran was milled and washed with deionized water and oven dried at 60 °C. Dried adsorbent was sieved under 40-50 mesh fraction. Later, it was washed again with deionized water and 0.1M NaOH followed by washing with pure water. It was left to dry overnight at 60 °C.	(Kaya, et al.,2014)
Sugarcane bagasse	Cr (VI)	Sugarcane bagasse collected from sugar-mill was separated from pith and sun dried. Later, it was boiled in distilled water for 30 minutes and dried again for 24 hours at 120 °C in an oven. After drying, it was grinded and sieved at 150 µm.	(Garg, et al., 2007)

Table 2.3 (Continued)

Orange peel	Ni (II)	Orange peel was rinsed with tap water and cut into small pieces. Then, it was oven dried about 100 °C followed by crushing and sieving to 1.80 mm size.	(Gonen and Serin, 2012)
Peanut shell	Cu (II) Cr (III)	The collected peanut shells were washed with tap water for 1-2 h to remove dirt and coloration. Then, distilled water was used to wash the shells followed by drying in an oven for one day at 50 °C. Dried peanut shells were crushed, milled and sieved to less than 30 µm.	(Witek-Krowiak, Szafran and Modelski, 2011)
Almond shell	Cr (VI)	Almond shells were grounded in ball mills to produce crumbs. The crumbs are then sieved to filter out particle size under 100 µm. Deionized water was used to wash the sieved biomass followed by drying for 24 hours at 100 °C.	(Pehlivan and Altun, 2008)
Walnut shell	Cr (VI)	Walnut shells were grounded in ball mills to produce crumbs. The crumbs are then sieved to filter out particle size under 100 µm. Deionized water was used to wash the sieved biomass followed by drying for 24 hours at 100 °C.	
Hazelnut shell	Cr (VI)	Hazelnut shells were grounded in ball mills to produce crumbs. The crumbs are then sieved to filter out particle size under 100 µm. Deionized water was used to wash the sieved biomass followed by drying for 24 hours at 100 °C.	
Barley straw	Ni (II)	Barley straw was dried under the sun, crushed and sieved to 0.425 - 3.35 mm sizes.	(Thevannan, Mungroo and Niu, 2010)

Table 2.3 (Continued)

Coffee grounds	Cr (VI)	The collected coffee grounds were oven dried at 60 °C for 3 days and stored in desiccators before use.	(Cherdchoo, Nithettham and Charoenpanich, 2019)
Mixed tea waste	Cr (VI)	Mixed tea leave waste collected from coffee shops were washed with boiling water until the water was virtually colourless to remove coloured and soluble components. Then, the washed leaves were dried in the sun for 3 days.	
Rice bran	Ni (II)	The samples were dried at 70 °C for one week. The dried sample were later protonated with three acids HCl, H ₂ SO ₄ and H ₃ PO ₄ . The samples were washed with deionized water after each treatment until reach near neutral. After treatment, the rice bran was dried in a drying oven at 60 °C for 24 hours.	(Zafar, et al., 2007)

2.6 Parameters Affecting Biosorption Efficiencies

The strongly influencing factors that contributes to the removal of metals from bulk such as pH of solution, agitation speed of samples, temperature during agitation, retention time of biosorption, preliminary metal ion concentration in the solution and initial biosorbent concentration readily affects the biosorption rate. However, the effects of these parameters are studied individually while maintaining the rest at fixed condition.

2.6.1 Influence of pH

The optimum pH required to achieve maximum adsorption by biosorbents differs according to the surface properties of the biosorbent and characteristics targeted heavy metals (Taşar, Kaya and Özer, 2014). This interrelation can be well explained by the functional groups (carboxyl, amino and phosphate groups) of biomass cell walls. The pH dependency for maximum removal efficiency differs according to the types of biomass as different biomass contains different functional groups (Nguyen, et al., 2013). Furthermore, the influence of pH largely affects the interaction between the surface charges on the biosorbent surface and the oppositely charged ions (counter ions). The solubility of metal ions in aqueous solution and the degree of ionization of biosorbent which hugely contributes to the adsorption process are also dependent on pH of solution (Park, Yun and Park, 2010).

Lower pH signifies increased concentration of protons (H^+) causing the overall surface charge on the biosorbent to be positive. However, the H^+ ions will compete effectively for active sites on biosorbent surface with the existing cationic metals (Cr^{6+} and Ni^{2+}) in aqueous solution causing a decrease in biosorption capacity. This is mainly because, H^+ ions are preferentially adsorbed onto the active binding sites rather than the metal ions due to its vast availability. The active sites on the biosorbent surface is protonated (rich in H^+) and will be incapable of binding the cations, at lower pH causing the metal ions to remain suspended in the solution (Witek-Krowiak, Szafran and Modelski, 2011).

Generally, the adsorption of heavy metals by biomass are conducted at a considerably higher initial pH of solution. Since higher pH of a solution provides a lower concentration of hydrogen (H^+) ions, larger number of negatively charged ligands are likely to promote metal ion adsorption through

electrostatic precipitation. Meanwhile, this condition inversely affects if the desired heavy metal present as anions in the solution. Although, a very high pH might affect the solubility of metal ions resulting in metal hydroxide precipitation (Witek-Krowiak, Szafran and Modelski, 2011). To avoid precipitation of such metal complex during adsorption, several investigations were conducted devoted to find the starting pH of the initial precipitation. Table 2.4 summarises the optimum pH of aqueous solution for Cr^{6+} and Ni^{2+} metal adsorption. In theory, high percentage removal of Cr^{6+} is supported by strong electrostatic force of attraction. This is mainly due to the greater attractive forces caused by the hydroxide ions (OH^-) surrounding the surface of adsorbate that enhances the interaction between Cr^{6+} with the biosorbents binding sites (Pehlivan and Altun, 2008).

Table 2.4: Optimum pH of Various Biosorbent on Maximum Removal of Cr (VI) and Ni (II) ions.

Biosorbent	Heavy Metals		References
	Ni (II)	Cr (VI)	
Camellia sinensis tea leaves	4.0	-	(Malkoc and Nuhoglu, 2005)
Sugarcane bagasse	-	2.0	(Garg, et al., 2007)
Orange peel	5.0	-	(Gonen and Serin, 2012)
Cashew nut shell	5.0	-	(Senthil Kumar, et al., 2011)
Almond shell	-	3.0	(Pehlivan and Altun, 2008)
Walnut shell	-	3.5	
Hazelnut shell	-	3.5	
Barley straw	4.85	-	(Thevannan, Mungroo and Niu, 2010)
Coffee grounds	-	2.0	(Cherdchoo, Nithettham and Charoenpanich, 2019)
Mixed waste tea	-	2.0	
Wheat bran	-	2.0	(Kaya, et al., 2014)
Rice bran	6.0	-	(Zafar, et al., 2007)

According to Table 2.4, previous studies show that the optimum pH for Ni^{2+} was reported to be in the range of 4.0-6.0 for various biosorbents. These results are in agreement with the theory of the negatively charged biosorbent surface that supports the adsorption of positively charged ion (Ni^{2+}) in the solution.

The influence of pH on Ni (II) was demonstrated by Thevannan, Mungroo and Niu (2010) where the pH of the nickel sulfate solutions was increased twice of its initial pH. It was noticed that, when the pH of the solution increased with the uptake of Ni^{2+} by Barley straw. However, further increase in pH resulted in decrease of Ni^{2+} uptake. Thus, pH of 4.85 was found to be the optimal value for achieving maximum adsorption capacity. According to Malkoc and Nuhoglu (2005), the batch biosorption of Ni (II) ions using *Camellia sinensis* tea leaves showed promising adsorption at pH 4.0 and significantly reduced as the pH value approached 2. This is due to the fact that at lower pH, the cationic Ni^{2+} have to compete with H^+ ions due to protonation of biosorbent surface. Consequently, Ni^{2+} would be hindered from reaching the active binding sites of the biosorbent surface. Meanwhile, at higher pH, the Ni^{2+} gets precipitated to nickel hydroxide precipitate due to presence of hydroxide anions (OH^-).

Conversely, the optimal level of pH was found to be in the range of 2.0-3.0 in removing Cr^{6+} . Pehlivan and Altun (2008) demonstrated the influence of pH on the adsorption of Cr^{6+} ions on almond shell under various pH of bulk solution. The study showed that, when the pH is in the range of 5.0-9.0, the percentage removal of Cr^{6+} decreased non-linearly. While the percentage removal exhibited an increase when the pH is in the range of 2.0 - 4.5. Thus, pH of 3.0 was selected as the optimal pH required to achieve highest percentage removal. Meanwhile, Cherdchoo, Nithettham and Charoenpanich (2019) stated that the pH of the aqueous solution show a strong influence on the degree of ionization of the metals and the surface charge of biosorbent. Previous thesis showed that, the removal of Cr^{6+} ions can achieve maximum value of 95.08 % at pH 2 and had progressively reduced as the pH improved. This could be due to the fact that, the different ionic forms of Cr^{6+} .

When investigating the influence of pH on the adsorption of Cr^{6+} ions, several mechanisms such as electrostatic force, ion exchanges and chemical

complexation must be considered. One of the common mechanisms considered is electrostatic interaction between biosorbent and adsorbate. Cr^{6+} ion forms stable complexes when dissolved in aqueous solution such as dichromate ($\text{Cr}_2\text{O}_7^{2-}$), hydrogen chromate (HCrO_4^-), chromate (CrO_4^{2-}) and hydrogen dichromate (HCr_2O_7^-). At lower pH, the presence of dichromate ions ($\text{Cr}_2\text{O}_7^{2-}$) tends to promote electrostatic attraction between the positively charged biosorbent and itself which exist as negative charged anion. The dominant anion HCrO_4^- which is considered as the dominant anion at lower pH of solution and the positively charged functional group on biosorbent surface plays a huge part in the high adsorption of Cr^{6+} ions.

2.6.2 Influence of Contact Time

The retention time provided for adsorption operation are also one of the influencing factors when discussing about the metal uptake capacity. The contact time can be well expressed with the time given for the immersion of a given amount of biosorbent in a constant volume and concentration of metal ion solution (Sadeek et al., 2015). When a pre-determined adsorbate volume is aimed to be used for the sequestration of heavy metal ions, rapid uptake of metal ions and the time need to achieve equilibrium adsorption state signifies the effectiveness of the adsorbent (Gonen and Serin, 2012). Hence, any adsorbent with the capability to provide high metal uptake capacity in a short period is considered as the ideal choice.

Sadeek, et al. (2015) denoted that the upsurge in contact time will cause the biosorbent fibres to swell which will eventually increases the area of contact. Thus, increasing the contact between the swelled fibres and metal ions, at the same time improving the interaction between the active functional groups and the metal ions. In other words, the increase in contact time significantly promotes sufficient time for the metal ions to be adsorbed onto the active sites of adsorbent surface. The optimum contact time of various biosorption studies on reaching adsorption equilibrium is demonstrated in Table 2.5 below.

Table 2.5: Optimum Contact Time of Various Biosorbent on Reaching Adsorption Equilibrium.

Biosorbent	Contact time to reach adsorption equilibrium (min)		References
	Ni (II)	Cr (VI)	
Heavy Metals			
Camellia sinensis tea leaves	120	-	(Malkoc and Nuhoglu, 2005)
Sugarcane bagasse	-	60	(Garg, et al., 2007)
Orange peel	14	-	(Gonen and Serin, 2012)
Cashew nut shell	30	-	(Senthil Kumar, et al., 2011)
Almond shell	-	60	(Pehlivan and Altun, 2008)
Walnut shell	-	100	
Hazelnut shell	-	100	
Barley straw	360	-	(Thevannan, Mungroo and Niu, 2010)
Coffee grounds	-	120	(Cherdchoo, Nithettham and Charoenpanich, 2019)
Mixed waste tea	-	80	
Wheat bran	-	180	(Kaya, et al., 2014)
Rice bran	240	-	(Zafar, et al., 2007)

Table 2.5 shows various optimal contact time that has been recorded, in order to establish maximum heavy metal ion removal. These results do not show any notable trend mainly due to the contribution of other influencing parameter that are independent of the retention time in achieving high adsorption efficiency.

Based on the study conducted by Senthil Kumar, et al., (2011), the contact time showed no correspondence with the other adsorption operating condition. Thus, the increase in time of contact between the adsorbent (cashew nut shell) and the heavy metal ion (Ni (II)) resulted in an increase in removal efficiency, despite any change in other operating conditions. It was deduced that

removal percentage increase along with the time of contact until equilibrium is reached at 78 % removal after 30 minutes.

Consequently, any provided contact period beyond the equilibrium point had negligible effect on the percentage removal of heavy metals. The rapid adsorption in the early stage is explained by the larger number of available binding sites of the cashew nut shell for the Ni (II) adsorption. As the adsorption proceeds, the adsorbed Ni (II) ion forms a monolayer due to the fact that each binding site can fit only one ion. As the active adsorption sites in a system remaining constant the metal uptake rate begins to decrease when the active sites on the biosorbent surface becomes saturated with adsorbate ions. This is because of the repulsion of the solid molecules on the surface and the bulk phase (Gonen and Serin, 2012). In addition, the cashew nut shell becomes exhausted during the formation of monolayer and the uptake rate of Ni (II) becomes dependent on the rate at which the ions are transferred from exterior to the interior sites of the biosorbent surface (Senthil Kumar, et al., 2011).

In overall, the results in Table 2.5 shows that longer retention of adsorbate during biosorption will result in larger percentage of metal ion removal. However, it only applies until the saturation point where maximum removal is achieved. Any contact beyond the maximum limit would not show any change in results. Thus, to avoid prolonged period of experimentation, the appropriate time frame of contact of biosorbent and the heavy metal ions are studied.

2.6.3 Influence of Agitation Speed

Generally, the adsorption operation will be conducted in a shaking incubator which agitates the mixture of adsorbent and adsorbate at a constant speed. Agitation is recommended in majority of the study to reduce the experimentation time. This could be explained by the mass transfer of metal ions across the bulk solution followed by its diffusion across the external liquid film surrounding the adsorbent particles. In most cases, the transport is considered as the rate limiting step due to the extensive resistance offered by the thin liquid film of biosorbent. Thus, it is essential to ensure that proper mixing with sufficient contact between adsorbate and adsorbent surface is achieved in order to overcome the resistance. In other words, increasing the

agitation speed could enhance degree of physio-chemical interaction between metal ions and charged biosorbents surface (Cherdchoo, Nithettham and Charoenpanich, 2019). However, above optimal limit might cause biomass break down and fragmentation.

2.6.4 Influence of Initial Biosorbent Dosage

Biosorbent is known to provide active binding sites for heavy metal ion adsorption. The percentage of metal removal and the biosorption capacity is directly ascribed to the biosorbent concentration, consequently relating to the number of available binding sites provided for adsorption. Thus, the initial dosage of biosorbent shows a strong influence of the adsorption operation (Abdel Ghani and El Chaghaby, 2014).

Studies on the influence of initial dosage of biosorbent are performed by increasing the biosorbent volume and determining the percentage removal and uptake capacity while maintaining the initial concentration of metal ions, pH and contact period at constant value. In theory, increasing the biosorbent concentration provides greater availability of active binding sites through larger surface area. However, the adsorption capacity will be significantly reduced due to lower adsorbate to binding site ratio where the metal ions are exposed to large surface area of binding sites. As the biosorbent dosage is at excessive level, overlapping or aggregation of binding sites available to the adsorbate, thus, longer diffusion path might cause lower adsorbate binding on to the active sites (Ferda Gönen, 2012). Whereas, at low adsorbent concentration the metal uptake by the biosorbent is denoted as relatively high. This is because of the high metal-biosorbent ratio resulting in large amount of metal ions being adsorbed per unit adsorbent (Abdel Ghani and El Chaghaby, 2014). The influence of adsorbent dosage on metal ions biosorption investigated by various researchers are shown in Table 2.6.

Table 2.6: Optimum Initial Biosorbent Dosage for Maximum Removal of Cr (VI) and Ni (II) ions.

Biosorbent	Optimum Initial Biosorbent Dosage (g/L)		Initial concentration of heavy metal ions (mg/L)	References
	Ni (II)	Cr (VI)		
Heavy Metals				
Camellia sinensis tea leaves	15	-	200	(Malkoc and Nuhoglu, 2005)
Sugarcane bagasse	-	20	50	(Garg, et al., 2007)
Orange peel	2	-	100	(Gonen and Serin, 2012)
Cashew nut shell	3	-	20	(Senthil Kumar, et al., 2011)
Almond shell	-	50	10.4	(Pehlivan and Altun, 2008)
Walnut shell	-	30	10.4	
Hazelnut shell	-	20	10.4	
Coffee grounds	-	5	10	(Cherdchoo, Nithettham and Charoenpanich, 2019)
Mixed waste tea	-	5	10	
Rice bran	5	-	100	(Zafar, et al., 2007)

Table 2.6 provides reported information about the initial dose of biosorbent used to obtain maximum percentage removal on Ni (II) and Cr (VI) ions. The optimum concentration of biosorbent is also strongly dependent on the metal ion concentration in the aqueous solution. The range of optimal initial dosage of biosorbent exists within range of 5 - 15 g/L for Ni (II) and 5-50 g/L Cr (VI) ion solution.

In a previous study, the adsorption of Ni (II) on cashew nut shell were studied by varying the initial biosorbent dosage. It was reported that, the removal percentage increased sharply with an increase in biosorbent dose before reaching a saturation point at where the removal percentage showed a constant value. This was mainly due to the decrease in concentration gradient across the biosorbent surface. The maximum adsorption capacity of Ni (II) on cashew nut shell was concluded as 73.69 % with initial biosorbent dosage of 3 g/L. It was further explained that the adsorption efficiency of metal ions is strongly affected by the increase in number of binding sites available for adsorption whereas the number of available sites are dependent on the amount of adsorbent used in the adsorption process (Senthil Kumar, et al., 2011).

According to Table 2.6, the overall trend shows that the amount of biosorbent used to achieve higher metal uptake is considerably higher compared to the concentration of metal ions removed from the solution. This concludes that, a higher biosorbent dosage will be desired up to an optimal point. Beyond this optimal point will not show any increase in adsorption frequency due to the effect of mass transfer limitation caused by accumulation and staking of dense biosorbents at higher concentration.

2.6.5 Influence of Initial Concentration of Heavy Metal Ions

The initial concentration of metal ion represents the amount of adsorbate that is required to be removed from the bulk solution. It is also said to be a major influencing factor in metal uptake rate, since it is directly attributed to the transport of adsorbate molecules. This is mainly because the concentration of metal ion act as the driving force for the mass transfer of adsorbate molecules across boundary layer of adsorbent particles through concentration gradient. According to the past studies, the initial concentration of heavy metal ions is deducted to be inversely proportional to the percentage removal of metal ions

while directly proportional to the biosorption capacity of the adsorbent (Abdel Ghani and El Chaghaby, 2014).

As the concentration of metal ions in the aqueous solution is increased, the biosorption capacity is observed to rise. This is mainly due to the strong driving force provided by the huge concentration of heavy metal ions to overcome the mass transfer resistance faced against the biosorbent boundary layer. When the concentration of metal ions in aqueous solution is relatively high the adsorbent surface can face overloading, which could lead to more ions to be left un-adsorbed due to the saturation of the binding sites. This could eventually result in lower percentage of heavy metal being removed from the non-changing volume of heavy metal solution. However, at lower concentration of metal ions the interaction between the metal ions and the biosorbent binding sites becomes intense, facilitating almost complete adsorption. Hence, a higher percentage removal of metal ions can be seen (Abdel Ghani and El Chaghaby, 2014). The influence of initial concentration of metal ions on biosorption investigated by various researchers are shown in Table 2.7.

Table 2.7: Optimum Initial concentration of heavy metal ions for Maximum Adsorption Capacity.

Biosorbent	Optimum Initial concentration of heavy metal ions (mg/L)		Initial Biosorbent Dosage (g/L)	References
	Ni (II)	Cr (VI)		
Heavy Metals				
Camellia sinensis tea leaves	50		10	(Malkoc and Nuhoglu, 2005)
Sugarcane bagasse	-	250	20	(Garg, et al., 2007)
Orange peel	10	-	2	(Gonen and Serin, 2012)
Cashew nut shell	20	-	3	(Senthil Kumar, et al., 2011)
Almond shell	-	26	25	(Pehlivan and Altun, 2008)
Walnut shell	-	26	25	
Hazelnut shell	-	26	25	
Coffee grounds	-	100	5	(Cherdchoo, Nithettham and Charoenpanich, 2019)
Mixed waste tea	-	80	5	
Rice bran	100	-	5	(Zafar, et al., 2007)

Table 2.7 provides information about the initial concentration of heavy metal ions required to obtain maximum percentage removal of metal ions. The optimum initial concentration of heavy metal ions is also strongly dependent on the biosorbent dosage. The range of optimal initial concentration of heavy metal ions exists at about 10 - 100 mg/L for Ni (II) and 26 - 250 mg/L Cr (VI) solution.

The past study involving adsorption of Cr (VI) on mixed waste tea and coffee grounds showed almost complete adsorption when the initial Cr⁶⁺ concentration was tested at 40 mg/L and 35 mg/L respectively. The results showed that the metal uptake efficiency decreased as the initial Cr⁶⁺ concentration increased. This is explained by the limited available binding sites to compensate the high concentration of heavy metals (Cherdchoo, Nithettham and Charoenpanich, 2019).

This was further supported by another study conducted on the adsorption of Ni (II) ions on cashew nut shell where the initial concentration of heavy metal ions was altered as (10–50 mg/L) with constant biosorbent dose. The results exhibited a decline in percentage removal of Ni (II) ions from 77.68 % to 65.35 % and an increase in adsorption capacity from 2.589 to 10.892 mg/g when the heavy metal concentration is increased from 10 to 50 mg/L. The decrease in the removal percentage can be well explained by the saturation of available binding sites on the adsorbent surface above the maximum concentration of Ni (II) ions can be adsorbed. On the other hand, the increase in adsorption capacity can be attributed by higher adsorption rate and the all available active sites to be completely occupied by the high Ni (II) ions present in the aqueous solution (Senthil Kumar, et al., 2011).

According to Table 2.7, the overall trend shows that the initial concentration of metal ions investigated is significantly lower compared to the dosage of biosorbent used. Thus, it shows that higher metal removal can be achieved at lower concentration of metal ions, mainly caused by near complete adsorption of metal ions. This leads to maximum percentage removal of heavy metals, avoiding saturation of binding sites and un-adsorbed metal ions in the solution.

2.7 Optimum Operating Conditions for Biosorption Process

As discussed earlier, there are some critical biosorption condition that significantly influence the biosorption of metals such as temperature, contact time, agitation speed, pH of the solution, initial concentration of heavy metal ions and initial biosorbent dosage. Among the mentioned parameters, initial concentration of heavy metal ions, initial biosorbent dosage and pH can be deduced to be significant parameter in affecting the removal of Ni (II) and Cr (VI) ions from aqueous solution. This is because of the drastic change that was observed in percentage removal of heavy metal ions when the parameters were varied. The summary of the discussed biosorbent towards Ni (II) and Cr (VI) along with the optimal conditions for biosorption is shown in the Table 2.8.

Based on Table 2.8, the optimum pH of heavy metal solution for adsorption of Cr (VI) is 2 - 3.5 while for Ni (II) is 4 - 6. Meanwhile, the optimum biosorbent dosage strongly depends on the initial concentration of heavy metal ions which showed dosage of 5 – 15 g/L and 5 - 25 g/L for heavy metal ion concentration of 20 - 100 mg/L and 10 – 250 mg/L for Ni (II) and Cr (VI) ion respectively. Finally, the optimal contact time could be affected by the physical properties of the biosorbent while includes the biosorbent size and surface area. Based on the literature review, the optimal contact time ranges from 14 – 360 minutes.

Table 2.8: Summary of the Optimum Condition for Maximum Removal of Cr (VI) and Ni (II) ions

Biosorbent	Metal ion	pH	Contact time (min)	Initial Biosorbent Dosage	Initial concentration of heavy metal ions (mg/L)	Reference
Camellia sinensis tea leaves	Ni (II)	4.0	120	15	50	(Malkoc and Nuhoglu, 2005)
Sugarcane bagasse	Cr (VI)	2.0	60	20	250	(Garg, et al., 2007)
Wheat bran	Cr (VI)	2.0	180	-	-	(Kaya, et al.,2014)
Orange peel	Ni (II)	5.0	14	2	100	(Gonen and Serin, 2012)
Cashew nut shell	Ni (II)	5.0	30	3	20	(Senthil Kumar, et al., 2011)
Almond shell	Cr (VI)	3.0	60	25	10.4	(Pehlivan and Altun, 2008)
Walnut shell	Cr (VI)	3.5	100	25	10.4	
Hazelnut shell	Cr (VI)	3.5	100	25	10.4	
Barley straw	Ni (II)	4.85	360	-	-	(Thevannan, Mungroo and Niu, 2010)
Coffee grounds	Cr (VI)	2.0	120	5	100	(Cherdchoo, Nithettham and Charoenpanich, 2019)
Mixed tea waste	Cr (VI)	2.0	80	5	80	
Rice bran	Ni (II)	6.0	240	5	100	(Zafar, et al., 2007)

CHAPTER 3

METHODOLOGY AND WORK PLAN

3.1 Introduction

The aim of the experiment was to identify the most effective biosorbent and to determine the most optimal biosorption condition for maximum percentage removal of Ni (II) and Cr (VI) ions. The experiment was conducted in batch mode, where the biosorbents of green tea leaves and peanut shells were added in synthetic wastewater containing Ni (II) and Cr (VI) ions. As the first part of the study, the green tea leaves and peanut shells were used for biosorption of Ni (II) and Cr (VI) ions at fixed initial concentration of heavy metal ions, initial biosorbent concentration, speed of agitation of adsorption samples in shaking incubator, contact time provided for biosorption and pH of aqueous solution. This screening study was conducted to determine the most effective biosorbent. On the second part of the study, the effects of initial biosorbent dosage and pH of aqueous solution related to removal efficiency of heavy metal ions (Cr (VI) and Ni (II)) were studied at 5 level Full Factorial Experimental Design of Design Expert @ Software Version 12 was used to design the experimental runs for optimization study. Later, the optimum condition to achieve maximum removal of heavy metal ions were determined through RSM in Design Expert software. The material and equipment required to perform the batch biosorption experiment is shown in Table 3.1 and Table 3.2, respectively.

3.1.1 Material Preparation

Table 3.1: List of Materials used.

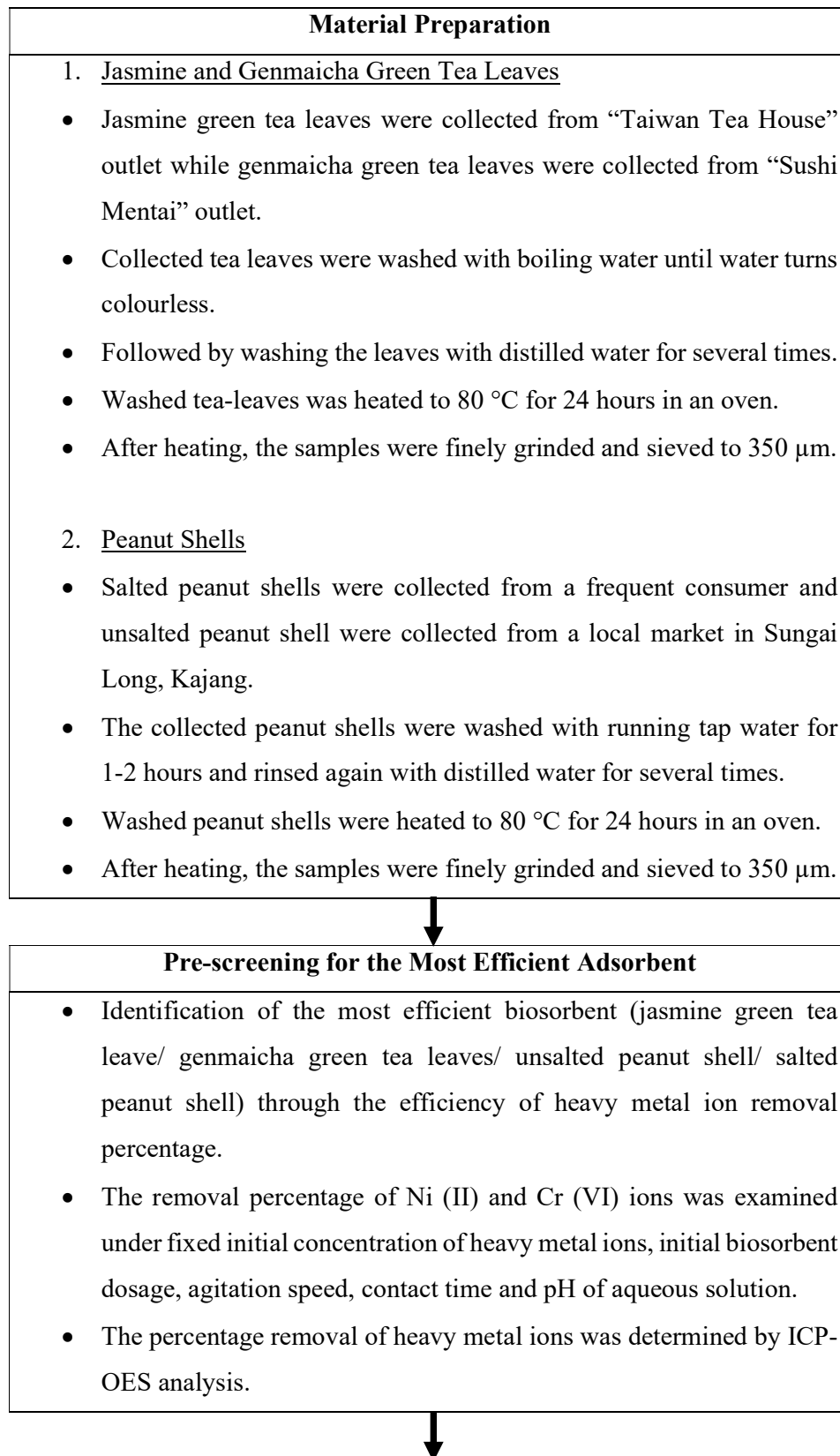
Materials	Source
Potassium dichromate, $K_2Cr_2O_7$	Friendemann Schmidt Chemical
Nickel (II) sulfate hexahydrate, $NiSO_4(H_2O)_6$	Sigma-Aldrich
Sodium hydroxide, NaOH	Merck Millipore
Hydrochloric acid, HCl	Merck Millipore
Deionized water	UTAR Laboratory
Distilled water	UTAR Laboratory

Table 3.2: List of Equipment used.

Equipment	Model	Manufacturer
Electronic balance	Entris 224-1S	Sartorius
Convection Drying oven	Beschickung	Memmert
Sieve shaker	300 μ m	Prada
Electrical blender	HR2056/90	Philips
pH probe and meter	PC 300	Eutech
Hotplate	LMS-1003	IKA
Shaking incubator	-	Labtech
Inductively Coupled Plasma Optical Emission Spectrometry (ICP-OES)	Optima 7000DV	Perkin Elmer
X-ray Diffractometer	XRD-6000	Shidmazu
Scanning Electron Microscopy with Energy Dispersive X-ray Spectroscopy (SEM-EDX)	S-3400N	Hitachi

3.2 Overview of Project Methodology

A summary of the work plan and methodology is represented below.



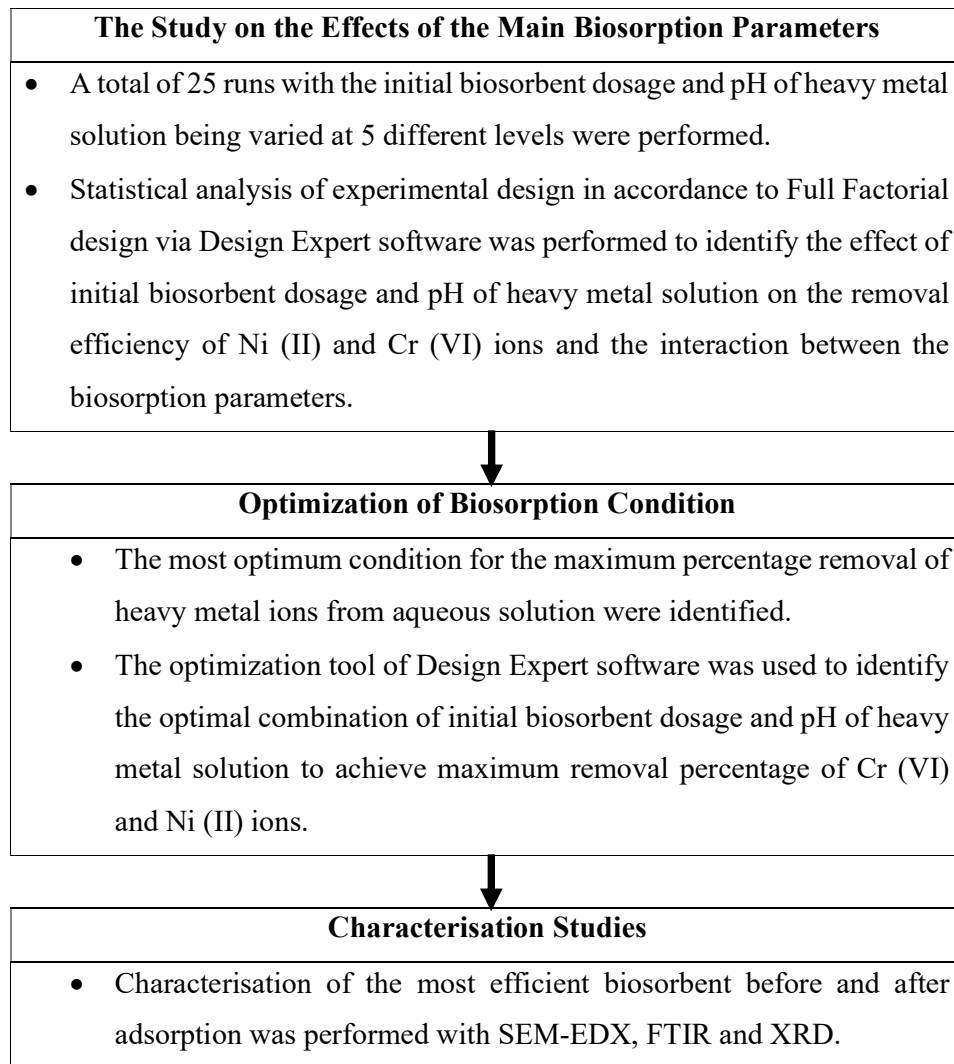


Figure 3.1: Experimental Flow Diagram

	2019							2020				
	Jun-15	Jul-15	Aug-15	Sep-15	Oct-15	Nov-15	Dec-15	Jan-15	Feb-15	Mar-15	Apr-15	May-15
Problem Formulation & Project Planning	■	■										
Literature search & Data gathering			■	■	■	■						
Designing, Planning and Preparation of Material for Experimentation.							■	■				
Pre-screening Stage (1 st stage of Experiment).								■	■			
Studying the Effects of Adsorption Parameters (2 nd stage of Experiment).									■	■		
Optimization of Parameters & Characterization studies (3 rd stage of Experiment)										■		
Tabulation and Discussion of Results and Thesis Write Up											■	
Finalize thesis											■	■

Figure 3.2: Gantt Chart

3.2.1 Biosorbent Preparation

Green Tea Leaves

Exhausted Jasmine green tea leaves were decided to be collected from a local “Taiwan Tea House” outlet in Sungai Long, Kajang. While, exhausted Genmaicha green tea leaves were collected from a local “Sushi Mentai” outlet in Sungai Long, Kajang. A total of 2 different kind of green tea leaves (jasmine green tea and genmaicha tea leaves) were collected from the outlet. The collected tea leaves are required to be washed with boiling water to remove soluble and coloured components. Hence, the leaves were washed until the wash water becomes colourless. Later, the washed leaves were sent to an oven to be heated at 80 °C for 24 hours to remove any the volatile components. After heating overnight, the samples were finely grinded and collected using a sieve shake with pore size of 300 µm.

Peanut Shell

Salted peanut shells were collected from a frequent peanut consumer and unsalted/ unprocessed peanut were collected from a local market in Sungai Long, Kajang. At the same time, unsalted peanut shells were collected from a nearby market. The collected peanut shells were extensively washed in running tap water for 1–2 hour to remove any sort of dirt and coloration. It was followed by washing with distilled water several times and heating in an oven at 80 °C for 24 hours to eliminate any water content present within the sample. After heating overnight, the dried samples were finely grinded and collected using a sieve shaker with pore size of 300 µm.

3.2.2 Biosorbate Preparation

The metal ions of Ni (II) and Cr (VI) can be obtained from Potassium dichromate, $K_2Cr_2O_7$ and Nickel (II) sulfate hexahydrate, $NiSO_4(H_2O)_6$ salts, respectively. The salts were obtained from UTAR laboratory inventory. The acquired heavy metal salts which exist in crystalline state were weighed in an electronic balance and mixed with 1L of deionised water in a 1L schottt bottle. Approximately, 226.30 mg of Potassium dichromate and 210.90 mg of Nickel (II) sulfate hexahydrate, $NiSO_4(H_2O)_6$ was mixed with 1L of deionised water to prepare 80 mg/L Cr (VI) and 80 mg/L Ni (II) stock solution, respectively. the

identification of the mass of heavy metal salts to prepare 80 mg/L of heavy metal solution are shown in Appendix A. Besides, heavy metal solutions of 100 mg/L concentration was also prepared and diluted to 20 ppm, 40 ppm, 60 ppm, 80 ppm and 100 ppm to construct a calibration curve that could be used as standard reference point for identification of heavy metal ion concentration left after adsorption. The calibration curve obtained from the analysis of ICP-OES for nickel and chromium elements are shown in Appendix D and E, respectively. Approximately, 84.87 mg of Potassium dichromate, $K_2Cr_2O_7$ and 74.08 mg of Nickel (II) sulfate hexahydrate, $NiSO_4 (H_2O)_6$ was mixed with 300 mL of deionised water to prepare 100 mg/L Cr (VI) and 100 mg/L Ni (II) solution, respectively.

3.3 Batch Adsorption Experiment

The adsorption experiment was conducted on batch mode operation using green tea leaves and peanut shells as biosorbents to remove Cr (VI) and Ni (II) ions from synthetic wastewater.

3.3.1 Pre-screening of the Most Effective Biosorbent

The pre-screening stage was divided into two set of experiment where each set of experiment employs different biosorbent. For the first set of experiment, 6 units of 250 mL Erlenmeyer flask was prepared for adsorption studies. Out of the 6 flask, 3 units were filled with 50 mL of Cr (VI) solution and the other with equal amount of Ni (II) solution. Then, each solution was added with constant dose of jasmine green tea leaves (biosorbent) of 3 g. After addition of jasmine green tea leaves, the pH of Cr (VI) solution and Ni (II) solution was adjusted with the addition of acidic or basic solutions as shown in Table 3.3. Hydrochloric acid, HCl of 0.1M and sodium hydroxide, NaOH of 0.1M were used to adjust the pH of the heavy metal solution. The preparation of 0.1 M of HCL and 0.1 M of NaOH are done according to Appendix B and C, respectively. Upon adjustments, the biosorbent and metal solution mixture was placed in a shaking incubator to be agitated at 120 rpm at 27-30 °C for 24 hours. After 24 hours, the biosorbents are separated from the solution through filtration process using 150 mm filter paper and Büchner funnel. Later, 10 mL of the collected filtrate was transferred to 15 mL centrifuge tubes. The collected samples in the

centrifuge tubes were then sent to ICP-OES analysis to determine the concentration of heavy metal ion left in the solution upon adsorption. These procedures were repeated using genmaicha green tea leaves, salted peanut shell and unsalted peanut shell as biosorbents.

Before analysing Ni (II) and Cr (VI) ions present in the solution, a calibration curve of heavy metal ion was plotted. The calibration curve was used as a standard when determining the concentration of the heavy metal ion present in the solution before and after adsorption. The equilibrium (final) and initial concentration of metal ions identified from the solution were used as the basis to determine the most effective biosorbent for the removal of the respective heavy metals. Thereon, the most effective biosorbent are employed in optimization study for maximum removal of Cr (VI) and Ni (II) ions.

Table 3.3: Summary of Pre-screening Test Runs for the Removal of using Jasmine Green Tea Leaves, Genmaicha Green Tea Leaves, Salted Peanut Shells and Unsalted Peanut Shells.

Heavy metal ions	Cr (VI)	Ni (II)
Temperature (°C)	27-30	27-30
pH	2	6
Initial concentration of heavy metal ions (mg/L)	80	80
Initial Biosorbent Dose (g)	3	3

3.3.2 Optimization Study via Full Factorial Experimental Design

After selecting the most efficient biosorbent for the removal of Ni (II) and Cr (VI) ions in the pre-screening stage, the experimentation was performed to study the effects of the most significant biosorption parameters (biosorbent dosage and initial pH of solution) using only the most efficient biosorbent. For each parameter study, 5 levels of test runs were performed based on the Full Factorial Design of Design Expert Software @ Version 12 as the removal percentage of Cr (VI) and Ni (II) ions being the response factor. Later, the optimal value of the main parameters to reach maximum removal percentage of heavy metal ions were identified using optimization tool of Design Expert software.

Firstly, the effect of biosorbent dosage was conducted by varying the adsorbent dosage in the range of 2 g to 4 g. Meanwhile, the effect of pH of solution was tested by varying the pH in the range of 2 to 6 for Cr (VI) solution and 4 to 8 for Ni (II) solution. A clear representation of the test runs performed can be well seen in Table 3.5 and Table 3.6. Finally, the data obtained from the experimental runs of Full Factorial Design were used to develop an empirical model to describe the response of the adsorption process. This inadvertently reduces the total number of experimental runs that is required in order to achieve the most optimal solution and better response. This not only reduces the overall cost of the study but also the period required for completion of the study. Full factorial design takes into account of the effect of the main factors and all possible interaction effects. Full Factorial runs various combinations of the affecting factors to establish a best way to estimate all the main and interaction effects on the removal percentage of heavy metals (Nist, 2020).

Through statistical analysis, the interaction between the initial biosorbent dosage and pH along with their effect on the removal percentage of Ni (II) and Cr (VI) ions were studied. Later, the empirical model developed from the response of the Full Factorial Design was used to compute the most optimum condition for maximum percentage removal of heavy metal ions through optimization tool of Design Expert Software @ Version 12.

3.3.2.1 Effect of Biosorbent Dosage and pH of Aqueous Solution

As mentioned earlier, the influence of initial biosorbent dosage on percentage removal of heavy metal ions was done by varying the biosorbent concentration in the range of 2 g to 4 g. In the meantime, other affecting parameters such as metal ion concentration, temperature, contact time and agitation speed are kept constant excluding the pH of the solution. Firstly, 50 units of Erlenmeyer flasks were prepared. The first 25 flask were filled with 50 mL of Cr (VI) solution and the rest with equal amount of Ni (II) solution with a concentration of 80 mg/L respectively. Then, the most efficient biosorbent in the pre-screening stage were weighed in an electronic balance and added to each flask containing stock solution in the range of 2 g, 2.5 g, 3 g, 3.5 g and 4 g.

The effect of pH of solution on the percentage removal of heavy metal ions was studied by varying the pH in the range of 2 to 6 for Cr (VI) solution

and 4 to 8 for Ni (II) solution. The study of effect of pH started with the preparation of 500mL of acidic solution, hydrochloric acid (HCl) and basic solution, sodium hydroxide (NaOH) with concentration of 0.1M for pH adjustments. Since, the maximum adsorption of Cr (VI) ion is observed in the pH range of 2 to 4, the pH of each set of Cr (VI) solution was adjusted to 2,3,4,5 and 6 with the addition of hydrochloric acid (HCl) and sodium hydroxide (NaOH). While, the maximum adsorption of Ni (II) ion was observed in the pH range of 4 to 6, the pH of each set of Ni (II) solution was adjusted to 4,5,6,7 and 8 for each sample solution by addition of hydrochloric acid (HCl). The pH of the solution was determined with a pH probe and meter.

After addition of biosorbent into the 50 units of Erlenmeyer flasks, the pH of the aqueous solution was adjusted in accordance with the Full Factorial Experimental runs developed as shown in Table 3.5 and Table 3.6. The, the mouth of the flask filled with adsorption media were sealed with aluminium foil and sent to a shaking incubator to agitate for 24 hours at 120 rpm and at temperature of 27-30 °C. After agitation, the solutions were transferred to 15 mL centrifuge tubes through filtration process using 150 mm filter paper and Büchner funnel. The filtrate is then taken to ICP-OES analysis to determine the concentration of heavy metal ion left in the solution after adsorption.

The range of the operating conditions for the each of the factors are shown in Table 3.4. While, the test runs that are planned to be conducted in relation to the two factors mentioned above are shown in Table 3.5 and Table 3.6. Finally, a peer representation of the optimization strategy is shown in Figure 3.3.

Table 3.4: High and Low Levels of Factors

Factor	Cr (VI)		Ni (II)	
	High	Low	High	Low
Initial Biosorbent	2	4	2	4
Dosage (g)				
pH	2	6	4	8

Table 3.5: Summary of Test Runs for the Removal of Cr⁶⁺ using the most efficient biosorbent Leaves as Biosorbents.

Test Run	pH	Initial Biosorbent Dose (g)
1	2	2.0
2	2	2.5
3	2	3.0
4	2	3.5
5	2	4.0
6	3	2.0
7	3	2.5
8	3	3.0
9	3	3.5
10	3	4.0
11	4	2.0
12	4	2.5
13	4	3.0
14	4	3.5
15	4	4.0
16	5	2.0
17	5	2.5
18	5	3.0
19	5	3.5
20	5	4.0
21	6	2.0
22	6	2.5
23	6	3.0
24	6	3.5
25	6	4.0

Table 3.6: Summary of Test Runs for the Removal of Ni²⁺ using the most efficient biosorbent Leaves as Biosorbents.

Test Run	pH	Initial Biosorbent Dose (g)
1	4	2.0
2	4	2.5
3	4	3.0
4	4	3.5
5	4	4.0
6	5	2.0
7	5	2.5
8	5	3.0
9	5	3.5
10	5	4.0
11	6	2.0
12	6	2.5
13	6	3.0
14	6	3.5
15	6	4.0
16	7	2.0
17	7	2.5
18	7	3.0
19	7	3.5
20	7	4.0
21	8	2.0
22	8	2.5
23	8	3.0
24	8	3.5
25	8	4.0

Table 3.5 and Table 3.6 shows the test runs that are to be performed for the adsorption of Ni (II) ions and Cr (VI) using the most efficient biosorbent. The optimum conditions for biosorption process are determined based on the maximum heavy metal removal percentage.

3.4 Analysis of Experimental Data

3.4.1 Percentage Removal of Heavy Metal Ions

The percentage removal of heavy metal ions was determined for both pre-screening and optimization stage. The percentage removal can be obtained as shown in Equation 3.1. The initial concentration of heavy metal ions (mg/L) is obtained through ICP-OES analysis before adsorption was performed. However, the equilibrium concentration (mg/L) was obtained through ICP-OES analysis after the aqueous solution has been in contact with biosorbent in a shaking incubator for 24 hours.

The percentage removal of metal ions can be determined by the following mass balance relationship:

$$\text{Percentage removal (\%)} = \frac{(C_0 - C_f)}{C_0} \times 100\% \quad (3.1)$$

where C_0 is initial concentration (mg/L) of heavy metal ion in aqueous solution and C_f is final concentration (mg/L) of heavy metal ion in aqueous solution.

3.4.2 Statistical Analysis of Experimental Data and Optimizing Factors

The experimental data were employed and analyzed under full factorial design in Design Expert Software @ Version 12. A full factorial design indicates an experiment which includes trial runs that are designed to run at all possible combination of the factor levels. It allows the possibility of studying all potential interactions between the factors (Jmp, 2020). In this case, the factors being initial biosorbent dosage and pH of aqueous solution while the response being removal percentage of heavy metal ions. Normally, full factorial designs are large compared to the conventional designs mainly because it takes into account of every combination of the factor levels. The two operating factors are decided to be studied on 5 levels, making the design a 5-level factor. Thus, the full factorial design has $5^2 = 25$ runs. Since, the 5-level factorial is not directly available in the Design Expert @ Software Version 12, the design constructed under user defined option. The optimizing factors were classified as discrete numeric factors and the levels were decided as shown in Table 3.4. Then, the statistical analysis was performed by extracting and interpreting the Analysis of Variance (ANOVA), model of the design, R-squared value, “Predicted vs

Actual” plot, Box Cox plot, contour and 3D surface graphs. After, the model is termed significant and the R-squared value achieved an acceptable range, the process optimization was performed. The optimum operating conditions were determined through point prediction to achieve the desired goal. The numerical optimization criteria set in Design Expert Software is shown in Table 3.7.

Table 3.7: Numerical Optimization Criteria

Criteria	Goal
Initial biosorbent dosage (g)	Minimize
pH	In range
Removal percentage (%)	Maximize

The optimization module will be set to maximize the percentage removal, where the best set of factor levels are selected to satisfy the target.

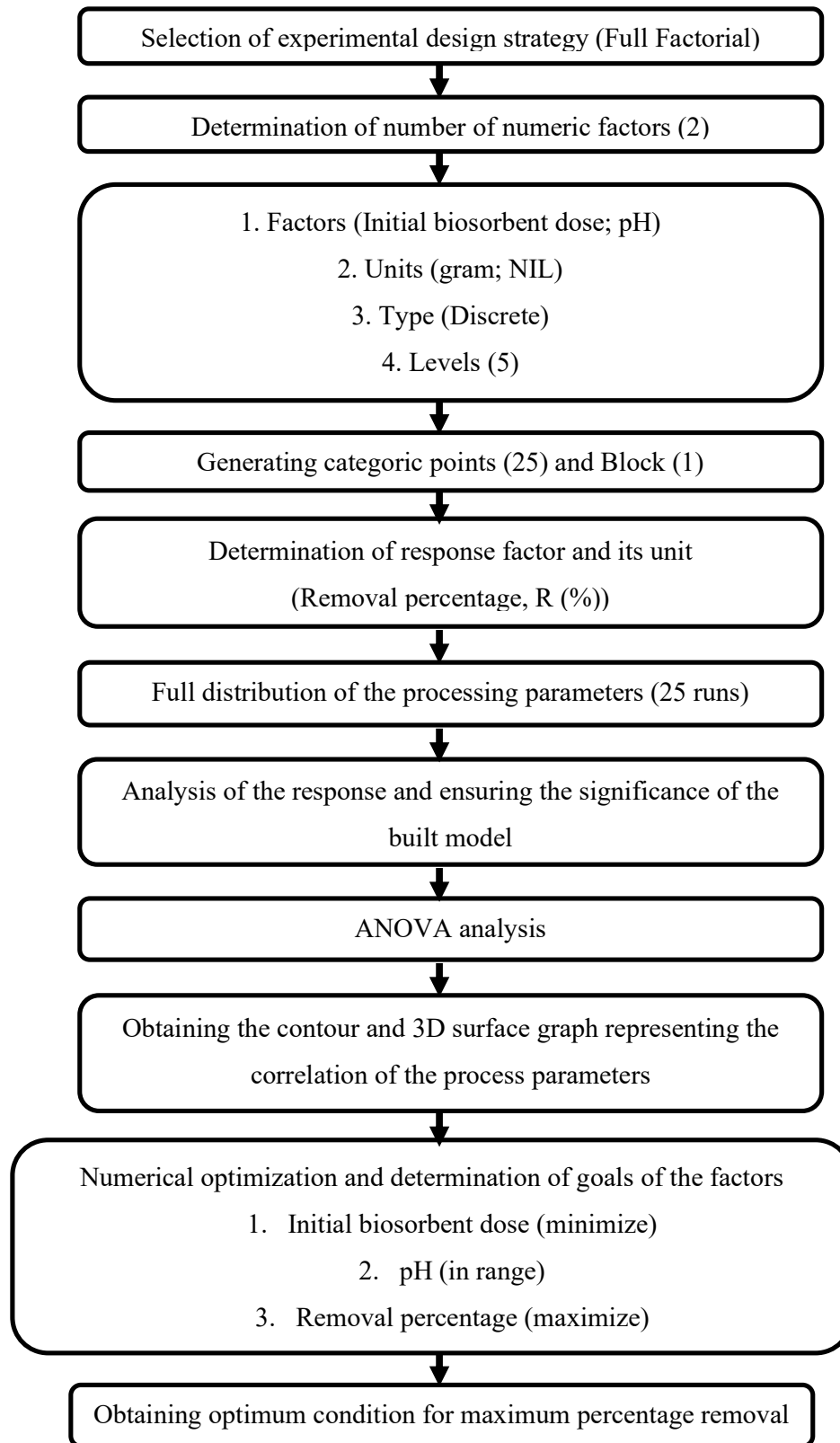


Figure 3.3: Overview of Full Factorial Design on Optimization Strategy

3.5 Instrumental Analysis of Heavy Metal Ion Concentration and Characterisation Study of Biosorbent

As mentioned earlier, the study begins with interpreting the removal efficiency of the adsorption process by identifying the final concentration of heavy metal ions left in the adsorption solution through Inductively Coupled Plasma-Optical Emission Spectrometry (ICP-OES) analysis. Later, the study proceeds with characterisation studies. The characterisation study refers to the study of the change in surface morphology and identification of elemental composition on biosorbent. Scanning Electron Microscopy with Energy Dispersive X-ray (SEM-EDX) is employed to evaluate the change in surface morphology of biosorbent before and after adsorption. Fourier Transform Infrared Spectroscopy (FTIR) was mainly employed to identify the functional groups that may in any manner could contribute to the biosorption and to characterise the adsorption mechanism. While, X-ray Diffraction (XRD) is employed to detect the change in structural properties of the biosorbent before and after adsorption. It is also used to identify any presence of crystalline materials on the biosorbent surface after adsorption via XRD spectrum.

3.5.1 Inductively Coupled Plasma Optical Emission Spectrometry (ICP-OES)

The adsorbent is added to the heavy metal ion solution and left in the shaking incubator for 24 hours at 120 rpm and 27-30 °C. After 24 hours, the adsorbent is separated from the solution through 150 mm filter paper and Büchner funnel. The filtrate is collected as samples and stored in 15 mL centrifuge tubes. The samples with unknown concentrations were then sent to Inductively Coupled Plasma-Optical Emission Spectrometry (ICP-OES) for analysis. The analysis in ICP-OES was aim to identify the heavy metal ion concentration that is left in the solution prior to adsorption. The final concentration of heavy metal ion also considered as the equilibrium concentration, C_e is later correlated with the initial concentration, C_o to identify the removal percentage of the adsorption.

The ICP-OES analysis begins with constructing calibration curve of the analysing heavy metal ion. Firstly, 100 ppm concentration of Cr (VI) solution were prepared by dissolving 84.87 mg of Potassium dichromate, $K_2Cr_2O_7$ in 300

mL of deionised water to prepare 100 mg/L Cr (VI) solution. Later, the prepared solution was diluted to 80 ppm, 60 ppm, 40 ppm and 20 ppm and stored in 50 mL centrifuge tubes. The different concentration of Cr (VI) solution were analysed in ICP-OES along with deionised water to plot the calibration curve based on their mean corrected intensity. The solutions were placed in the Perkin Elmer autosampler followed by injecting the solution into the spray chamber of ICP-OES by a peristaltic pump through a nebulizer. The atomized aerosol is lead into an argon plasma. The concentration of the element is determined based on the intensity of the photon rays. The operating conditions of the ICP-OES maintained during the analysis are shown in Table 3.8. After the calibration curve was plotted, the adsorption samples were compared with the calibration curve to obtain the final concentration of adsorption. These steps were repeated for the analysis of Ni (II) solution were 74.08 mg of Nickel (II) sulfate hexahydrate, $\text{NiSO}_4 (\text{H}_2\text{O})_6$ was dissolved in 300 mL of deionised water to prepare 100 mg/L solution.

Table 3.8: Operating conditions of Inductively Coupled Plasma Optical Emission Spectrometry (ICP-OES).

Operating parameters	Operating condition
RF power	1300 W
Plasma Gas	Argon
Plasma Gas Flow	15 L/min
Peristaltic pump flow rate	1.5 mL/min
Spray chamber	Cyclonic
Replicates	3
Cleaning effluent	Deionized water

3.5.2 Scanning Electron Microscopy with Energy Dispersive X-ray Spectroscopy (SEM-EDX)

The samples of biosorbent was analysed in Scanning Electron Microscopy with Energy Dispersive X-ray (SEM-EDX) before and after adsorption. SEM was employed to study the change in surface morphology before and after adsorption, while the EDX was employed to confirm the presence of the heavy metals on the binding sites. SEM-EDX provides a visual perspective of high depth and detailed image of the porosity and surface structure of the biosorbent. While, SEM is used for just surface visual, EDX aims to detect the presence of unknown elements near the surface of the biosorbent. In this study, the before and after adsorption samples of the most efficient biosorbent were sent to SEM-EDX to observe the change in surface morphology and to determine the presence of heavy metals on the surface prior to adsorption. The heavy metal loaded biosorbent residues were separated from the solution through filtration and dried in oven at 80 °C overnight. The dried biosorbents were crushed to powders in pestle and mortar and sent to the SEM-EDX analysis. The powders were placed on the SEM pin mount specimen holder. The specimen holders were then sent to the sputter coating where the samples will be coated with Gold and Palladium. Then, the coated samples were mounted onto the SEM sample stage. The change in surface structure and porosity were identified from SEM analysis while the elemental composition on the surface are obtained from EDX analysis. The operating conditions of the SEM-EDX analysis are shown in Table 3.9.

Table 3.9: Operating conditions of Scanning Electron Microscopy with Energy Dispersive X-ray Spectroscopy (SEM-EDX)

Operating parameters	Operating condition
Coating	Gold (Ag) and Palladium (Pd)
Electron Energy	15 kV
EDX Mode	Low vacuum
Magnification	500x - 3000x

3.5.3 Fourier Transform Infrared Spectroscopy (FTIR)

Fourier Transform Infrared Spectroscopy (FTIR) analysis shows the presence of many functional group, indicating the complex structure of the biosorbent. The heavy metal loaded residues of biosorbents from the adsorption process were filtered and dried in the oven at 80 °C overnight. The dried biosorbents were then crushed to powders using pestle and mortar. Later, they were placed on the FTIR analysis stage for analysis. The peaks and bands obtained from the spectra can be used to identify the changes in the functional group of the biosorbent before and after adsorption. The change in the vibrational frequency and intensity indicates adsorption had occurred with the involvement of functional groups present on the surface of the biosorbent. The FTIR spectra of the sample were analysed in the range of 4000-600 cm^{-1} . The operating condition that is maintained during the analysis is shown in Table 3.10.

Table 3.10: Operating conditions of Fourier Transform Infrared Spectroscopy (FTIR)

Operating parameters	Operating condition
Temperature	26 °C
Humidity	42 %
Resolution	4 cm^{-1}

3.5.4 X-ray Diffraction (XRD)

X-ray Diffraction (XRD) is mainly used for identification of unknown crystalline materials such as inorganic compounds. The biosorbent was also required to be analysed under XRD before and after adsorption to identify the change in the peak obtained from the XRD spectrum. The peak observed in the spectrum indicates the presence of inorganic compounds such as heavy metals and presence of functional groups in the biosorbent due to its primary constituents such as cellulose and lignin. After adsorption, the change in peak could be evaluated to identify the kinetics of adsorption that has been occurred. In this study, the most efficient biosorbent was analysed in XRD, before and after adsorption to determine the presence of crystalline materials via the change in crystallinity of the biosorbent surface. After separating the biosorbents from

the solution prior to adsorption, the heavy metal loaded solid residues are dried in the oven at 80 °C for 24 hours. The dried biosorbents are then crushed to powder in pestle and mortar and sent to XRD analysis. The biosorbent powder are placed in the sample holder and fitted into the XRD sample stage. The XRD analysis is carried out with a measuring range of 10° to 70° at 2° per min as shown in Table 3.11.

Table 3.11: Operating conditions of X-ray Diffractometer (XRD)

Operating parameters	Operating condition
Measuring angle range	10-70°
Rotation speed	2° / min

The calculation of crystallite size from the XRD raw data can be obtained with the use of Debye Scherrer's equation is shown as Equation 3.2.

$$\text{Crystallite size, } d_x(\text{nm}) = \frac{0.94 \lambda}{FWHM \cdot \cos \theta} \quad (3.2)$$

where,

d_x = Crystallite size, nm

λ = X-ray wavelength (CuK α) = 0.15406 nm

FWHM = Full Width Half Maximum, rad

θ = Bragg's angle, rad

CHAPTER 4

RESULTS AND DISCUSSION

In this study, two factors influencing the removal percentage of Cr (VI) and Ni (II) ions using biosorbents were studied in detail. As discussed in the literature review, initial biosorbent dosage and initial pH of aqueous solution showed the most prominent influence on the percentage removal of nickel and chromium ions. Therefore, these parameters were varied based on the Full Factorial Experimental Design of Design Expert @ Software Version 12. The experimental data obtained from the biosorption process were used as input for the response in Design Expert Software. The results obtained from the software were subjected to statistical analysis where the data were evaluated based on individual and interactive effects of the parameters on heavy metal adsorption. Response Surface Methodology (RSM) explores the relationships between several manipulated variables and one or more response variables. The influence of the operating parameters on the removal efficiency of Cr (VI) and Ni (II) ions were discussed based on the results and graphs obtained from the ANOVA analysis of Design Expert. Later, the empirical model developed from the input of response was used to optimize the initial biosorbent dosage and pH to achieve maximum removal percentage of Cr (VI) and Ni (II) ions. At the final stage, characterisation study was performed on fresh and used biosorbents with X-ray Diffraction (XRD), Scanning Electron Microscopy (SEM) and Fourier Transformed Infrared (FTIR) to display the physical and chemical properties of the biosorbents.

4.1 Pre-screening of the Most Efficient Biosorbents (Green tea leaves and Peanut shells)

As mentioned in the methodological section, exhausted green tea leaves and peanut shells were selected as potential biosorbents to adsorb Ni (II) and Cr (VI) ions. The batch adsorption process was carried out in accordance to the operating condition of the heavy metal ions as shown in Table 3.3. Based on the availability of raw material supply, two different kinds of green tea leaves and

two different kinds of peanut shells were attempted. The biosorbents used in this study were jasmine green tea leaves, genmaicha green tea leaves, salted peanut shells and unsalted peanut shells. These raw materials were used as biosorbents for the removal of Ni (II) and Cr (VI) ions from aqueous solution. The corresponding percentage removal observed from the experiment are displayed in Table 4.1. The percentage removal of heavy metal ions was deduced based on the final metal ion concentration obtained from ICP-OES as shown in Appendix G after correlating with the percentage removal equation 3.1. Meanwhile, the sample calculation of percentage removal of Cr (VI) using jasmine green tea leaves were well shown in Appendix F. Based on the removal percentage obtained, it can be deduced that both the green tea leaves showed greater affinity towards heavy metal ions (Cr (VI) and Ni (II)) compared to both salted and unsalted peanut shells. The removal percentage for Cr (VI) and Ni (II) by jasmine green tea leaves were 91.95 % and 96.16 % while the removal percentage by genmaicha green tea leaves were 89.21 % and 92.04 % respectively. Whereas, the removal percentage by salted peanut shell for Cr (VI) and Ni (II) were 81.94 % and 92.61 % while by unsalted peanut shell were 56.26 % and 61.60 % respectively. On average, the results clearly showed that jasmine green tea leaf was the most effective biosorbent for the removal of both Cr (VI) and Ni (II) ions. Hence, jasmine green tea leaf was chosen to be used in the subsequent stages of biosorption studies.

Table 4.1: Pre-screening Results for Jasmine Green Tea, Genmaicha Green Tea, Salted Peanut Shell and Unsalted Peanut Shell

Biosorbent	Final Metal Ion Concentration (mg/L)		Concentration of Metal Ion Removed (mg/L)		Percentage Removal, R (%)	
	Cr (VI)	Ni (II)	Cr (VI)	Ni (II)	Cr (VI)	Ni (II)
Heavy Metal Ions						
Jasmine Green Tea	6.442	3.073	73.56	76.93	91.95	96.16
Genmaicha Green Tea	8.635	6.366	71.37	73.63	89.21	92.04
Salted Peanut Shell	14.450	5.912	65.55	74.09	81.94	92.61
Unsalted Peanut Shell	34.99	30.72	45.01	49.28	56.26	61.60

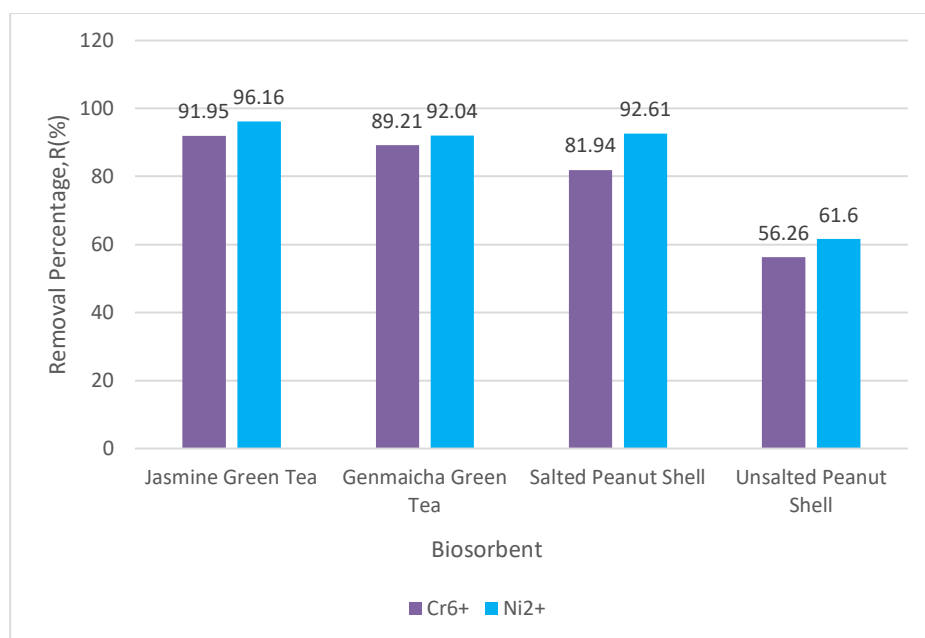


Figure 4.1: Pre-screening of Different Biosorbents on their Removal Percentage, R (%) of Cr (VI) and Ni (II) ions.

4.2 Influence of Initial Biosorbent Dosage and pH of Aqueous Solution on Percentage Removal of Cr (VI) and Ni (II) ions

During pre-screening stage, jasmine green tea leave was selected to be used in the batch biosorption of Cr (VI) and Ni (II) ions. The batch biosorption process was performed based on the experimental runs generated via full factorial experimental design of Design Expert @ Software Version 12. The initial biosorbent dosage and the pH of the aqueous solution were studied at five different levels. The initial biosorbent dosage and pH being the main manipulated factor, the removal percentage was measured as the response factor. The removal percentage of Cr (VI) and Ni (II) obtained from experimental runs at different initial biosorbent dosage and pH combinations is shown in Table 4.2 and Table 4.3 respectively. The initial biosorbent dosage and pH of aqueous solution are varied at five different levels. The removal percentage of Ni (II) is tested twice and the average removal percentage was considered while for removal of Cr (VI) only one reading is obtained due to time constraint. Later, the trend of the removal percentage influenced by both initial biosorbent dosage and pH of aqueous solution were plotted and analysed as shown in Figure 4.2.

Table 4.2: Removal Percentage, R (%) of Cr (VI) Obtained at Different Biosorbent Dose and pH combination.

Removal Percentage, R (%)						
pH	pH 2	pH 3	pH 4	pH 5	pH 6	
Initial Biosorbent Dose						
2.0 g	99.92	99.89	99.93	99.96	97.42	
2.5 g	66.40	90.21	98.08	94.94	92.48	
3.0 g	79.76	92.57	98.32	93.51	91.45	
3.5 g	88.80	95.33	98.49	98.59	97.90	
4.0 g	100.00	100.00	99.99	99.87	99.87	

Table 4.3: Removal Percentage, R (%) of Ni (II) Obtained at Different Biosorbent Dose and pH combination.

Removal Percentage, R (%)															
pH	pH 4			pH 5			pH 6			pH 7			pH 8		
Initial															
Biosorbent	1	2	Average												
Dose															
2.0 g	78.23	78.88	78.55	87.46	86.38	86.92	86.65	86.93	86.79	93.00	93.38	93.19	76.53	61.73	69.13
2.5 g	80.16	82.26	81.21	85.00	87.08	86.04	85.63	93.14	89.38	92.96	93.35	93.15	81.09	71.78	76.43
3.0 g	85.45	78.36	81.91	84.30	91.30	87.80	88.47	88.59	88.53	92.29	92.60	92.44	84.93	82.58	83.75
3.5 g	84.23	99.24	91.73	89.68	99.14	94.41	89.62	89.90	89.76	92.54	92.89	92.71	86.45	83.93	85.19
4.0 g	93.00	83.51	88.25	89.57	98.97	94.27	90.18	87.84	89.01	88.93	88.87	88.90	87.36	84.78	86.07

4.2.1 Influence of Initial Biosorbent Dosage

The initial biosorbent dosage plays a significant role in the biosorption efficiency of the adsorbents. The study on the influence of the initial biosorbent dosage of jasmine green tea leaves was conducted by varying the biosorbent dosage while maintaining the concentration of heavy metal solution at 80 mg/L. The effect of biosorbent dosage on the removal percentage of heavy metal ions were studied in the range of 2 to 4 g with an interval of 0.5 g. Figure 4.2 (a) and 4.2 (b) depicts the percentage removal of Cr (VI) and Ni (II) ions at varying the biosorbent dosage and pH of solution, respectively.

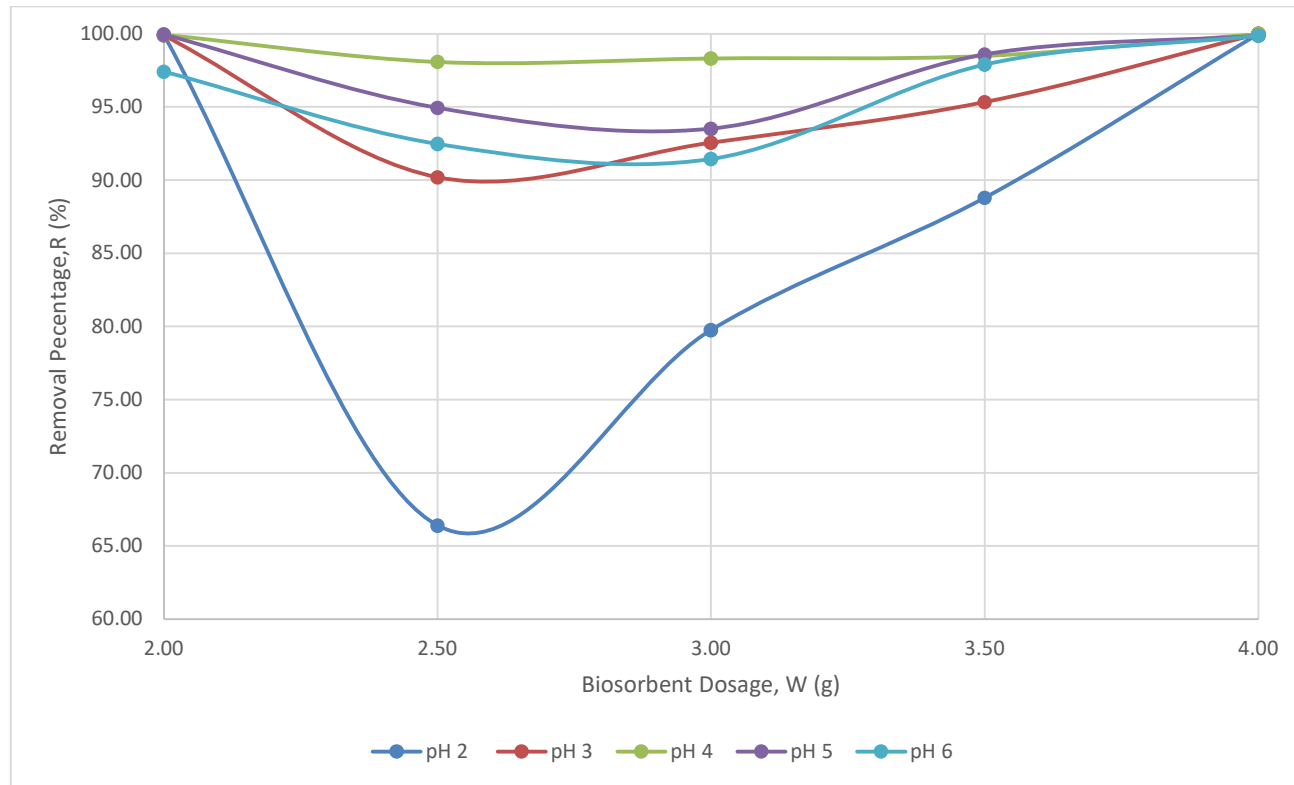
Theoretically, the increase in dosage of biosorbent for the same amount of available heavy metal ions will lead to an increase in adsorption frequency, thus higher removal percentage can be seen. The increase in removal efficiency of heavy metal ions from aqueous solutions can be caused by the increase in number of exchangeable sites available for adsorption (Senthil Kumar, 2011). This was mainly due to the largely available adsorption binding sites offered by the large surface area of biosorbent in high dosage. Thus, more binding sites will be available, resulting in higher amount of metal uptake (Abdel Ghani and El Chaghaby, 2014). The optimum initial biosorbent dosage was deduced based on the maximum removal percentage of the heavy metal ions at equilibrium. This trend has been widely expressed in the study of Cherdchoo, Nithettham and Charoenpanich (2019); Amarasinghe and Williams (2007) and Nigam, et al. (2019). This theory can be well fitted to be result obtained for the removal of Ni (II) ions in Figure 4.2 (b).

The overall trend shown in Figure 4.2 (a) shows a slow decline at the initial stage from 2 g to 3 g followed by a gradual increase from 3 g to 4 g. The highest removal percentage of Cr (VI) ions of 100.00 % was obtained at pH 2 and pH 3 with the biosorbent dosage of 4 g. This shows the optimal initial biosorbent dosage to achieve maximum removal percentage was 4g where all of the heavy metal ions present in the solution were completely adsorbed onto the adsorption sites. However, the overall trend of the removal percentage of heavy metal ions from aqueous solution against the biosorbent dosage does not fit the theoretical normalities mentioned earlier. This could be caused by several reasons that might have potentially affected the result of the experimentation.

Firstly, the analysis for the 2 g of biosorbent at different pH was analysed in ICP-OES at different period compared to the rest of the included data. The environment of the ICP-OES such as spectral interference, matrix effects and operating mode during analysis highly affects the performance of the analysis (HORIBA, n.d.). This could have potentially affected the result. Secondly, the green tea used for the 2 g of biosorbent analysis, was freshly prepared adsorbent material unlike the adsorbent material used for the rest of the analysis. Thus, the period of storage on jasmine green tea leaves could have affect the efficiency of the adsorbent towards adsorbing the Cr (VI) ions.

Figure 4.2 (b) shows an overall increased trend in the removal percentage, before reaching a saturation point (peak). The removal percentage of Ni (II) ions shows a slow increase from biosorbent dosage 2 g to 3 g. The lowest peak (83.75%) was obtained at pH 8 with the biosorbent dosage of 3 g and the highest peak (94.41%) was obtained at pH 5 with biosorbent dosage of 3.5 g. This was caused by the equilibrium has been achieved. Higher concentration of biosorbent resulted in higher amount of biosorption sites, however after the optimal point, the agglomeration of the biosorbent particles can lead to overlapping of binding sites and longer diffusional path of the metal ions (Cherdchoo, Nithettham and Charoenpanich, 2019). This will eventually restrict the adsorption process of the heavy metal ions and unsaturation of adsorbent sites. Despite employing agitation in a shaking incubator to enhance the mixing during adsorption, further addition of biosorbent beyond equilibrium will only show reduced adsorption efficiency due to some of the adsorption sites remain unsaturated caused by overlapping (Nigam, et al., 2019). The optimal initial biosorbent dosage was highly dependent on the pH of the aqueous solution.

a)



b)

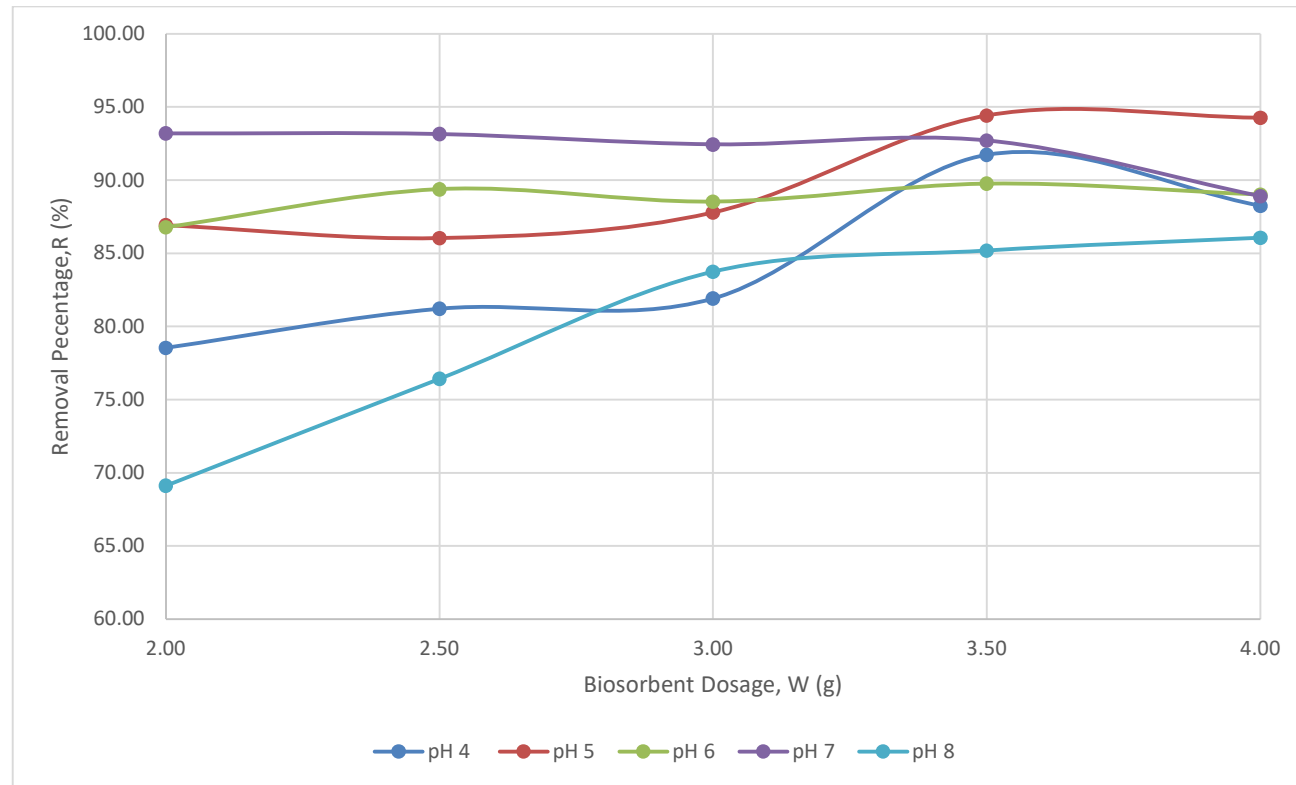


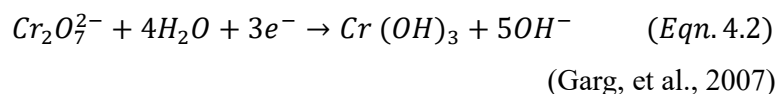
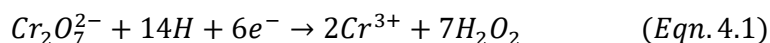
Figure 4.2: Percentage Removal, R (%) of Heavy Metal Ions at Different pH and at Different Initial Biosorbent Dosage of Jasmine Green Tea Leave on the Removal of (a) Cr (VI) and (b) Ni (II) ions.

4.2.2 Influence of pH of Aqueous Solution

Influence of pH of heavy metal solution during adsorption on the removal percentage was studied in detailed. The initial pH of the solution was varied at five different level where the pH of Cr (VI) solution was studied with pH 2,3,4,5 and 6 whereas the pH of Ni (II) solution was studied with pH 4,5,6,7 and 8. In order to prevent precipitation, the pH range was not exceeded beyond pH 8 (Nigam, et al., 2019). The pH range for the respective heavy metal ion solution were decided based on the formation of cation or anion when dissociated in water. Figure 4.3 (a) and 4.3 (b) represents at constant biosorbent dosage, the effect of pH on the removal of Cr (VI) and Ni (II) ions respectively. Based on Figure 4.3 (a), the removal percentage of Cr (VI) from aqueous solution has reached maximum of 98.32 % at pH 4. While, the maximum removal percentage of Ni (II) of 94.41 % was observed at pH 5. The effect of pH on the removal percentage of heavy metal ions was decided to be studied at initial biosorbent dosage of 3 g, 3.5 g and 4 g. The optimum biosorbent dosage found earlier for removal of both Cr (VI) and Ni (II) ions were about 3 - 4 g. Thus, 3 g to 4 g adsorbent dosage was chosen as the ideal range, during the study of the effects of pH on removal percentage.

Based on Figure 4.3 (a), the maximum removal percentage was observed at system of pH 4. As mentioned in the literature review, the optimum pH range published for the removal of Cr (VI) ions were typically in the range of 2 to 4. Hence, Figure 4.3 (a) supports the results obtained in the previously studied thesis. The removal percentage of heavy metals was increased slowly with the pH increment till pH 4. Thereafter, removal percentage reduced as the pH increased to 6. Thus, system of pH 4 was determined as the optimal pH required to remove highest amount of hexavalent chromium. This was mainly because, Cr (VI) solution dissociate into different chromate anions (CrO_4^{2-} , H_2CrO_4 , HCrO_4^- and $\text{Cr}_2\text{O}_7^{2-}$) in water. The stability of these ions were highly dependent on the pH of the aqueous solution (Pehlivan and Altun, 2008). At the same time, the pH of the aqueous solution strongly affects the adsorbent surface charge and the degree of ionization of the heavy metals (Abdel Ghani and El Chaghaby, 2014).. At acidic condition of pH 4, these anions will be dominantly available and the adsorbent surface will be protonated. Among the wide group of anions,

HCrO_4^- that was dominantly available at high acidic condition were strongly attracted to the positively charged adsorbent surface via electrostatic attraction (Cherdchoo, Nithettham and Charoenpanich, 2019). At lower pH, the green tea leaves surface will be surrounded by hydronium ions (H^+ and H_3O^+) which promotes the attraction of chromate anions onto the binding sites of the biosorbent (Pehlivan and Altun, 2007). The most dominantly available chromium species at lower pH is hydrogen chromate ion (HCrO_4^-) which would transform into chromium oxoanion (CrO_4^-) and chromate anion ($\text{Cr}_2\text{O}_7^{2-}$) as the pH increases. Since, higher removal of Cr (VI) ions were observed at more acidic condition on the positively charged green tea leaves, it can be deduced that hydrogen chromate ion (HCrO_4^-) was the active chromium species observed to be adsorbed onto the green tea (Sarin, et al., 2006). Besides, it was also reported that, the dichromate ions go through reduction to form Cr^{3+} at lower system pH. Thus, having a much smaller ionic size, Cr^{3+} can be easily replaced by cationic hydronium (H^+ and H_3O^+) on the biosorbent surface, resulting in higher adsorption at acidic condition. The reduction of dichromate ion ($\text{Cr}_2\text{O}_7^{2-}$) into Cr^{3+} is shown below in Equation 4.1 and 4.2.



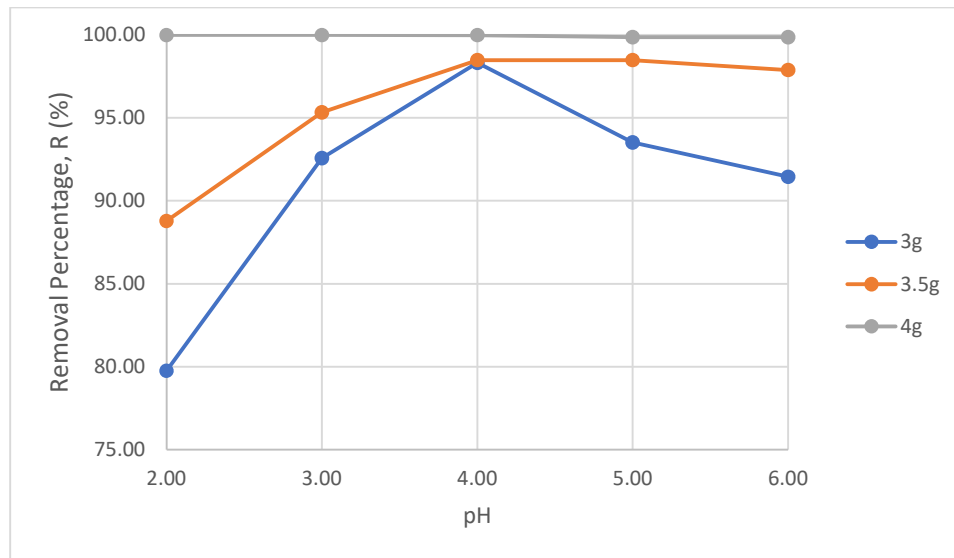
On the contrary, at pH above 4 the removal percentage showed a steep decline was mainly because of the interference caused by decrease in electrostatic attraction and the presence of hydroxide ions (OH^-) in bulk solution. The presence of OH^- ions will lead to competitive adsorption with chromium oxoanion (CrO_4^-) and chromate anion ($\text{Cr}_2\text{O}_7^{2-}$) that could significantly reduce the adsorption efficiency due to lower adsorption sites availability for chromium species ions due to the occupation of binding sites (Pehlivan and Altun, 2007).

According to Figure 4.3 (b), the optimal removal percentage of Ni (II) ions was observed at system of pH 5. Beyond pH 5, steep decline can be seen when the pH was approaching system pH 8. As mentioned earlier, at lower pH, the

adsorbent surface will be protonated leading to electrostatic repulsion between the positively charged ligands on the biosorbent surface and Ni (II). At the same time, the competitive adsorption of protons (H^+ and H_3O^+) and Ni (II) ions could also hugely reduce the metal uptake rate (Flores-Garnica, et al., 2013). Higher concentration and mobility of H^+ and H_3O^+ ions at lower pH conditions which will hinder the Ni (II) ions from reaching the adsorbent active sites due to repulsive forces (Senthil Kumar, et al., 2011). In addition, adsorption of Ni (II) ions also decreases at lower pH hinders the due to surface functional group that contribute to the removal of heavy metals, experiencing repulsive forces by the H^+ ions. As the pH progress to the optimal value, the removal efficiency gradually increases as the adsorption of cationic Ni (II) build-up due to the increase in negatively charged biosorbent surface (Zafar, et al., 2007). Increase in pH of the system until optimal level of 5 will reduce the H^+ ions along with the competition for adsorption onto the binding sites. However, the decrease in removal percentage beyond pH 5 can be caused by hydroxylated complex formation due to precipitation of Ni (II) into nickel hydroxide due to the presence of OH^- ions as reported by Malkoc and Nuhoglu (2005). Such insoluble complexes formation, not only reduce the amount of nickel available for adsorption but also reduces the affinity of nickel ions towards the biosorbent (Zafar, et al., 2007).

Anyhow, the trend of the removal percentage at different pH at initial biosorbent dosage of 4 g shows that the initial biosorbent dosage acts as the predominant force in affecting the removal percentage of Cr (VI) ions rather than the pH of the aqueous solution which resulted in least changes in removal percentage over the range of pH.

a)



b)

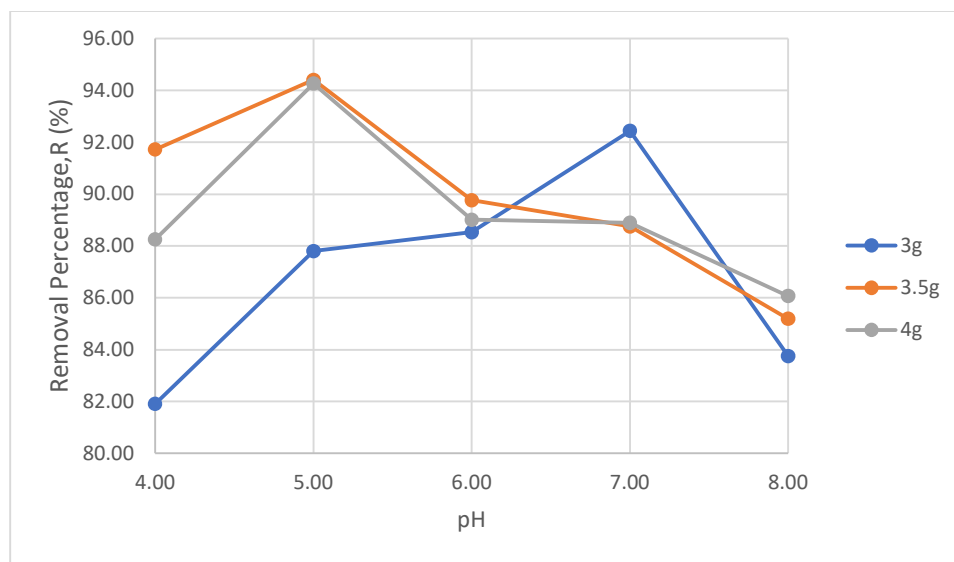


Figure 4.3: Percentage Removal, R (%) of Heavy Metal Ions with 3g, 3.5g and 4g Dosage of Jasmine Green Tea Leave on the Adsorption of (a) Cr (VI) and (b) Ni (II) ions.

4.3 Statistical Analysis in Design Expert Software

After studying the effects of initial biosorbent dosage and pH on the removal percentage of Cr (VI) and Ni (II) ion, statistical analysis was performed on experimental data collected via Full Factorial Experimental run in Design Expert @ Software Version 12. The influences of the individual effects of two parameters and the interaction effect between these two parameters on the adsorption efficiency of heavy metal ions were evaluated through response surface methodology (RSM). As mentioned earlier, each parameter was studied on five different levels. The experimental design for the Full Factorial Design which includes two factors (Factor A: Initial biosorbent dosage; Factor B: pH) at five levels was shown in Table 4.4 and Table 4.5. A total of 25 experimental runs for each Cr (VI) and Ni (II) ion removal were designed. Meanwhile, removal percentage of heavy metal ions (Cr (VI) and Ni (II)) was considered a response factor to measure the performance of the biosorption process.

Both of the affecting factors, initial biosorbent dosage (A) and pH (B) were analysed quantitatively (numerical) and thus a qualitative judgement was made. Thus, Table 4.2 and 4.3 shows the removal percentage corresponding to varying biosorbent dosage and pH of aqueous solution. The response variable was collected from various experimental runs with different combination of Factor A and B. The removal percentage was obtained from Equation 3.1 by correlating the initial concentration of heavy metal ions and final metal ion concentration of the aqueous solution that was measured with ICP-OES. This model represents a 5^2 full factorial design with a total of 25 runs which fully complement all possible factor combination to measure the interaction as well as the main effects on the responding variable (Witek-Krowiak, et al., 2014).

Table 4.4: Experimental Design Matrix with Response for Adsorption of Cr (VI) ion

TEST RUNS	Factor A	Factor B	Response
	Initial biosorbent dose	pH	Removal percentage
	(g)		(%)
1	2.0	2	99.92
2	2.5	2	66.40
3	3.0	2	79.76
4	3.5	2	88.80
5	4.0	2	100.00
6	2.0	3	99.89
7	2.5	3	90.21
8	3.0	3	92.57
9	3.5	3	95.33
10	4.0	3	100.00
11	2.0	4	99.93
12	2.5	4	98.08
13	3.0	4	98.32
14	3.5	4	98.49
15	4.0	4	99.99
16	2.0	5	99.96
17	2.5	5	94.94
18	3.0	5	93.51
19	3.5	5	98.59
20	4.0	5	99.87
21	2.0	6	97.42
22	2.5	6	92.48
23	3.0	6	91.45
24	3.5	6	97.90
25	4.0	6	99.87

Table 4.5: Experimental Design Matrix with Response for Adsorption of Ni (II) ion

TEST RUNS	Factor A	Factor B	Response
	Initial biosorbent dose (g)	pH	Removal percentage (%)
1	2.0	4	78.55
2	2.5	4	81.21
3	3.0	4	81.91
4	3.5	4	91.73
5	4.0	4	88.25
6	2.0	5	86.92
7	2.5	5	86.04
8	3.0	5	87.80
9	3.5	5	94.41
10	4.0	5	94.27
11	2.0	6	86.79
12	2.5	6	89.38
13	3.0	6	88.53
14	3.5	6	89.76
15	4.0	6	89.01
16	2.0	7	93.19
17	2.5	7	93.15
18	3.0	7	92.44
19	3.5	7	92.71
20	4.0	7	88.90
21	2.0	8	69.13
22	2.5	8	76.43
23	3.0	8	83.75
24	3.5	8	85.19
25	4.0	8	86.07

4.3.1 Analysis of Variance (ANOVA)

Analysis of Variance (ANOVA) was a critical module in statistical analysis where it defines the significance of the design model as well as the term included in the model (StatEase, 2020).. The significance of the model was normally based on the model P-value in association with the model F-value. The model was termed significant if the “P-value > F-value”. In the meantime, the model terms were deemed significant only if the P-value < 0.0500 (StatEase, 2020).. Table 4.6 and 4.7 represents the findings from ANOVA for the removal of Cr (VI) and Ni (II) respectively. Most importantly, the model suggested for the response variable of Cr (VI) and Ni (II) removal percentage was Quartic model. These models were later modified by eliminating the most insignificant model terms that do not support the hierarchy. This was to ensure that the significance of the model and the precision of the empirical model was maximized. From Table 4.6, the empirical model with F-value 13.75 was termed significant in accordance with the P-value ($0.0001 < 0.0500$). In this case, the terms that were significant with “P-value > F-value” less than 0.1000 were A, B, AB, B², A²B, A³, A²B² and A³B. Meanwhile, Table 4.5 representing the empirical model of Ni (II) removal with F-value 20.39 was also termed significant in accordance with the P-value ($0.0001 < 0.0500$). The significant model terms with “P-value > F-value” less than 0.1000 were B, AB, B², AB², B³, AB³ and B⁴. To be noted that, there was only 0.01 % chance that the F-values for both Cr (VI) and Ni (II) removal could be affected by noise.

Table 4.6: Analysis of Variance (ANOVA) for removal of Cr (VI)

Source	Sum of Squares	df	Mean Square	F-value	P-value	Remark
Model	1296.12	10	129.61	13.75	< 0.0001	significant
A-Initial biosorbent dosage	80.05	1	80.05	8.49	0.0113	
B-pH	356.27	1	356.27	37.79	< 0.0001	
AB	63.79	1	63.79	6.77	0.0209	
A ²	7.51	1	7.51	0.7962	0.3873	
B ²	358.73	1	358.73	38.05	< 0.0001	
A ² B	156.01	1	156.01	16.55	0.0012	
AB ²	22.31	1	22.31	2.37	0.1462	
A ³	101.93	1	101.93	10.81	0.0054	
A ² B ²	133.12	1	133.12	14.12	0.0021	
A ³ B	56.85	1	56.85	6.03	0.0277	
Residual	131.98	14	9.43			
Cor Total	1428.10	24				

Table 4.7: Analysis of Variance (ANOVA) for removal of Ni (II)

Source	Sum of Squares	df	Mean Square	F-value	P-value	Remark
Model	818.21	11	74.38	20.39	< 0.0001	significant
A-Initial biosorbent dosage	8.49	1	8.49	2.33	0.1512	
B-pH	26.64	1	26.64	7.30	0.0181	
AB	57.65	1	57.65	15.80	0.0016	
A ²	9.78	1	9.78	2.68	0.1255	
B ²	25.23	1	25.23	6.91	0.0208	
A ² B	13.50	1	13.50	3.70	0.0766	
AB ²	106.26	1	106.26	29.13	0.0001	
A ³	9.84	1	9.84	2.70	0.1245	
B ³	35.11	1	35.11	9.62	0.0084	
AB ³	60.81	1	60.81	16.67	0.0013	
B ⁴	67.87	1	67.87	18.60	0.0008	
Residual	47.43	13	3.65			
Cor Total	865.64	24				

The reliability of the empirical model can further be ensured by evaluating the coefficient of determination, R^2 value. The R^2 value shows the accuracy of the response generated with the predicted response (Connor, 2020). At the same time, it shows the variation observed in the response by the selected model towards the predicted manipulated variable. The R^2 value ranges from 0 to 1 and a higher value depicts a more accurate representation of the response. Besides that, the predicted R^2 value indicates the ability to predict the future observation based on the response variable provided. The adjusted R^2 value in association with the predicted R^2 value which adjusts the number of irrelevant model terms (StatEase, 2020). The difference between adjusted R^2 and predicted R^2 value was at < 0.20 to be considered as they were in reasonable agreement. Meanwhile, adequate precision parameter was used to determine the signal to noise ratio and compares the average prediction errors to the range of predicted values at the design points. An adequate precision value of greater than 4 was desirable (StatEase, 2020).

Table 4.8 shows the summary of the ANOVA for the removal of Cr (VI) ions. The R^2 value of the empirical model was indicated as 0.9076. It shows that 90.76 % of the variation in the response variable can be explained through the empirical model. Since, there was no insignificant model terms that lays out of the model hierarchy support to be eliminated, the adjusted R^2 value cannot be further optimized. These could be an effect of the response variable (removal percentage) experimental data that has been recorded that does not fit the normalities.

Table 4.8: Summary of Analysis of Variance (ANOVA) for removal of Cr (VI)

Significant Model Terms	A, B, AB, A^2 , B^2 , A^2B , AB^2 , A^3 , A^2B^2 , A^3B
R^2	0.9076
Adjusted R^2	0.8416
Predicted R^2	0.4562
Adeq Precision	13.7315

Table 4.9 summarises the ANOVA of the removal of Ni (II) ion. The predicted R^2 was obtained as 0.7041 which was in reasonable agreement with the adjusted R^2 of 0.8988. While, the adequate precision measures the signal to noise ratio of (18.361 > 4.00) indicating that was it an adequate signal. This ensures that the model can be used to navigate the design space. The empirical model has shown prominent significance which could ensure precision results during optimization

Table 4.9: Summary of Analysis of Variance (ANOVA) for removal of Ni (II)

Significant Model Terms	A, B, AB, A ² , B ² , A ² B, AB ² , A ³ , B ³ , AB ³ , B ⁴
R²	0.9452
Adjusted R²	0.8988
Predicted R²	0.7041
Adeq Precision	18.3613

Based on the ANOVA analysis, the empirical model of the removal of Cr (VI) and Ni (II) ions were shown in Table 4.10 and 4.11 respectively.

Table 4.10: Empirical Equation in Terms of Coded and Actual Factors for removal of Cr (VI)

Mathematical Model	
Coded Factors	Removal percentage = $97.89 + 8.18A + 8.32B - 9.60AB + 2.04A^2 - 14.11B^2 - 8.45A^2B + 3.19AB^2 - 9.52A^3 + 13.19A^2B^2 + 10.05$
Actual Factors	Removal percentage = $1349.30300 - 1189.78367$ (initial biosorbent dosage) - 345.12948 (pH) + 308.10180 (initial biosorbent dosage) + 338.30400 (initial biosorbent dosage) + 23.74565 (pH) ² - 75.83482 (initial biosorbent dosage) ² (pH) - 18.98076 (initial biosorbent dosage)(pH) ² - 29.62533 (initial biosorbent dosage) ³ + 3.29653 (initial biosorbent dosage) ² (pH) ²

Table 4.11: Empirical Equation in Terms of Coded and Actual Factors for removal of Ni (II)

Mathematical Model	
Coded Factors	Removal percentage = $89.44 + 2.66A + 4.72B - 9.13AB - 1.50A^2 + 14.08B^2 - 2.48A^2B + 6.97AB^2 - 2.96A^3 - 5.59B^3 + 10.40AB^3 - 20.55B^4$
Actual Factors	Removal percentage = $-614.34286 - 303.54752$ (initial biosorbent dosage) + 638.51776 (pH) + 122.34419 (initial biosorbent dosage)(pH) + 32.57257 (initial biosorbent dosage) ² – 196.37195 (pH) ² – 1.24200 (initial biosorbent dosage) ² (pH) – 21.65157 (initial biosorbent dosage)(pH) ² – 2.95733 (initial biosorbent dosage) ³ + 26.22667 (pH) ³ + 1.29967 (initial biosorbent dosage)(pH) ³ – 1.28433 (pH) ⁴

4.3.2 Diagnostic Plots

As the R^2 value for the model of Ni (II) and Cr (VI) ion removal were discussed in the earlier section, this section demonstrates the predicted plots of the empirical model. These confirms the correct prediction of the statistical model on the heavy metal ions removal efficiency. Figure 4.4 and 4.5 depicts the plot of experimental responses versus the predicted responses on removal percentage of Cr (VI) and Ni (II) ions respectively. Based on Figure 4.4 and 4.5, it can be seen that the experimental values of removal percentage of Ni (II) ions lie closer to the predicted values compared to removal percentage of Cr (VI). This can be supported by the R^2 value for the model discussed earlier where for the removal percentage of Cr (VI) (R^2 : 0.9075) while for removal percentage of Ni (II) (R^2 : 0.9452). Hence, this shows that the empirical model of Ni (II) removal was able to predict the response more accurately compared to empirical model of Cr (VI) removal based on the range of data provided.

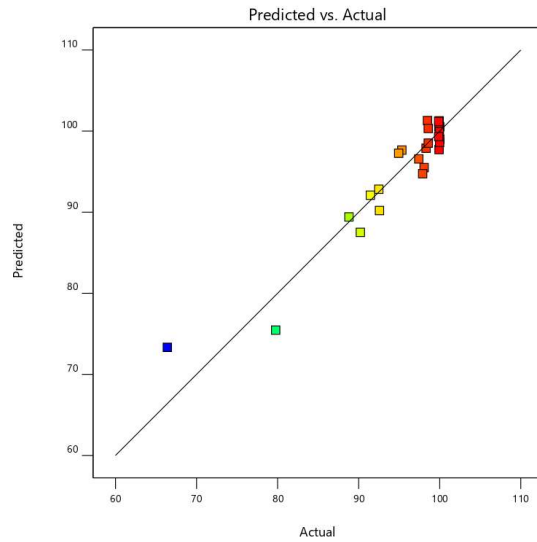


Figure 4.4: Predicted vs Actual Plot for Removal Percentage of Cr (VI).

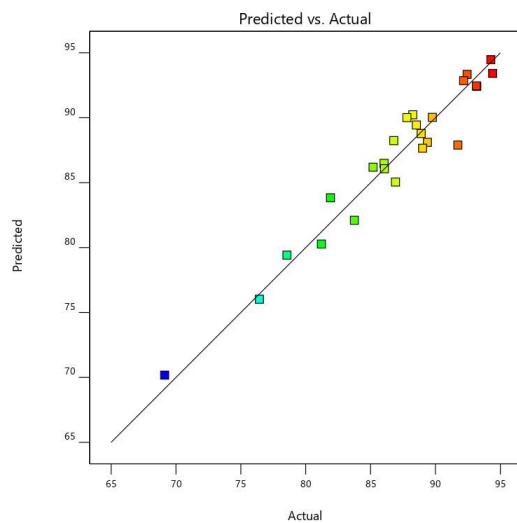


Figure 4.5: Predicted vs Actual Plot for Removal Percentage of Ni (II).

4.3.3 Box-Cox Plot for Power Transformation

A Box-Cox plot acts as a tool to aid the users to determine the most suitable power transformation required for a response data. The power transformation was commonly described with the value of lambda, λ . Power transformation is commonly applied to a set of test data that are not ascertain with the assumption of normality. When the real data that was obtained goes through an appropriate transformation, it can yield a data set that can follow the normal distribution as expected (Nist, 2020). The Design Expert software shows the current power

transformation as well as considers the minimum lambda value and the lambdas at 95 % confidence interval, if it was within ± 3 lambda limits.

Based on the results obtained from Design Expert @ Software Version 12, the initial Box-Cox plot obtained from the ANOVA analysis for the removal of Ni (II) and Cr (VI) was shown in Figure 4.6 and 4.7 respectively. Both the plot shows the current lambda value to be at 1. Even though, both Box-Cox plot provided a recommended logarithmic function ($\lambda = 3$), there was no recommendation indicated for power transformation. This shows that the power transformation that was intended to be recommended falls outside the confidence interval (StatEase, 2020). Since, there was no recommendation provided by the Design Expert software for any transform of logarithmic function, the current logarithmic function ($\lambda = 1$) was followed to obtain the results of normality.

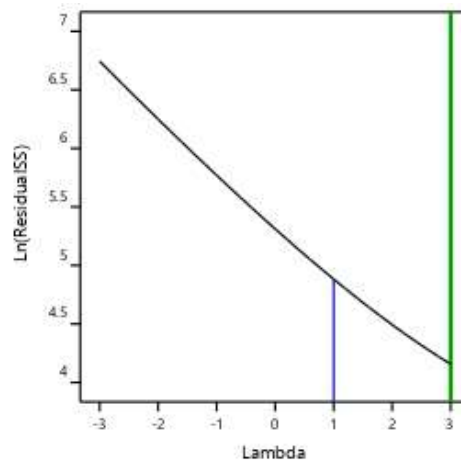


Figure 4.6: Box-Cox Plot for Power Transform for removal of Cr (VI).

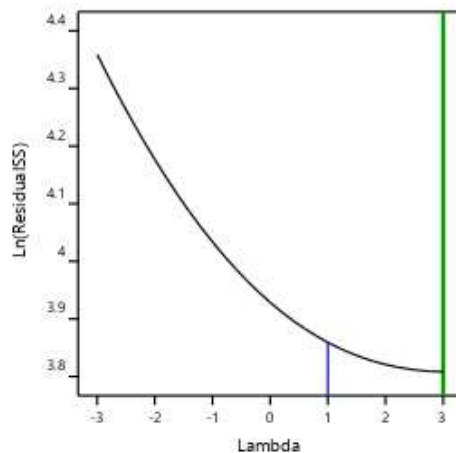


Figure 4.7: Box-Cox Plot for Power Transform for removal of Ni (II).

4.3.4 Model Graphs

In general, high biosorbent dosage of jasmine green tea leaves has indicated higher removal efficiency of heavy metal ions. However, the removal efficiency was also strongly affected by the pH of the aqueous solution. Therefore, the interaction between these numeric factors at fixed initial concentration of heavy metal ions of 80 mg/L were identified using model graphs such as contour plot and 3D surface plot with the removal percentage being the measurement of the biosorption efficiency. In the current study, the trend of interaction between the Factor A (initial biosorbent dosage) and Factor B (pH) on the Response (removal percentage) of the model was projected through a 3D surface plot and contour plot extracted from Design Expert Software. From the model graphs obtained, the regions can be subdivided into “productive” and “non-productive” region of the empirical model which were classified based on the colour of the region. The bright red colour indicates the region of peak which shows the highest removal percentage of heavy metal ions, followed by yellow, green and blue colour (El-Naggar, et al., 2018).

Figure 4.8 and Figure 4.9 show the contour plot and 3D surface plot of model term of Factor A and Factor B on the removal percentage of Cr (VI) ions respectively. From the plots, when the initial biosorbent dosage was just at 2 g and the pH of the aqueous solution has increased to 4, the removal percentage of Cr (VI) ions increased substantially, indicating high adsorption efficiency. At initial biosorbent dosage of 2 g and pH of 4, almost all the Cr (VI) ions have been removed. However, at the region with higher initial biosorbent dosage of 2.5 g and 3 g, removal percentage of heavy metal ions were low. This might be due to occurrence of overlapping of active binding sites at saturated biosorbent dosage (Cherdchoo, Nithettham and Charoenpanich, 2019). In contrast, when the pH decreased below 4, the removal percentage of Cr (VI) ions from aqueous solution has decreased regardless on the initial biosorbent dosage. This indicates lower adsorption efficiency by the green tea leaves at pH lower than 4. It can be deduced that the combination of pH and initial biosorbent dosage at red “productive region” was favourable whereas the combination of pH and initial biosorbent dosage at blue to red “non-productive region” should be avoided to achieve maximum Cr (VI) removal percentage.

Figure 4.9 shows a 3D surface plot of interaction between the Factor A (initial biosorbent dosage) and Factor B (pH) the removal percentage of Cr (VI) ions. It shows a broad peak at pH 4, irrespective of initial biosorbent dosage, indicating maximum removal percentage. Therefore, pH was considered as the most evident factor in the adsorption of Cr (VI) ions. In the meantime, the removal percentage of Cr (VI) did not show any increase beyond pH 4 regardless of initial biosorbent dosage. Thus, the optimal value for removal of Cr (VI) could be strongly fall at pH 4. This deduction was further supported by the claim provided by Nigam, et al. (2019) which stated that maximum removal of Cr (VI) using tea waste was observed at pH 3.9.

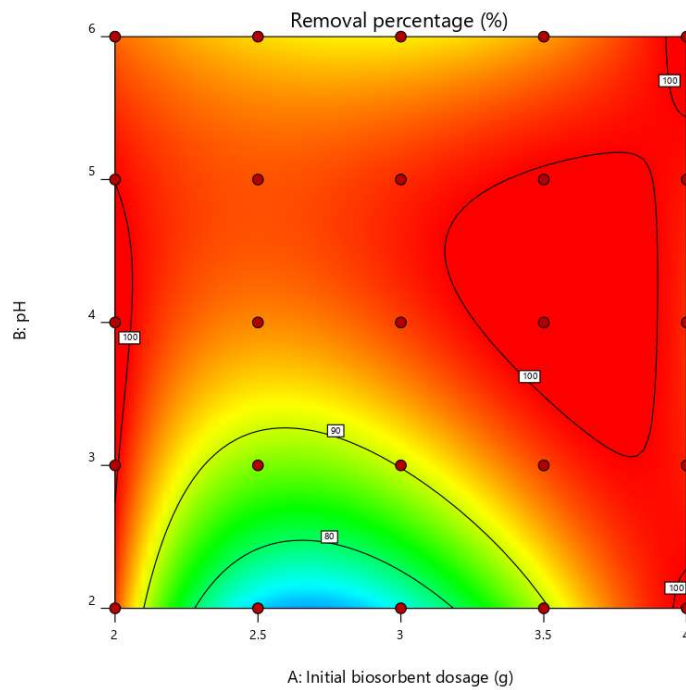


Figure 4.8: Contour Plot for Interaction between Initial Biosorbent Dosage (g) and pH of on Removal Percentage of Cr (VI).

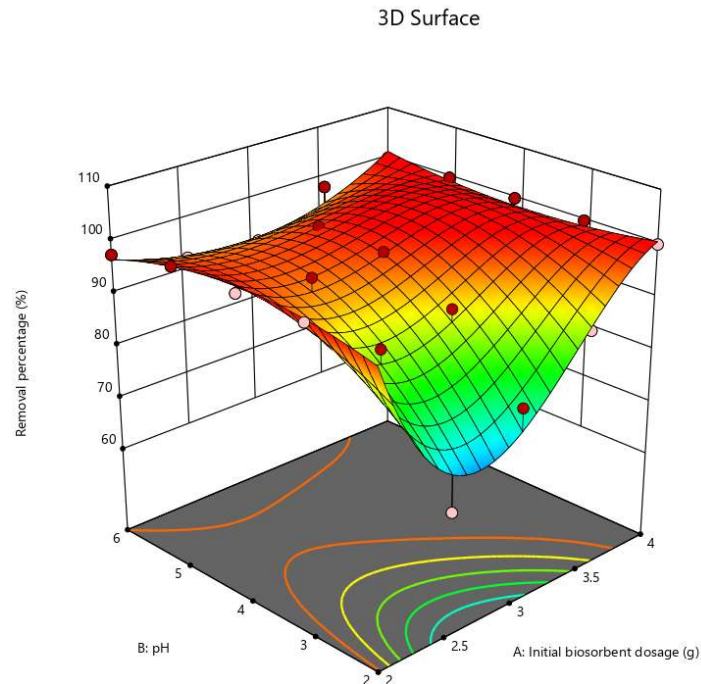


Figure 4.9: 3D Surface Plot for Interaction between Initial Biosorbent Dosage (g), pH and Removal Percentage of Cr (VI).

Figure 4.10 and Figure 4.11 show the contour plot and 3D surface plot of model term of Factor A and Factor B on the removal percentage of Ni (II) ions respectively. The current view shows that, when the pH was increased to 7 and the biosorbent dosage was increased to 4 g, the removal percentage of Ni (II) ions showed a strong increase in removal percentage, indicating high adsorption efficiency. In contrast, when the pH decreased below 7, the removal percentage of Ni (II) ions from aqueous solution has decreased substantially regardless on the initial biosorbent dosage. This indicates lower adsorption efficiency by the green tea leaves at pH lower than 7. However, this did not comply when the initial biosorbent dosage reaches 4 g, where the removal percentage was optimum at pH 4 to 5. This could be caused by the initial biosorbent dosage appeared as the significant factor on the removal of Ni (II). Thus, when the system was in the range of pH 4 to 5 and biosorbent concentration at 4 g, Ni (II) removal percentage showed significant drop. This could be caused by the accumulation of biosorbent due to excessive biosorbent concentration resulting in unsaturation of adsorption sites (Cherdchoo, Nithettham and Charoenpanich, 2019). Based on Figure 4.10, the combination

of pH and initial biosorbent dosage at red “productive region” was favourable whereas the combination of pH and initial biosorbent dosage at blue to red “non-productive region” should be avoided to achieve maximum Ni (II) removal percentage.

Figure 4.11 shows a 3D surface plot of interaction between the Factor A (initial biosorbent dosage) and Factor B (pH) the removal percentage of Ni (II) ions. It shows a broad peak at pH 7, irrespective of initial biosorbent dosage, for higher removal percentage. At the same time, an optimum peak was found at pH 4 to 5 and at initial biosorbent dosage of 4 g. On the contrary, pH was considered as the most significant factor in the adsorption of Ni (II) ions. Thus, the optimal value for removal of Ni (II) was at pH 7 and at initial biosorbent dosage of 4 g. This deduction was further supported by the claim provided by Shah, et al. (2015) which stated that the optimal pH to obtain maximum Ni (II) removal using tea waste can be seen at system pH 7. The adsorption of Ni (II) ions has been proven to show poor removal efficiency below pH 7 due to high concentration of competing H^+ ions and beyond pH 7 due to the metal hydroxide precipitation.

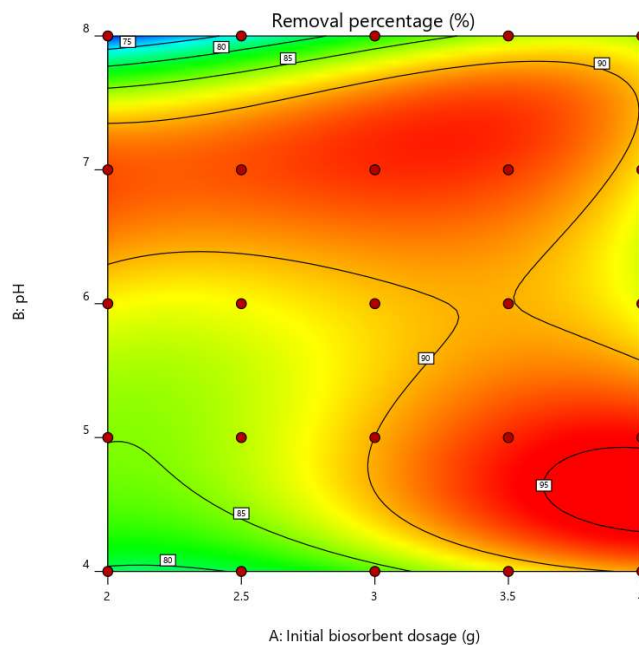


Figure 4.10: Contour Plot for Interaction between Initial Biosorbent Dosage (g) and pH of on Removal Percentage of Ni (II).

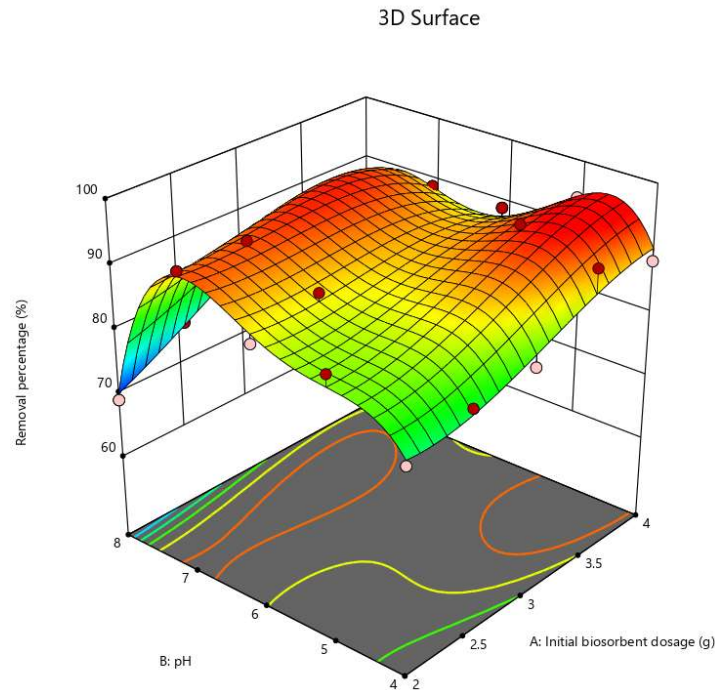


Figure 4.11: 3D Surface Plot for Interaction between Initial Biosorbent Dosage (g), pH and Removal Percentage of Ni (II).

4.4 Optimization of Operating Condition using Design Expert

The process optimization was performed under numerical optimization in Design Expert @ Software Version 12. The numerical optimization tool takes into account of the design evaluation, ANOVA statistics data and diagnostic graphs of the model that was developed. This was to makes sure, the optimization tool provides a good estimation of the true response surface based on the model (StatEase, 2020). In this case, the empirical model of Cr (VI) and Ni (II) from the ANOVA analysis was used. The main aim of the optimization process is to determine the optimal value of initial biosorbent dosage and initial pH of the aqueous solution to yield the maximum removal percentage of heavy metal ions (Cr (VI) and Ni (II)). The criteria set for the removal of Cr (VI) and Ni (II) ions in Design Expert Numerical Optimization tool were shown in Table 4.12 and Table 4.13, respectively. The response (removal percentage %) was given the most importance as it correlates with the objective of the study. The best optimal solution was selected based on the highest removal percentage of heavy metal ions followed by minimum biosorbent dosage. In industry, an optimized process always uses less resources to achieve their goal. In this case,

to achieve maximum removal of heavy metal ions, minimal amount of biosorbent is expected to reduce the processing cost. Thus, the goal of optimization process was to obtain the best combination of condition that fulfil all the goals and achieve a high desirability value.

Table 4.12: Constraints and Goals of Numerical Optimization of Cr (VI) Removal

Criteria	Lower Limit	Upper Limit	Goal
Initial biosorbent dosage (g)	2	4	Minimize
pH	2	6	In range
Removal percentage (%)	66.4	100	Maximize

Table 4.13: Constraints and Goals of Numerical Optimization of Ni (II) Removal

Criteria	Lower Limit	Upper Limit	Goal
Initial biosorbent dosage (g)	2	4	Minimize
pH	4	8	In range
Removal percentage (%)	69.13	100	Maximize

Based on the constraint and goals shown in Table 4.12 and Table 4.13, it can be seen that the removal percentage of heavy metal ion was desired to reach maximum while maintaining initial biosorbent dosage at minimum and pH in range. Once optimize, a series of solutions that falls within these constraints was generated as shown in Table 4.14 and Table 4.15. Table 4.14 represents a total of 8 solutions for Cr (VI) removal with desirability ranging from 0.329 to 0.999 and removal percentage ranging from 90.070 % to 100.000 %. Meanwhile, Table 4.15 represents a total of 5 solutions with desirability ranging from 0.460 to 0.868 that offers removal percentage of Ni (II) ranging from 79.419 % to 92.415 %.

Table 4.14: Solution of Numerical Optimization of Cr (VI) Removal

No.	Initial biosorbent dosage (g)	pH	Removal percentage (%)	Desirability
1	2.000	5.000	99.947	0.999
2	2.011	3.000	100.000	0.998
3	2.056	4.000	100.000	0.989
4	2.000	2.000	97.726	0.957
5	2.000	6.000	96.568	0.935
6	3.522	2.000	90.070	0.470
7	3.881	5.000	100.000	0.347
8	3.897	4.000	100.000	0.329

Table 4.15: Solution of Numerical Optimization of Ni (II) Removal

No.	Initial biosorbent dosage (g)	pH	Removal percentage (%)	Desirability
1	2.000	7.000	92.415	0.868
2	2.000	6.000	88.239	0.787
3	2.000	5.000	85.049	0.718
4	2.000	4.000	79.419	0.577
5	2.931	8.000	81.332	0.460

From Table 4.14, solution 2 was chosen as the optimum solution for the removal of Cr (VI) ion with initial biosorbent dosage of 2.011 g and pH value 3 to yield complete removal percentage of Cr (VI). The optimal solution was chosen based on the main goal of the study which was the percentage removal percentage of heavy metal ion. Solution 2 provides the highest removal percentage (100 %) at higher desirability of 0.998. Another aspect to consider was the initial biosorbent dosage, where solution 2 requires almost the least amount of biosorbent to achieve highest removal efficiency. As a supporting factor, pH 3 that was included in the solution correlates with the optimum pH recorded in the literature review. The optimum pH value obtained falls close to the value obtained in the study of Cherdchoo, Nithettham and Charoenpanich

(2019) and Nigam, et al. (2019). Hence, solution 2 falls under the feasible range of adsorption condition.

From Table 4.15, solution 1 was selected as the optimum solution for the removal of Ni (II) ion with initial biosorbent dosage of 2.000 g and pH 7 to yield a maximum removal percentage of 92.415 %. Based on the solution 1 provides the highest removal percentage at the desirability of 0.868 which was a fairly high value. Thus, the desirability of the solution does not range far from zero outside of the limits to the goal (StatEase, 2020). In comparison, none of the other solution able to achieve removal efficiency of more than 86 % as given in solution 1. In addition, the low desirability function value of the other solutions also indicates that the solution falls far from the limits of the goal. Besides, solution 1 also offers the least amount of initial biosorbent dosage to achieve highest removal efficiency. As another supporting factor, pH value of 7 that was included in the solution correlates with the optimum pH recorded in the literature review of the previous studies involving Cr (VI) by biosorbents where the optimum pH falls within 6 to 8 (Singh, H., 2013). The pH value obtained falls close to the value obtained in the study of Malakahmad, Tan and Yavari (2016) and Malkoc and Nuhoglu (2005). Hence, solution 1 was decided to be the feasible and optimal adsorption condition for the removal of Ni (II) ion. The summary of the optimum condition generated by Design Expert Software for the removal of Cr (VI) and Ni (II) ions were shown in Table 4.16.

Table 4.16: Summary of Optimized Condition Generated from Design Expert for the Removal of Cr (VI) and Ni (II)

Criteria	Cr (VI)	Ni (II)
A: Initial biosorbent dosage (g)	2.011	2.000
B: pH	3.000	7.000
Response: Removal percentage (%)	100.00	92.42
Desirability Reliability	0.998 0.9075	0.868 0.9452

4.5 Characterisation of Green Tea Leaves

Various characterisation tests were performed on exhausted jasmine green tea leaves to study the physical and chemical changes in relative to the heavy metal uptake of the biosorbent. Characterisation study such as SEM-EDX, XRD and FTIR were performed and discussed in the upcoming section. The results attained were compared with literatures findings to check for any abnormalities and discrepancies of the results.

4.5.1 Scanning Electron Microscopy- Energy Dispersive X-ray Spectroscopy (SEM-EDX)

The surface morphology of an adsorbent can be well displayed through Scanning Electron Microscopy (SEM). This analysis was performed on exhausted jasmine green tea leaf powder with particle size less than 350 μm . The green tea leaf powder was examined before and after adsorption of heavy metal ions (Cr (VI) and Ni (II)). This test aims to identify any changes in the surface topology or composition of the biosorbent prior to adsorption. The analysis was performed with a working distance of 6800 μm , accelerating voltage of 15.0 kV and magnification ranging from 1000x to 2700x, which ever that was able to provide clear and detailed representation of the biosorbent surface. Figure 4.12 illustrates the SEM micrographs of exhausted jasmine green tea leaf powder before adsorption while Figure 4.13 and Figure 4.14 represents the SEM micrographs after adsorption of Cr (VI) and Ni (II) respectively.

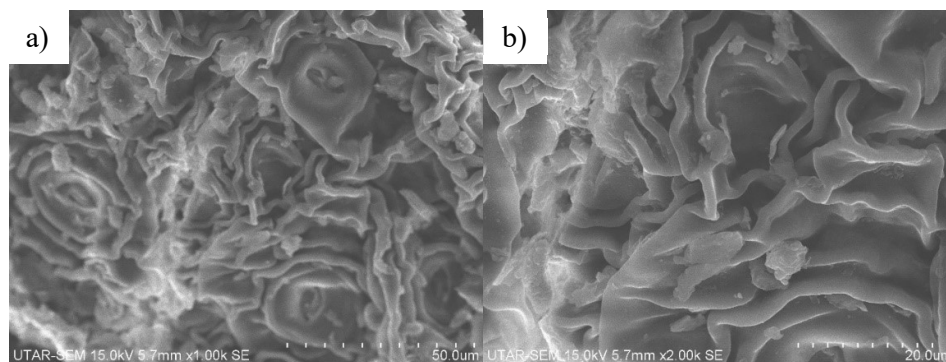


Figure 4.12: SEM Images of Jasmine Green Tea Leaves Before Adsorption at a) 1000x and b) 2000x Magnification.

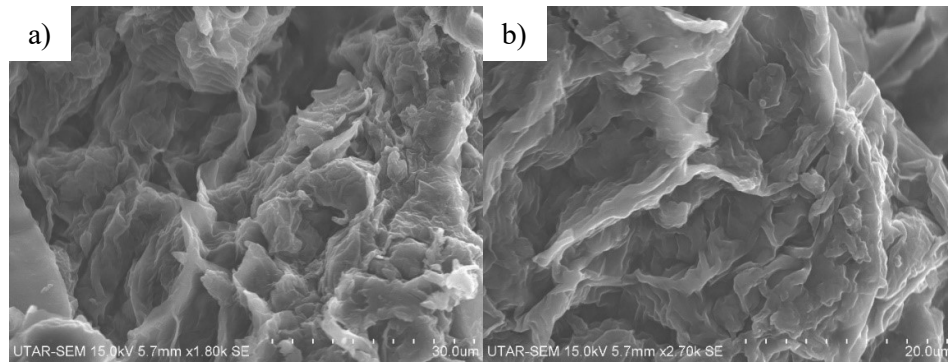


Figure 4.13: SEM Images of Jasmine Green Tea Leaves After Adsorption of Cr (VI) ions at a) 1800x and b) 2700x Magnification.

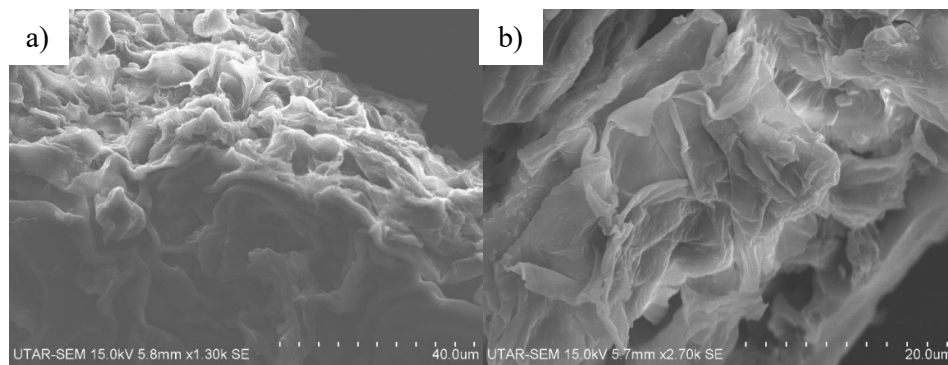


Figure 4.14: SEM Images of Jasmine Green Tea Leaves After Adsorption of Ni (II) ions at a) 1300x and b) 2700x Magnification.

In Figure 4.12, the SEM micrograph of virgin jasmine green tea leaf displays uneven and rough surface that depicts large volume of asymmetric pores on the surface of the adsorbent. These porous structures were deemed to have large internal surface area with abundant adsorption sites which could offer higher biosorption rate (Harikishore Kumar, Ramana, Sessaiah and Reddy, 2011). This supports the metal uptake capacity of green tea leaves that has been recorded earlier in the pre-screening stage. The larger area of adsorption sites allows high amount of metal ions to efficiently adhere on to the adsorbent. This can be clearly seen in Figure 4.13 and Figure 4.14 where prior to adsorption, the total pores volume of the biosorbent surface have significantly reduced. A smoother surface was formed covered with brighter and shiny coating, indicates the presence of heavy metals (Venugopal, Mohanty and Kaustubha, 2011).

The presence of Ni (II) and Cr (VI) ions on the green tea leaf surface were validated with EDX spectroscopy as shown in Table 4.18 and Table 4.19 respectively. While, Table 4.17 depicts the composition of virgin jasmine green tea leaves before adsorption of heavy metal ions. The EDX results are displayed in Appendix H.

Table 4.17: Energy Dispersive X-ray (EDX) Microanalysis Report of Virgin Jasmine Green Tea Leaves

Element	Weight, Wt. (%)	After Matrix, At (%)
Carbon (<i>CK</i>)	50.50	57.21
Nitrogen (<i>NK</i>)	05.78	05.62
Oxygen (<i>OK</i>)	43.71	37.17

Table 4.18: Energy Dispersive X-ray (EDX) Microanalysis Report of Jasmine Green Tea Leaves After Adsorption of Cr (VI)

Element	Weight, Wt. (%)	After Matrix, At (%)
Carbon (<i>CK</i>)	62.44	68.64
Nitrogen (<i>NK</i>)	04.84	04.56
Oxygen (<i>OK</i>)	32.37	26.71
Chromium (<i>CrK</i>)	00.35	00.09

Table 4.19: Energy Dispersive X-ray (EDX) Microanalysis Report of Jasmine Green Tea Leaves After Adsorption of Ni (II)

Element	Weight, Wt. (%)	After Matrix, At (%)
Carbon (<i>CK</i>)	41.68	54.13
Nitrogen (<i>NK</i>)	02.04	01.38
Oxygen (<i>OK</i>)	40.60	39.58
Nickel (<i>NiK</i>)	02.02	00.54

Table 4.18 indicates the presence of the Cr (VI) at about (00.35 %) in the jasmine green tea leaves after adsorption process. Meanwhile, Table 4.19 confirms the presence Ni (II) at about (02.02 %) in the jasmine green tea leaves after adsorption process. Although, the detected value of the weight percentage

of heavy metals on the biosorbent surface was not an accurate representation of the actual value, this ultimately confirmed the adsorption of heavy metal ions on the green tea leaves. Based on Table 4.17, it was observed that virgin jasmine green tea leaf was composed of high amount of carbon, calcium and oxygen on its surface (Nigam, et al., 2019). Based on the results, jasmine green tea leaves exhibit high adsorption efficiency due to its rich content of carbon and calcium as similar to activated carbon (Malakahmad, Tan and Yavari, 2016).

4.5.2 Fourier Transform Infrared Spectroscopy (FTIR)

The raw jasmine green tea leaves along with the green tea leaves collected prior to the adsorption of Cr (VI) and Ni (II) were analysed with Fourier Transformed Infrared (FTIR) using Perkin Elmer Spectrum RXI spectrophotometer. The biosorbent were studied before and after adsorption to identify the presence of functional group on the biosorbent surface that could in any manner interact with the heavy metal ions during adsorption. Analysis of FTIR spectrum of biosorbent on the shift of peaks indicated the functional group involved in the adsorption process have bonded with heavy metal ions (Malakahmad, Tan and Yavari, 2016). The functional group and their respective wavenumber of FTIR were shown in Table 4.20. The FTIR spectrum was measured in wavelength range of 600 - 4000 cm^{-1} . Hence, a plot of transmittance (%) against wavelength (cm^{-1}) for raw green tea leaves, after adsorption of Ni (II) and after adsorption of Cr (VI) was displayed in Figure 4.15 (a), 4.15 (b) and 4.15 (c) respectively.

Based on Figure 4.15 (a), several peaks were undergoing peak shift for biosorbent after adsorption process, compared to virgin biosorbent. Each peak represents a single or complex functional group. The difference in peak wavelength observed was listed in Table 4.17. The peaks of 3287.91 cm^{-1} , 2917.65 cm^{-1} , 2849.68 cm^{-1} , 1734.05 cm^{-1} , 1617.67 cm^{-1} and 1027.05 cm^{-1} have been spotted in the FTIR spectrum of raw biosorbent. The strong and broad band at 3287.91 cm^{-1} represents a strong band of hydroxyl (O-H) group (Nigam, et al., 2019). The band observed at 2917.65 cm^{-1} and 2849.68 cm^{-1} could be assigned to aliphatic compounds with (C-H) stretch (Cherdchoo, Nithettham and Charoenpanich 2019). While, the band at 1734.05 cm^{-1} showed (C-O-C) stretching in polysaccharides ether functional group (Senthilkumar and

Sivakumar, 2014). The peak at 1617.67 cm^{-1} might be caused by (C=C) stretch in aromatic ring and (C=O) stretch in polyphenols (Malkoc and Nuhoglu, 2005). Lastly, the steep and strong peak at 1027.05 cm^{-1} could be assigned to (C-OH) stretching vibration of carboxylic acid and alcohol (Nigam, et al., 2019). On overall, it can be deduced that green tea leaves were rich in polysaccharides, polyphenols, carboxylic acid and amines.

After adsorption of Ni (II) ions, Figure 4.15 (b) shows the shift in peaks of 3287.91 cm^{-1} , 1734.05 cm^{-1} and 1617.67 cm^{-1} to 3305.83 cm^{-1} , 1732.09 cm^{-1} and 1619.08 cm^{-1} . This indicates that hydroxyl (O-H) group, carbonyl (C=O) and ether (C-O-C) group were involved in the adsorption of Ni (II) ions. Other than that, Figure 4.15 (c) shows the shift in peaks of 3287.91 cm^{-1} , 2917.65 cm^{-1} , 1734.05 cm^{-1} , 1617.67 cm^{-1} and 1027.05 cm^{-1} to 3292.30 cm^{-1} , 2918.79 cm^{-1} , 1730.89 cm^{-1} , 1624.38 cm^{-1} and 1025.34 cm^{-1} , after adsorption of Cr (VI) ions. Hence, hydroxyl (O-H) group, alkene (C=C), carbonyl (C=O), aliphatic group (C-H), carboxyl (C-OH) and ether (C-O-C) were involved in Cr (VI) uptake (Nigam, et al., 2019). In addition, possible stretching in vibrations of (C-H) group on the green tea leaf surface can also be noted. The shifting of peaks and stretching of bands observed after heavy metal loading can be attributed to the changes in ionic functional group caused by the counter ions (Ni (II) and Cr (VI)), supporting their contribution towards metal adsorption (Sanusi, et al., 2018). Jasmine green tea is composed of high amount of oxygenated functional group such as hydroxyl (O-H), carbonyl (C=O), ether (C-O-C) and carboxyl (C-OH) group (Malakahmad, Tan and Yavari, 2016). These functional group observed to be involved in the uptake of Ni (II) and Cr (VI), demonstrates that the adsorption can be expressed as physical adsorption supported by electrostatic columbic forces between oxygenated functional group and heavy metal ions (Malakahmad, Tan and Yavari, 2016).

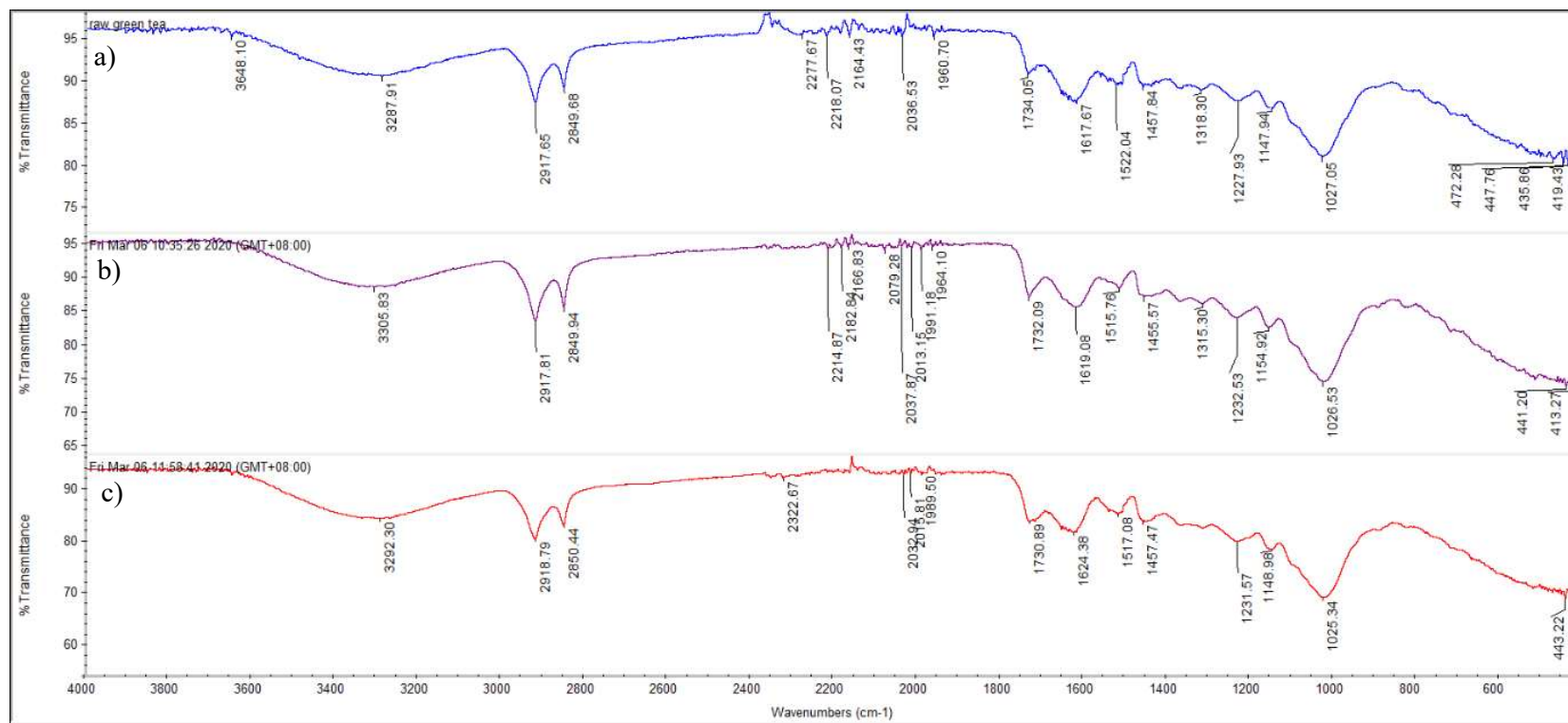


Figure 4.15: Fourier Transformed Infrared (FTIR) Spectra of Jasmine Green Tea Leaves Before and After Adsorption (a)Raw, (b) After adsorption of Ni (II) and (c) After adsorption of Cr (VI).

Table 4.20: Fourier Transformed Infrared (FTIR) Peak Wavelengths with Respective Functional Groups

Raw Jasmine Green Tea Leave	Wavenumber (cm ⁻¹)		Bond		Functional Group	Reference
	Ni (II) Loaded	Band Difference	Cr (VI) Loaded	Band Difference		
3287.91	3305.83	-17.92	3292.30	-4.39	O-H stretching, H-bonding	Alcohol, phenols and amines (Nigam, et al., 2019); (Senthilkumar and Sivakumar, 2014)
2917.65	2917.81	-0.16	2918.79	-1.14	C-H stretching	Alkanes (Senthilkumar and Sivakumar, 2014)
2849.68	2849.94	-0.26	2850.44	-0.76		
1734.05	1732.09	1.96	1730.89	3.16	C-O-C stretch	Ethers (Senthilkumar and Sivakumar, 2014)
1617.67	1619.08	-1.41	1624.38	-6.71	C=C and C=O stretching	Alkenes and carbonyl (Malkoc and Nuhoglu, 2005)
1027.05	1026.53	0.52	1025.34	1.71	C-OH stretching	Carboxylic acid, alcohol and aliphatic amines (Nigam, et al., 2019)

4.5.3 X-ray Diffraction (XRD)

The exhausted jasmine green tea leaves were examined with X-ray Diffraction (XRD) in angle range of 10 - 70° at a rotation speed of 2° per minute using Cu K α spectral line at 40 kV. The biosorbent were analysed before and after adsorption of Cr (VI) and Ni (II) ions using X-ray diffractometer. The aim of the analysis was to study the changes of crystalline structure of the biosorbent. The presence of heavy metals on the biosorbent surface were generally identified through the changes in X-ray diffraction patterns of the raw green tea leaves after adsorption process (Cai, et al., 2015). A plot of X-ray diffracted intensities against the rotation angle of the samples was measured and recorded. Figure 4.16, Figure 4.17 and Figure 4.18 depicts the X-ray diffraction pattern of raw jasmine green tea, Cr (VI) loaded jasmine green tea and Ni (II) loaded jasmine green tea respectively. The XRD raw data is displayed in Appendix I. The crystallinity of the biosorbent was evaluated quantitatively based on the peak height or peak area observed from the diffraction patterns.

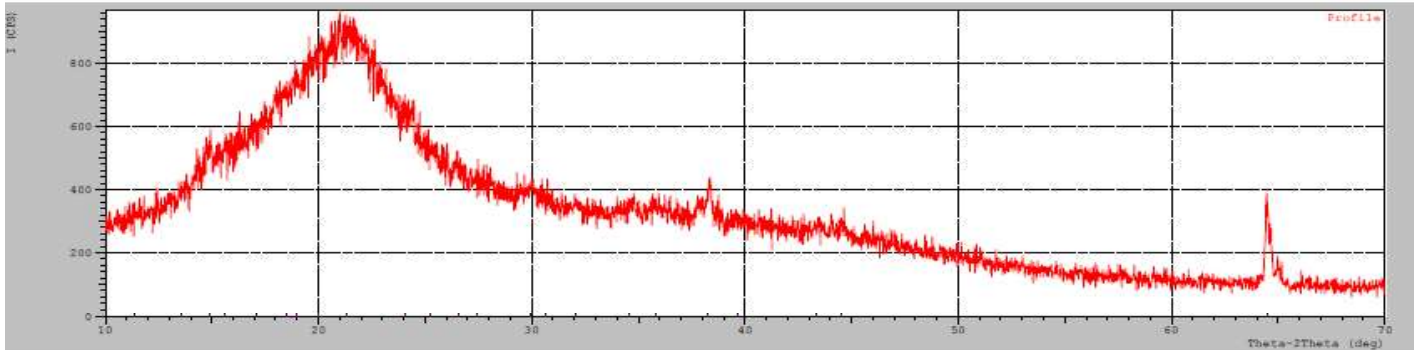


Figure 4.16: XRD Spectra of Raw Jasmine Green Tea Leaves.

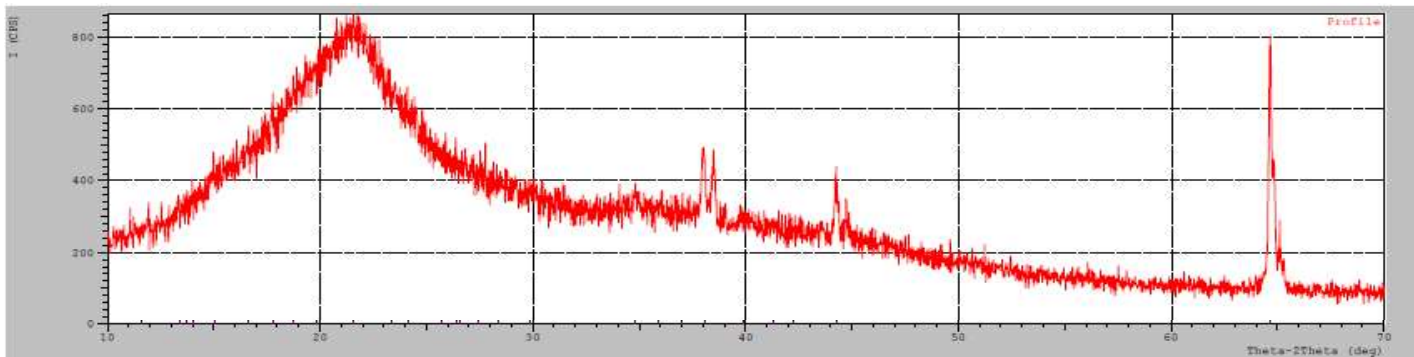


Figure 4.17: XRD Spectra of Jasmine Green Tea Leaves After Adsorption of Cr (VI) ions.

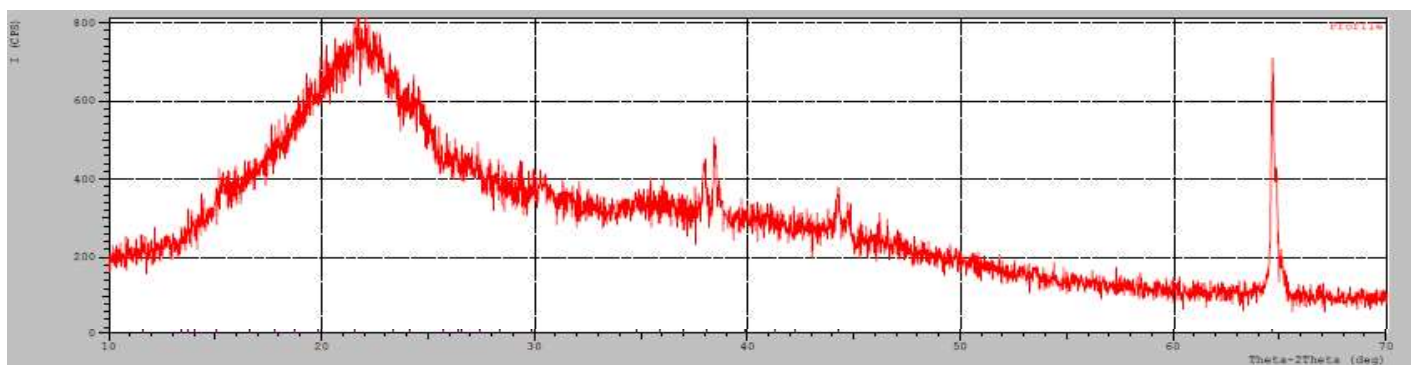


Figure 4.18: XRD Spectra of Jasmine Green Tea Leaves After Adsorption of Ni (II) ions.

Based on Figure 4.16, XRD profile shows a broad peak around $2\theta = 21.3400^\circ$ but without any sharp peaks with one or two sharp peaks with low intensity. This indicates that raw green tea leaves had a less crystalline structure. The majority of the species present in the green tea leaves were amorphous. Amorphous materials were said to be filled with large volume of active sites rendering higher metal uptake capacity (Cai, et al., 2015). In addition, the presence of broad peak at $2\theta = 21.3400^\circ$, could be associated with the organic functional group of related to lignin and cellulose that were widely present in most tea leaves (Lin, et al., 2020).

Based on Figure 4.17, a distinct peak at 2θ of 64.6382° has been observed on green tea leaves after the adsorption of Cr (VI) ions. While, Figure 4.18 showed a distinct peak at 2θ of 64.6312° has been observed on green tea leaves after the adsorption of Ni (II) ions.

When a specific foreign element presents on a surface, the changes in X-ray diffraction pattern of the biosorbent will decide the crystallinity of the element. In this case, both Cr (VI) and Ni (II) loaded green tea samples showed distinct peaks at $2\theta = 64.6382^\circ$ and 64.6312° , respectively. This strongly suggests that these heavy metal adsorption on to the biosorbent has distorted the amorphous structure of the virgin jasmine green tea leaves into crystalline structure (Shrestha, et al., 2016).

The crystallite size of the XRD raw data obtained through Debye Scherrer's equation according to Eqn. 3.2, are shown in Table 4.21, 4.22 and 4.23. The sample calculation to obtain crystallite size for peak No.9 of virgin jasmine green tea was shown in Appendix J. Table 4.21, 4.22 and 4.23 represent the crystallite size calculated from the 2θ (deg) and FWHM (deg) obtained from the three most significant peaks of XRD raw data. Table 4.21 representing virgin jasmine green tea XRD analysis, showed average crystallite size of 2.1109 nm. However, the average crystallite size showed massive increase after the adsorption of Cr (VI) and Ni (II) ions which showed crystallite size of 13.7927 nm and 58.8390 nm, respectively. This proves that the surface area of the virgin jasmine green tea has showed significant decrease after the biosorption of heavy metals (Singh, et al., 2020). Besides the phase change from

amorphous to crystalline structure, the decrease in surface area caused by the increase in crystallite size, further confirms that adsorption has taken place.

Table 4.21: Crystallite Size of Virgin Jasmine Green Tea

No	Peak No.	2 Theta, 2θ (deg)	2 Theta, 2θ (rad)	FWHM (deg)	FWHM (rad)	Crystallite size (nm)
1	9	21.24	0.3707	4	0.0698	2.1109
2	8	20.02	0.3494	0	0	0
3	7	18.98	0.3313	0	0	0
Average						2.1109

Table 4.22: Crystallite Size of Jasmine Green Tea After Adsorption of Cr (VI)

No	Peak No.	2 Theta, 2θ (deg)	2 Theta, 2θ (rad)	FWHM (deg)	FWHM (rad)	Crystallite size (nm)
1	10	21.54	0.3759	0	0	0
2	27	64.6328	1.1280	0.6036	0.0105	13.7927
3	9	19.88	0.3470	0	0	0
Average						13.7927

Table 4.23: Crystallite Size of Jasmine Green Tea After Adsorption of Ni (II)

No	Peak No.	2 Theta, 2θ (deg)	2 Theta, 2θ (rad)	FWHM (deg)	FWHM (rad)	Crystallite size (nm)
1	14	64.7105	1.1294	0.16	0.002792	61.3895
2	11	38.0513	0.6641	0.1583	0.002763	55.4442
3	13	44.2986	0.7732	0.1501	0.002620	59.6833
Average						58.8390

CHAPTER 5

CONCLUSION AND RECOMMENDATIONS

5.1 Conclusion

In this study, the jasmine green tea leaves, genmaicha green tea leaves, salted peanut shells and unsalted peanut shells were screened for the biosorbent efficiencies in removing two hazardous heavy metal ions (Cr (VI) and Ni (II)) in aqueous solution. Based on the results obtained, jasmine green tea leaves emerged as the most effective biosorbent with the highest affinity towards Cr (VI) and Ni (II) ions where removal percentage of 90.98 % and 96.13 % respectively had been recorded. Therefore, jasmine green tea leaf was selected to be used as optimum biosorbent in the study to determine the effects of initial biosorbent dosage and initial pH of aqueous solution on the removal percentage of Cr (VI) and Ni (II) ions. In overall, the removal percentage of those heavy metal ions increased initially with the increased in biosorbent dosage and pH and decreased after reaching the optimum point.

Hence, the initial biosorbent dosage and initial pH of aqueous solution are declared as the dominant parameters affecting the removal percentage of Cr (VI) and Ni (II) ions by jasmine green tea leaves. The optimal condition for the removal of Cr (VI) ions are at pH 3 with initial biosorbent dosage of 2.011 g. Meanwhile, optimal condition for the removal of Ni (II) ions are at pH 7 with initial biosorbent dosage of 2.000 g. Under optimum operating conditions, the maximum removal percentage of Cr (VI) and Ni (II) ions by jasmine green tea leaves can be reach at 100.00 % and 92.415 %, respectively. SEM-EDX analysis showed that after adsorption, the surface porosity on the biosorbent surface was reduced and covered with shiny coating of heavy metals after adsorption. The presence of Cr and Ni on the biosorbent surface by elemental identification confirmed that after adsorption of heavy metal ions by jasmine green tea leaves had successfully occurred. The FTIR analysis exhibited that the functional hydroxyl (O-H) group, carbonyl (C=O) and ether (C-O-C) group were involved in the biosorption of Ni (II) ions while hydroxyl (O-H) group, alkene (C=C), carbonyl (C=O), aliphatic group (C-H), carboxyl (C-OH) and ether (C-O-C)

contributed to the adsorption of Cr (VI). From XRD analysis, the amorphous surface of virgin jasmine green tea leaves had been distorted into crystalline structure after adsorption of Cr (VI) and Ni (II) ions.

5.2 Recommendations for Future Work

The main goal of the current study was to identify the most efficient biosorbent for the removal of Ni (II) and Cr (VI) ions and to optimize the biosorption condition statistically using Design Expert Software. However, due to time constraint and sample limitations, only the effects of initial biosorbent dosage and initial pH of aqueous solution were studied. Therefore, it was recommended to include contributing adsorption parameters such as initial concentration of heavy metal ions, contact time, temperature and agitation speed in the future work. In this way, a higher level of factorial design with multiple independent variables can be developed to further enhance the accuracy of the biosorption condition through optimization.

In addition, the effect of initial biosorbent dosage of the removal percentage of Ni (II) and Cr (VI) ions are studied by varying the dosage from 2 g to 4 g. In majority of the combination, almost complete removal of Cr (VI) ions can be seen, despite higher levels of pH (6). This clearly indicates that, the biosorbent dosage provided to 50 mL of Cr (VI) with 80 mg/L concentration was excessive. While, almost complete removal can be achieved even at the lowest biosorbent dosage limit of 2 g, the future studies can focus on the effects of initial biosorbent dosage less than 2g.

Other than that, kinetic study of using several kinetic models such pseudo-first order and pseudo-second order can be used to determine the biosorption mechanism. The study was performed on time dependency, where the equilibrium biosorption capacity was recorded at varying contact period and fitted to the kinetic plots. In the meantime, the pH, initial biosorbent dosage and agitation speed of the biosorption process are maintained at fixed value. Based on the rate constant, k obtained from the kinetic plots, the value of activation energy, E_a was calculated (Taşar, Kaya and Özer, 2014). Then, the value of activation energy, E_a correlated with the adsorption mechanism that has been observed.

Besides that, the study of isotherm to describe the biosorption equilibrium can also be included. Generally, the biosorption equilibrium data obtained from batch experiments are fitted to the isotherm models to identify the distribution of adsorbate molecules between the liquid phase (aqueous solution) and the solid phase (adsorbent). A graph of equilibrium adsorption capacity, q_e against equilibrium heavy metal concentration, C_e was plotted under constant pH and temperature. The experimental data are fitted to the isotherm models using the method of linear least-squares regression. For a single solute system, the two widely accepted and studied equilibrium adsorption isotherm models are Langmuir and Freundlich models (Ahalya, Ramachandra, and Kanamad, 2005). The properties of the adsorption are determined by correlating data obtained from experimentation into Langmuir and Freundlich isotherm models while the best fitted model can be said to be well describe the adsorption. To study the behavior of the adsorption through isotherm studies, the batch biosorption process have to be performed with varying initial concentration of heavy metal ions at fixed optimum pH, temperature and initial biosorbent dosage (Witek-Krowiak, Szafran and Modelski, 2011). The equilibrium adsorption capacity, $Q_{e,exp}$ obtained from experimental data was compared with equilibrium adsorption capacity, $Q_{e,cal}$ obtained from the isotherm model. The best fitted model can be expressed through the identification of correlation coefficient (R^2). The correlation coefficient ranges from 0 to 1. The closer the value of R^2 to 1, the well fitted the data to the isotherm models.

REFERENCES

Abdel Ghani, N.T. and El Chaghaby, G.A., 2014. Biosorption for metal ions removal from aqueous solutions: A review of recent studies. *International Journal of Latest Research in Science and Technology*, [online] Available at: <<http://www.mnkjournals.com/ijlrst.htm>> [Accessed 15 July 2019].

Abdolali, A., Ngo, H.H., Guo, W., Lu, S., Chen, S.S., Nguyen, N.C., Zhang, X., Wang, J. and Wu, Y., 2016. A breakthrough biosorbent in removing heavy metals: Equilibrium, kinetic, thermodynamic and mechanism analyses in a lab-scale study. *Science of the Total Environment*, 542, pp.603–611.

Ahalya, N., Kanamadi, R. D. and Ramachandra, T. V., 2005. Biosorption of chromium (VI) from aqueous solutions by the husk of Bengal gram (*Cicer arietinum*), *Electronic J Biotechnol*, 8, pp.258-264.

Amarasinghe, B.M.W.P.K. and Williams, R.A., 2007. Tea waste as a low cost adsorbent for the removal of Cu and Pb from wastewater. *Chemical Engineering Journal*, 132(1–3), pp.299–309.

Cai, H.M., Chen, G.J., Peng, C.Y., Zhang, Z.Z., Dong, Y.Y., Shang, G.Z., Zhu, X.H., Gao, H.J. and Wan, X.C., 2015. Removal of fluoride from drinking water using tea waste loaded with Al/Fe oxides: A novel, safe and efficient biosorbent. *Applied Surface Science*, pp.34–44.

Cherdchoo, W., Nithettham, S. and Charoenpanich, J., 2019. Removal of Cr(VI) from synthetic wastewater by adsorption onto coffee ground and mixed waste tea. *Chemosphere*, 221, pp.758–767.

Connor, S., 2020. *How-To: Analyse A 2-Level Factorial Design Using Design-Expert 10 Software | Prism*. [online] Available at: <<https://www.prismtc.co.uk/resources/blogs-and-articles/how-to-analyse-a-2-level-factorial-design-using-design-expert-10-software>> [Accessed 29 March 2020].

Daneshfozoun, S., Abdullah, M.A. and Abdullah, B., 2017. Preparation and characterization of magnetic biosorbent based on oil palm empty fruit bunch fibers, cellulose and *Ceiba pentandra* for heavy metal ions removal. *Industrial Crops and Products*, 105, pp.93–103.

Department of Environment, 2010. *Environmental Requirements: A Guide For Investors*. 11th ed. Putrajaya, Malaysia: Ministry of Natural Resources and Environment, pp.62.

El-Naggar, N.E.A., Hamouda, R.A., Mousa, I.E., Abdel-Hamid, M.S. and Rabei, N.H., 2018. Biosorption optimization, characterization, immobilization and application of *Gelidium amansii* biomass for complete Pb²⁺ removal from aqueous solutions. *Scientific Reports*, 8(1), pp.1–19.

Flores-Garnica, J.G., Morales-Barrera, L., Pineda-Camacho, G. and Cristiani-Urbina, E., 2013. Biosorption of Ni(II) from aqueous solutions by Litchi chinensis seeds. *Bioresource Technology*, 136, pp.635–643.

Gadd, G.M., 1993. Interactions of fungi with toxic metals. *Phytologist*, 124, pp.25–60.

Garg, U.K., Kaur, M.P., Garg, V.K. and Sud, D., 2007. Removal of hexavalent chromium from aqueous solution by agricultural waste biomass. *Journal of Hazardous Materials*, 140(1–2), pp.60–68.

Gautam, R.K., Sharma, S.K., Mahiya, S. and Chattopadhyaya, M.C., 2014. CHAPTER 1. Contamination of Heavy Metals in Aquatic Media: Transport, Toxicity and Technologies for Remediation. *Heavy Metals In Water*, pp.1–24.

Gonen, F. and Serin, D.S., 2012. Adsorption study on orange peel: Removal of Ni(II) ions from aqueous solution. *African Journal of Biotechnology*, 11(5), pp.1250–1258.

Gunatilake, S.K., 2015. Methods of Removing Heavy Metals from. *Journal of Multidisciplinary Engineering Science Studies Industrial Wastewater*, 1(1), pp.13–18.

Harminder Singh, 2011. Adsorption of Nickel from aqueous solutions using low cost bio-waste adsorbents. *Water Quality Research Journal of Canada*.

HORIBA. n.d. *Performances In ICP-OES*. [online] Available at: <https://www.horiba.com/en_en/icp-oes-performances/> [Accessed 30 March 2020].

Ifthikar, J., Wang, T., Khan, A., Jawad, A., Sun, T., Jiao, X., Chen, Z., Wang, J., Wang, Q., Wang, H. and Jawad, A., 2017. Highly Efficient Lead Distribution by Magnetic Sewage Sludge Biochar: Sorption Mechanisms and Bench Applications. *Bioresource Technology*, 238, pp.399–406.

Jmp.com. 2020. *Full Factorial Designs. Statistical Discovery*. [online] Available at: <<https://www.jmp.com/support/help/14-2/full-factorial-designs.shtml>> [Accessed 18 March 2020].

José, A.F.-L., José, M.A. and María, D.A., 2014. Biosorption of Hexavalent Chromium from Aqueous Medium with Opuntia Biomass. *The Scientific World Journal*, 2014, pp.670249.

Joseph, L., Jun, B.M., Flora, J.R.V., Park, C.M. and Yoon, Y., 2019. Removal of heavy metals from water sources in the developing world using low-cost materials: A review. *Chemosphere*, 229, pp.142–159.

Joshi, N.C., 2017. Heavy metals, conventional methods for heavy metal removal, biosorption and the development of low cost adsorbent. *European Journal of Pharmaceutical and Medical Research*, [online] Available at: <http://www.ejpmr.com/admin/assets/article_issue/1485854916.pdf> [Accessed 2 August 2019].

Kaya, K., Pehlivan, E., Schmidt, C. and Bahadir, M., 2014. Use of modified wheat bran for the removal of chromium(VI) from aqueous solutions. *Food Chemistry*, 158, pp.112–117.

Lin, D., Wu, F., Hu, Y., Zhang, T., Liu, C., Hu, Q., Hu, Y., Xue, Z., Han, H. and Ko, T.H., 2020. Adsorption of Dye by Waste Black Tea Powder: Parameters, Kinetic, Equilibrium, and Thermodynamic Studies. *Journal of Chemistry*, 2020.

Malakahmad, A., Tan, S. and Yavari, S., 2016. Valorization of Wasted Black Tea as a Low-Cost Adsorbent for Nickel and Zinc Removal from Aqueous Solution. *Journal of Chemistry*, 2016.

Malkoc, E. and Nuhoglu, Y., 2005. Investigations of nickel (II) removal from aqueous solutions using tea factory waste. 127, pp.120–128.

Naskar, A., Guha, A.K., Mukherjee, M. and Ray, L., 2016. Adsorption of nickel onto *Bacillus cereus* M116: A mechanistic approach. *Separation Science and Technology (Philadelphia)*, 51(3), pp.427–438.

Nguyen, T.A.H., Ngo, H.H., Guo, W.S., Zhang, J., Liang, S., Yue, Q.Y., Li, Q. and Nguyen, T. V., 2013. Applicability of agricultural waste and by-products for adsorptive removal of heavy metals from wastewater. *Bioresource Technology*, 148, pp.574–585.

Nigam, M., Rajoriya, S., Rani Singh, S. and Kumar, P., 2019. Adsorption of Cr (VI) ion from tannery wastewater on tea waste: Kinetics, equilibrium and thermodynamics studies. *Journal of Environmental Chemical Engineering*. [online] Available at: <<https://linkinghub.elsevier.com/retrieve/pii/S2213343719303112>> [Accessed 19 July 2019].

Nist.gov. 2020. 5.3.3.3.2. *Full Factorial Example*. [online] Available at: <<https://www.itl.nist.gov/div898/handbook/pri/section3/pri3332.htm>> [Accessed 29 March 2020].

Park, D., Yun, Y. S. and Park, J. M., 2010. The past, present, and future trends of biosorption. *Biotechnol Bioproc E*, 15, 86–102.

Pehlivan, E. and Altun, T., 2008. Biosorption of chromium(VI) ion from aqueous solutions using walnut, hazelnut and almond shell. *Journal of Hazardous Materials*, 155(1–2), pp.378–384.

Pieper, D.H. and Reineke, W., 2000. Engineering bacteria for bioremediation. *Current Opinion in Biotechnology*, 11(3), pp.262–270.

Raval, N.P., Shah, P.U. and Shah, N.K., 2016. Adsorptive removal of nickel(II) ions from aqueous environment: A review. *Journal of Environmental Management*, 179, pp.1–20.

Reddy, D.H.K., Ramana, D.K.V., Sessaiah, K. and Reddy, A.V.R., 2011. Biosorption of Ni(II) from aqueous phase by Moringa oleifera bark, a low cost biosorbent. *Desalination*, 268(1–3), pp.150–157.

Sadeek, S.A., Negm, N.A., Hefni, H.H.H. and Abdel Wahab, M.M., 2015. Metal adsorption by agricultural biosorbents: Adsorption isotherm, kinetic and biosorbents chemical structures. *International Journal of Biological Macromolecules*, 81, pp.400–409.

Sanusi, K.A., Sunday, N.S., Hassan, M.S. and Abdulqadir, T.A., 2018. The effect of operational parameters on biosorption of Cd²⁺, Ni²⁺ and Cr⁶⁺ using Glycine max pod (Soya Bean). *Environmental Risk Assessment and Remediation*, 02(02).

Sarin, V. and Pant, K.K., 2006. Removal of chromium from industrial waste by using eucalyptus bark. *Bioresource Technology*, 97(1), pp.15–20.

Senthil Kumar, P.S., Ramalingam, S., Kirupha, S.D., Murugesan, A., Vidhyadevi, T. and Sivanesan, S., 2011. Adsorption behavior of nickel(II) onto cashew nut shell: Equilibrium, thermodynamics, kinetics, mechanism and process design. *Chemical Engineering Journal*, 167(1), pp.122–131.

Shah, J., Jan, M.R., Ul Haq, A. and Zeeshan, M., 2015. Equilibrium, kinetic and thermodynamic studies for sorption of Ni (II) from aqueous solution using formaldehyde treated waste tea leaves. *Journal of Saudi Chemical Society*, [online] 19(3), pp.301–310.

Shrestha, B., Kour, J. and Ghimire, K.N., 2016. Adsorptive Removal of Heavy Metals from Aqueous Solution with Environmental Friendly Material—Exhausted Tea Leaves. *Advances in Chemical Engineering and Science*, 06(04), pp.525–540.

Singh, S., Kumar, V., Datta, S., Dhanjal, D.S., Sharma, K., Samuel, J. and Singh, J., 2020. Current advancement and future prospect of biosorbents for bioremediation. *Science of the Total Environment*, 709.

Statease.com. 2020. *Stat-Ease » VII » Adequate Precision*. [online] Available at: <<https://www.statease.com/docs/v11/navigation/adequate-precision/>> [Accessed 29 March 2020].

Sud, D., Mahajan, G. and Kaur, M.P., 2008. Agricultural waste material as potential adsorbent for sequestering heavy metal ions from aqueous solutions - A review. *Bioresource Technology*, 99(14), pp.6017–6027.

Taşar, Ş., Kaya, F. and Özer, A., 2014. Biosorption of lead(II) ions from aqueous solution by peanut shells: Equilibrium, thermodynamic and kinetic studies. *Journal of Environmental Chemical Engineering*, 2(2), pp.1018–1026.

Thevannan, A., Mungroo, R. and Niu, H.C., 2010. Biosorption of nickel with barley straw. *Bioresource Technology*, 101(6), pp.1776–1780.

Venugopal, V. and Mohanty, K., 2011. Biosorptive uptake of Cr (VI) from aqueous solutions by Parthenium hysterophorus weed: Equilibrium, kinetics and thermodynamic studies. *Chemical Engineering Journal*, [online] 174(1), pp.151–158.

Vijayaraghavan, K. and Balasubramanian, R., 2015. Is biosorption suitable for decontamination of metal-bearing wastewaters? A critical review on the state-of-the-art of biosorption processes and future directions. *Journal of Environmental Management*, 160, pp.283–296.

Volesky, B., 2001. Detoxification of metal-bearing effluents: Biosorption for the next century, *Hydrometallurgy*, 59, pp.203-216.

Volesky, B. and Holan, Z. R., 1995. Biosorption of heavy metals. *Biotechnol Prog.*, 11, pp.235–250.

Wang, J., Chen, C., 2006. Biosorption of heavy metals by *Saccharomyces cerevisiae*: a review. *Biotechnol. Adv.*, 24, pp.427-451.

Witek-Krowiak, A., Chojnacka, K., Podstawczyk, D., Dawiec, A. and Pokomeda, K., 2014. Application of response surface methodology and artificial neural network methods in modelling and optimization of biosorption process. *Bioresource Technology*, 160, pp.150–160.

Witek-Krowiak, A., Szafran, R.G. and Modelski, S., 2011. Biosorption of heavy metals from aqueous solutions onto peanut shell as a low-cost biosorbent. *Desalination*, 265(1–3), pp.126–134.

Zafar, M.N., Nadeem, R. and Hanif, M.A., 2007. Biosorption of nickel from protonated rice bran. *J. Hazard. Mater.*, 143, pp. 478–485.

APPENDICES

Appendix A: Preparation of Heavy Metal Ion Solution

The biosorption process was performed with relative biosorbents with constant metal ion concentration of 80 mg/L solution. In this study, Ni (II) solution and Cr (VI) solution were used for the biosorption of heavy metal ions. Nickel (II) sulfate hexahydrate, $\text{NiSO}_4 (\text{H}_2\text{O})_6$ and Potassium dichromate, $\text{K}_2\text{Cr}_2\text{O}_7$ salts were used to prepare 1L of Ni (II) and Cr (VI) heavy metal solution.

A. Preparation of 1 Litre of 80 mg/L (80 ppm) of Ni (II) solution

- i. Determining the percentage of Ni (II) ions in $\text{NiSO}_4 (\text{H}_2\text{O})_6$:

Given,

Molecular weight of $\text{NiSO}_4 (\text{H}_2\text{O})_6$: 154.75 g/mol

Molecular weight of Ni (II): 58.693 g/mol

$$\frac{58.693 \text{ g/mol}}{154.75 \text{ g/mol}} \times 100\% = 37.93 \% \text{ of Ni (II) ions in } \text{NiSO}_4 (\text{H}_2\text{O})_6$$

This also proves that 100 g of Nickel (ii) sulfate hexahydrate, $\text{NiSO}_4 (\text{H}_2\text{O})_6$ would consists of 37.93 g of Ni (II) ions.

- ii. Determining the mass of $\text{NiSO}_4 (\text{H}_2\text{O})_6$ required to obtain 80 mg of Ni (II):

$$100 \text{ g of } \text{NiSO}_4 (\text{H}_2\text{O})_6 \rightarrow 37.93 \text{ g of Ni (II) ions}$$

$$x \text{ mg of } \text{NiSO}_4 (\text{H}_2\text{O})_6 \rightarrow 80 \text{ mg of Ni (II) ions}$$

$$x = \frac{80 \text{ mg} \times \frac{1 \text{ g}}{1000 \text{ mg}} \times 100 \text{ g } \text{NiSO}_4 (\text{H}_2\text{O})_6}{37.93 \text{ g of Ni (II)}} = 0.2109 \text{ g } \text{NiSO}_4 (\text{H}_2\text{O})_6$$

Thus, this shows that 0.2109 g of $\text{NiSO}_4 (\text{H}_2\text{O})_6$ is required to prepare 80 mg of Ni (II) solution.

- iii. Determining the mass of $\text{NiSO}_4 (\text{H}_2\text{O})_6$ required to obtain 80 mg/L of Ni (II) in 1 litre:

$$\frac{80 \text{ mg of Ni (II) ion}}{1 \text{ Litre}} = 80 \frac{\text{mg}}{\text{L}} \approx 80 \text{ ppm Ni (II) ions}$$

Therefore, to prepare 1 litre of 80 mg/L Ni (II) solution 0.2109 g of $\text{NiSO}_4 (\text{H}_2\text{O})_6$ has to be dissolved.

B. Preparation of 1 Litre of 80 mg/L (80 ppm) of Cr (VI) solution

- i. Determining the percentage of Cr (VI) ions in Potassium dichromate, $\text{K}_2\text{Cr}_2\text{O}_7$:

Given,

Molecular weight of $\text{K}_2\text{Cr}_2\text{O}_7$: 294.19 g/mol

Molecular weight of Cr (VI): 51.996 g/mol

$$\frac{2 \times 51.996 \text{ g/mol}}{294.19 \text{ g/mol}} \times 100\% = 35.35 \% \text{ of Cr (VI) ions in } \text{K}_2\text{Cr}_2\text{O}_7$$

This also proves that 100 g of Potassium dichromate, $\text{K}_2\text{Cr}_2\text{O}_7$ would consists of 35.35 g of Cr (VI) ions.

- ii. Determining the mass of $\text{K}_2\text{Cr}_2\text{O}_7$ required to obtain 80 mg of Cr (VI):

$$100 \text{ g of } \text{K}_2\text{Cr}_2\text{O}_7 \rightarrow 35.35 \text{ g of Cr (VI) ions}$$

$$x \text{ mg of } \text{K}_2\text{Cr}_2\text{O}_7 \rightarrow 80 \text{ mg of Cr (VI) ions}$$

$$x = \frac{80 \text{ mg} \times \frac{1 \text{g}}{1000 \text{mg}} \times 100 \text{ g } \text{K}_2\text{Cr}_2\text{O}_7}{35.35 \text{ g of Cr (VI)}} = 0.2263 \text{ g of } \text{K}_2\text{Cr}_2\text{O}_7$$

- iii. Determining the mass of $K_2Cr_2O_7$ required to obtain 80 mg/L of Cr (VI) in 1 Litre:

$$\frac{80 \text{ mg of Cr (VI) ion}}{1 \text{ Litre}} = 80 \frac{\text{mg}}{\text{L}} \approx 80 \text{ ppm Cr (VI) ions}$$

Therefore, to prepare 1 litre of 80 mg/L Cr (VI) solution 0.2263 g of $K_2Cr_2O_7$ has to be dissolved.

Appendix B: Preparation of 0.1 M of 37 % HCl

- i. Determining the Molarity of 37 % HCl:

Molecular weight of HCl = 36.46 g/mol

Specific gravity of 37% HCl = 1.19 g/mL

HCl (37%) volume/volume percent = 37 mL/100 mL

$$\text{HCl Molarity (M)} = \frac{37 \text{ mL}}{100 \text{ mL}} \times \frac{1.19 \text{ g}}{\text{mL}} \times \frac{1000 \text{ mL}}{1 \text{ L}} \times \frac{\text{mol}}{36.46 \text{ g}}$$

$$\text{HCl Molarity (M)} = 12.07 \text{ mol/L}$$

- ii. Determining the volume of 37 % HCl required to prepare 500 mL of 0.1 M of HCl solution:

$$M_1V_1 = M_2V_2$$

$$(12.07 \text{ M})V_1 = (0.1 \text{ M})(0.5 \text{ L})$$

$$V_1 = 0.004125 \text{ L} \approx 4.143 \text{ mL}$$

where

M_1 = Initial concentration of 37 % HCl solution, mol/L

V_1 = Volume of 37 % HCl solution, L

M_2 = Final concentration of diluted HCl solution, mol/L

V_2 = Final volume of diluted HCl solution, L

Therefore, 4.143 mL of 37 % of HCl solution was added to prepare 500 ml of 0.1 M HCl solution.

Appendix C: Preparation of 0.1 M of NaOH

- i. Determining the mass of NaOH pellets to prepare 1 litre of 0.1 M NaOH solution:

Given,

Concentration of NaOH pellets = 97 %

Molecular weight of NaOH = 40.00 g/mol

$$\text{mass of (NaOH)} = \text{Molarity (M)} \times \text{Volume (L)} \times MW_{\text{NaOH}} \times \text{Purity}$$

$$\text{mass of (NaOH)} = \frac{0.1 \text{ mol}}{\text{L}} \times \left(500 \text{ mL} \times \frac{1\text{L}}{1000\text{mL}} \right) \times \frac{40 \text{ g}}{\text{mol}} \times \frac{100}{97}$$

$$\text{mass of (NaOH)} = 2.06 \text{ g}$$

Hence, 2.08 g of NaOH was dissolved to prepare 500 mL of 0.1 M of NaOH solution.

Appendix D: Calibration Curve of Ni (II) Standard Solution

Ni 231.604

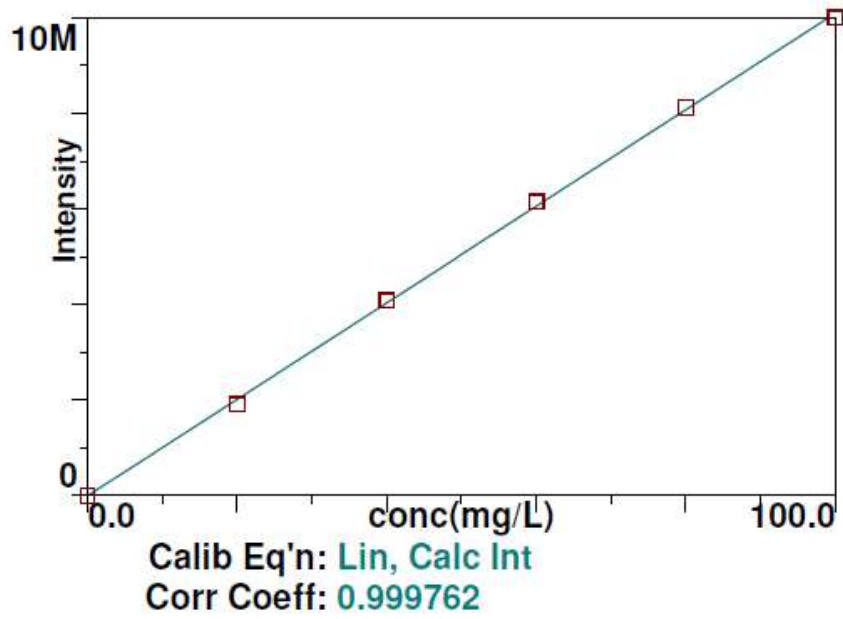


Figure D-1: Calibration Curve of Ni (II) Obtained from ICP-OES

Appendix E: Calibration Curve of Cr (VI) Standard Solution

Cr 267.716

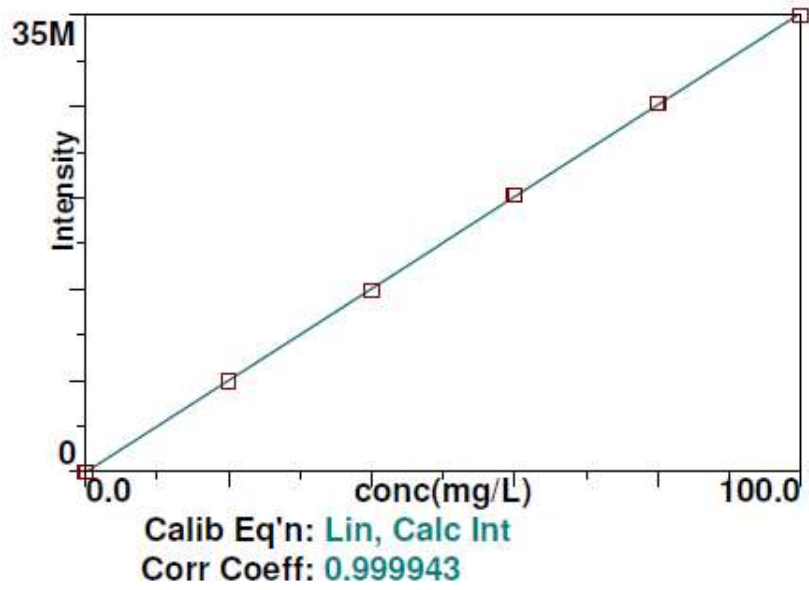


Figure E-1: Calibration Curve of Cr (VI) Obtained from ICP-OES

Appendix F: Sample Calculation of Removal Percentage, R (%) of Heavy Metal
Ions

From Table 4.1, the biosorption of Cr (VI) ion using jasmine green tea leave during the pre-screening stage resulted in final metal ion concentration of 6.442 mg/L.

Given,

Initial concentration, C_0 (mg/L) of heavy metal ion = 80 mg/L

Final concentration, C_e (mg/L) of heavy metal ion = 6.442 mg/L

$$\text{Percentage removal, } R (\%) = \frac{(C_0 - C_f)}{C_0} \times 100\%$$

$$\text{Percentage removal, } R (\%) = \frac{(80 - 6.442)}{80} \times 100\%$$

$$\text{Percentage removal, } R (\%) = 91.95 \%$$

Appendix G: Spreadsheets of ICP-OES Results

=====
Analysis Begun

Start Time: 1/22/2020 2:43:41 PM

Plasma On Time: 1/22/2020 1:51:38 PM

Logged In Analyst: Perkin Elmer

Technique: ICP Continuous

Spectrometer: Optima 7000

Autosampler: S10

Sample Information File: C:\Documents and Settings\All Users\PerkinElmer\ICP\Data\Sample Information\
dhivesh, prescreening Ni.sif

Batch ID:

Results Data Set: Nickel

Results Library: C:\Documents and Settings\Perkin Elmer\Desktop\student results\2020\dhivesh\
Results.mdb=====
Method Loaded

Method Name: Dhivesh2

Method Last Saved: 1/22/2020 2:38:32 PM

IEC File:

MSF File:

Method Description: Nickel calibration

=====
Sequence No.: 1

Autosampler Location: 1

Sample ID: Calib Blank 1

Date Collected: 1/22/2020 2:43:41 PM

Analyst:

Data Type: Original

Initial Sample Wt:

Initial Sample Vol:

Dilution:

Sample Prep Vol:

Wash Time:

Replicate Data: Calib Blank 1

Repl#	Analyte	Net Intensity	Corrected Intensity	Conc. Units	Calib. Units	Analysis Time
1	Ni 231.604	-954.5	-954.5	[0.00]	mg/L	2:44:50 PM
2	Ni 231.604	-928.7	-928.7	[0.00]	mg/L	2:45:00 PM
3	Ni 231.604	-986.0	-986.0	[0.00]	mg/L	2:45:10 PM

Mean Data: Calib Blank 1

Analyte	Mean Corrected Intensity	Std.Dev.	RSD	Conc. Units	Calib. Units
Ni 231.604	-956.4	28.70	3.00%	[0.00]	mg/L

=====
Sequence No.: 2

Autosampler Location: 2

Sample ID: 20ppm

Date Collected: 1/22/2020 2:45:57 PM

Analyst:

Data Type: Original

Initial Sample Wt:

Initial Sample Vol:

Dilution:

Sample Prep Vol:

Wash Time: 30

Auto Dilution Factor: 1

Replicate Data: 20ppm

Repl#	Analyte	Net Intensity	Corrected Intensity	Conc. Units	Calib. Units	Analysis Time
1	Ni 231.604	1951793.5	1952750.0	[20]	mg/L	2:47:06 PM
2	Ni 231.604	1955726.9	1956683.3	[20]	mg/L	2:47:08 PM
3	Ni 231.604	1950903.8	1951860.2	[20]	mg/L	2:47:10 PM

Mean Data: 20ppm

Analyte	Mean Corrected Intensity	Std.Dev.	RSD	Conc. Units	Calib. Units
Ni 231.604	1953764.5	2566.60	0.13%	[20]	mg/L

=====
Sequence No.: 3

Autosampler Location: 3

Sample ID: 40ppm

Date Collected: 1/22/2020 2:47:51 PM

Analyst:

Data Type: Original

Initial Sample Wt:
Dilution:
Wash Time: 30

Initial Sample Vol:
Sample Prep Vol:
Auto Dilution Factor: 1

Replicate Data: 40ppm

Repl#	Analyte	Net Intensity	Corrected Intensity	Calib. Conc. Units	Analysis Time
1	Ni 231.604	3816182.8	3817139.2	[40] mg/L	2:48:59 PM
2	Ni 231.604	3877244.2	3878200.6	[40] mg/L	2:49:02 PM
3	Ni 231.604	3903752.0	3904708.4	[40] mg/L	2:49:04 PM

Mean Data: 40ppm

Analyte	Mean Corrected Intensity	Std.Dev.	RSD	Calib Conc. Units
Ni 231.604	3866682.7	44906.41	1.16%	[40] mg/L

Sequence No.: 4

Sample ID: 60ppm

Analyst:

Initial Sample Wt:

Dilution:

Wash Time: 30

Autosampler Location: 4

Date Collected: 1/22/2020 2:49:45 PM

Data Type: Original

Initial Sample Vol:

Sample Prep Vol:

Auto Dilution Factor: 1

Replicate Data: 60ppm

Repl#	Analyte	Net Intensity	Corrected Intensity	Calib. Conc. Units	Analysis Time
1	Ni 231.604	5608940.2	5609896.6	[60] mg/L	2:50:54 PM
2	Ni 231.604	5647878.7	5648835.2	[60] mg/L	2:50:57 PM
3	Ni 231.604	5688064.4	5689020.9	[60] mg/L	2:51:00 PM

Mean Data: 60ppm

Analyte	Mean Corrected Intensity	Std.Dev.	RSD	Calib Conc. Units
Ni 231.604	5649250.9	39563.75	0.70%	[60] mg/L

Sequence No.: 5

Sample ID: 80ppm

Analyst:

Initial Sample Wt:

Dilution:

Wash Time: 30

Autosampler Location: 5

Date Collected: 1/22/2020 2:51:41 PM

Data Type: Original

Initial Sample Vol:

Sample Prep Vol:

Auto Dilution Factor: 1

Replicate Data: 80ppm

Repl#	Analyte	Net Intensity	Corrected Intensity	Calib. Conc. Units	Analysis Time
1	Ni 231.604	7180131.2	7181087.6	[80] mg/L	2:52:51 PM
2	Ni 231.604	7315350.5	7316306.9	[80] mg/L	2:52:54 PM
3	Ni 231.604	7325956.0	7326912.5	[80] mg/L	2:52:57 PM

Mean Data: 80ppm

Analyte	Mean Corrected Intensity	Std.Dev.	RSD	Calib Conc. Units
Ni 231.604	7274769.0	81303.58	1.12%	[80] mg/L

Sequence No.: 6

Sample ID: 100ppm

Analyst:

Initial Sample Wt:

Dilution:

Wash Time: 30

Autosampler Location: 6

Date Collected: 1/22/2020 2:53:39 PM

Data Type: Original

Initial Sample Vol:

Sample Prep Vol:

Auto Dilution Factor: 1

Replicate Data: 100ppm

Repl#	Analyte	Net Intensity	Corrected Intensity	Calib. Conc. Units	Analysis Time
1	Ni 231.604	8502424.0	8503380.5	[100] mg/L	2:54:46 PM
2	Ni 231.604	8536435.3	8537391.7	[100] mg/L	2:54:49 PM
3	Ni 231.604	8584299.2	8585255.6	[100] mg/L	2:54:52 PM

Mean Data: 100ppm

Analyte	Mean Corrected Intensity	Std.Dev.	RSD	Calib Conc. Units
Ni 231.604	8542009.3	41132.43	0.48%	[100] mg/L

Calibration Summary

Analyte	Stds.	Equation	Intercept	Slope	Curvature	Corr. Coef.	Reslope
Ni 231.604	5	Lin, Calc Int	229486.9	86370	0.00000	0.997462	

=====

Sequence No.: 7	Autosampler Location: 7
Sample ID: blank	Date Collected: 1/22/2020 2:55:33 PM
Analyst:	Data Type: Original
Initial Sample Wt:	Initial Sample Vol:
Dilution:	Sample Prep Vol:
Wash Time: 30	Auto Dilution Factor: 1

Replicate Data: blank

Repl#	Analyte	Net Intensity	Corrected Intensity	Calib. Conc. Units	Sample Conc. Units	Analysis Time
1	Ni 231.604	12173.3	13129.7	-2.505 mg/L	-2.505 mg/L	2:56:41 PM
2	Ni 231.604	10707.9	11664.4	-2.522 mg/L	-2.522 mg/L	2:56:49 PM
3	Ni 231.604	9763.2	10719.6	-2.533 mg/L	-2.533 mg/L	2:56:58 PM

Mean Data: blank

Analyte	Mean Corrected Intensity	Calib. Conc. Units	Std.Dev.	Sample Conc. Units	Std.Dev.	RSD
Ni 231.604	11837.9	-2.520 mg/L	0.0141	-2.520 mg/L	0.0141	0.56%

QC value less than the lower limit for Ni 231.604 Recovery = Not calculated
QC Failed. Continue with analysis.

=====

Sequence No.: 8	Autosampler Location: 8
Sample ID: 60ppm	Date Collected: 1/22/2020 2:59:14 PM
Analyst:	Data Type: Original
Initial Sample Wt:	Initial Sample Vol:
Dilution:	Sample Prep Vol:
Wash Time: 120	Auto Dilution Factor: 1

Replicate Data: 60ppm

Repl#	Analyte	Net Intensity	Corrected Intensity	Calib. Conc. Units	Sample Conc. Units	Analysis Time
1	Ni 231.604	5584546.1	5585502.5	62.02 mg/L	62.02 mg/L	3:00:23 PM
2	Ni 231.604	5595716.2	5596672.6	62.15 mg/L	62.15 mg/L	3:00:26 PM
3	Ni 231.604	5587744.0	5588700.4	62.05 mg/L	62.05 mg/L	3:00:28 PM

Mean Data: 60ppm

Analyte	Mean Corrected Intensity	Calib. Conc. Units	Std.Dev.	Sample Conc. Units	Std.Dev.	RSD
Ni 231.604	5590291.9	62.07 mg/L	0.067	62.07 mg/L	0.067	0.11%

QC value within limits for Ni 231.604 Recovery = 103.45%
All analyte(s) passed QC.

```

=====
Sequence No.: 9                      Autosampler Location: 9
Sample ID: stock                     Date Collected: 1/22/2020 3:02:39 PM
Analyst:                             Data Type: Original
Initial Sample Wt:                   Initial Sample Vol:
Dilution:                           Sample Prep Vol:
Wash Time: 120                       Auto Dilution Factor: 1
=====

```

Replicate Data: stock

Repl#	Analyte	Net Intensity	Corrected Intensity	Calib. Conc. Units	Sample Conc. Units	Analysis Time
1	Ni 231.604	7004285.2	7005241.7	78.45 mg/L	78.45 mg/L	3:03:47 PM
2	Ni 231.604	7149614.9	7150571.3	80.14 mg/L	80.14 mg/L	3:03:51 PM
3	Ni 231.604	7079367.8	7080324.2	79.32 mg/L	79.32 mg/L	3:03:54 PM

Mean Data: stock

Analyte	Mean Corrected Intensity	Calib. Conc. Units	Std.Dev.	Sample Conc. Units	Std.Dev.	RSD
Ni 231.604	7078712.4	79.31 mg/L	0.842	79.31 mg/L	0.842	1.06%

```

=====
Sequence No.: 10                     Autosampler Location: 10
Sample ID: green tea Ni              Date Collected: 1/22/2020 3:06:06 PM
Analyst:                             Data Type: Original
Initial Sample Wt:                   Initial Sample Vol:
Dilution:                           Sample Prep Vol:
Wash Time: 120                       Auto Dilution Factor: 1
=====

```

Replicate Data: green tea Ni

Repl#	Analyte	Net Intensity	Corrected Intensity	Calib. Conc. Units	Sample Conc. Units	Analysis Time
1	Ni 231.604	486656.8	487613.3	2.989 mg/L	2.989 mg/L	3:07:15 PM
2	Ni 231.604	505782.4	506738.8	3.210 mg/L	3.210 mg/L	3:07:18 PM
3	Ni 231.604	489281.3	490237.7	3.019 mg/L	3.019 mg/L	3:07:21 PM

Mean Data: green tea Ni

Analyte	Mean Corrected Intensity	Calib. Conc. Units	Std.Dev.	Sample Conc. Units	Std.Dev.	RSD
Ni 231.604	494863.3	3.073 mg/L	0.1200	3.073 mg/L	0.1200	3.91%

```

=====
Sequence No.: 11                     Autosampler Location: 11
Sample ID: geinmacha Ni              Date Collected: 1/22/2020 3:09:32 PM
Analyst:                             Data Type: Original
Initial Sample Wt:                   Initial Sample Vol:
Dilution:                           Sample Prep Vol:
Wash Time: 120                       Auto Dilution Factor: 1
=====

```

Replicate Data: geinmacha Ni

Repl#	Analyte	Net Intensity	Corrected Intensity	Calib. Conc. Units	Sample Conc. Units	Analysis Time
1	Ni 231.604	760418.5	761375.0	6.159 mg/L	6.159 mg/L	3:10:41 PM
2	Ni 231.604	779754.8	780711.3	6.382 mg/L	6.382 mg/L	3:10:43 PM
3	Ni 231.604	794886.6	795843.1	6.558 mg/L	6.558 mg/L	3:10:45 PM

Mean Data: geinmacha Ni

Analyte	Mean Corrected Intensity	Calib. Conc. Units	Std.Dev.	Sample Conc. Units	Std.Dev.	RSD
Ni 231.604	779309.8	6.366 mg/L	0.2000	6.366 mg/L	0.2000	3.14%

```

=====
Sequence No.: 12                     Autosampler Location: 12
Sample ID: salted peanut Ni          Date Collected: 1/22/2020 3:12:56 PM
=====

```

Analyst: Data Type: Original
 Initial Sample Wt: Initial Sample Vol:
 Dilution: Sample Prep Vol:
 Wash Time: 120 Auto Dilution Factor: 1

 Replicate Data: salted peanut Ni

Repl#	Analyte	Net Intensity	Corrected Intensity	Calib. Conc. Units	Sample Conc. Units	Analysis Time
1	Ni 231.604	742393.0	743349.4	5.950 mg/L	5.950 mg/L	3:14:06 PM
2	Ni 231.604	732264.5	733220.9	5.833 mg/L	5.833 mg/L	3:14:09 PM
3	Ni 231.604	742692.3	743648.7	5.953 mg/L	5.953 mg/L	3:14:12 PM

 Mean Data: salted peanut Ni

Analyte	Mean Corrected Intensity	Calib. Conc. Units	Std.Dev.	Sample Conc. Units	Std.Dev.	RSD
Ni 231.604	740073.0	5.912 mg/L	0.0687	5.912 mg/L	0.0687	1.16%

=====

Sequence No.: 13

Autosampler Location: 13

Sample ID: unsalted peanut Ni

Date Collected: 1/22/2020 3:16:23 PM

Analyst:

Data Type: Original

Initial Sample Wt:

Initial Sample Vol:

Dilution:

Sample Prep Vol:

Wash Time: 120

Auto Dilution Factor: 1

 Replicate Data: unsalted peanut Ni

Repl#	Analyte	Net Intensity	Corrected Intensity	Calib. Conc. Units	Sample Conc. Units	Analysis Time
1	Ni 231.604	2868960.4	2869916.8	30.57 mg/L	30.57 mg/L	3:17:32 PM
2	Ni 231.604	2849847.2	2850803.6	30.35 mg/L	30.35 mg/L	3:17:35 PM
3	Ni 231.604	2924956.1	2925912.6	31.22 mg/L	31.22 mg/L	3:17:37 PM

 Mean Data: unsalted peanut Ni

Analyte	Mean Corrected Intensity	Calib. Conc. Units	Std.Dev.	Sample Conc. Units	Std.Dev.	RSD
Ni 231.604	2882211.0	30.72 mg/L	0.452	30.72 mg/L	0.452	1.47%

=====
Analysis Begun

Start Time: 3/5/2020 10:08:36 AM

Plasma On Time: 3/5/2020 10:03:30 AM

Logged In Analyst: Perkin Elmer

Technique: ICP Continuous

Spectrometer: Optima 7000

Autosampler: S10

Sample Information File: C:\Documents and Settings\All Users\PerkinElmer\ICP\Data\Sample Information\
dhivesh, prescreening Ni2.sif

Batch ID:

Results Data Set: ni parameters

Results Library: C:\Documents and Settings\Perkin Elmer\Desktop\student results\2020\dhivesh\
Results.mdb=====
Method Loaded

Method Name: Dhivesh3

Method Last Saved: 2/18/2020 2:15:52 PM

IEC File:

MSF File:

Method Description:

=====
Sequence No.: 1

Autosampler Location: 1

Sample ID: DI blank

Date Collected: 3/5/2020 10:08:36 AM

Analyst:

Data Type: Original

Initial Sample Wt:

Initial Sample Vol:

Dilution:

Sample Prep Vol:

Wash Time:

Replicate Data: DI blank

Repl#	Analyte	Net Intensity	Corrected Intensity	Calib. Conc. Units	Sample Conc. Units	Analysis Time
1	Ni 231.604	-800.1	16.5	0.689 mg/L	0.689 mg/L	10:09:45 AM
2	Ni 231.604	-826.2	-9.7	0.688 mg/L	0.688 mg/L	10:09:58 AM
3	Ni 231.604	-735.6	81.0	0.689 mg/L	0.689 mg/L	10:10:09 AM

Mean Data: DI blank

Analyte	Mean Corrected Intensity	Calib. Conc. Units	Std.Dev.	Sample Conc. Units	Std.Dev.	RSD
Ni 231.604	29.3	0.689 mg/L	0.0006	0.689 mg/L	0.0006	0.09%

=====
Sequence No.: 2

Autosampler Location: 9

Sample ID: dose-2.0_pH4-reading1

Date Collected: 3/5/2020 10:12:27 AM

Analyst:

Data Type: Original

Initial Sample Wt:

Initial Sample Vol:

Dilution:

Sample Prep Vol:

Wash Time: 120

Auto Dilution Factor: 1

Replicate Data: dose-2.0_pH4-reading1

Repl#	Analyte	Net Intensity	Corrected Intensity	Calib. Conc. Units	Sample Conc. Units	Analysis Time
1	Ni 231.604	1257445.4	1258262.0	17.76 mg/L	17.76 mg/L	10:13:35 AM
2	Ni 231.604	1217925.8	1218742.4	17.22 mg/L	17.22 mg/L	10:13:38 AM
3	Ni 231.604	1221161.0	1221977.6	17.27 mg/L	17.27 mg/L	10:13:40 AM

Mean Data: dose-2.0_pH4-reading1

Analyte	Mean Corrected Intensity	Calib. Conc. Units	Std.Dev.	Sample Conc. Units	Std.Dev.	RSD
Ni 231.604	1232994.0	17.42 mg/L	0.298	17.42 mg/L	0.298	1.71%

=====
Sequence No.: 3

Autosampler Location: 10

Sample ID: dose-2.5_pH4-reading1

Date Collected: 3/5/2020 10:15:51 AM

Analyst:

Data Type: Original

Initial Sample Wt:
Dilution:
Wash Time: 120

Initial Sample Vol:
Sample Prep Vol:
Auto Dilution Factor: 1

Replicate Data: dose-2.5_pH4-reading1

Repl#	Analyte	Net Intensity	Corrected Intensity	Calib. Conc. Units	Sample Conc. Units	Analysis Time
1	Ni 231.604	1125217.3	1126033.9	15.96 mg/L	15.96 mg/L	10:17:01 AM
2	Ni 231.604	1121413.2	1122229.8	15.91 mg/L	15.91 mg/L	10:17:04 AM
3	Ni 231.604	1107357.5	1108174.1	15.72 mg/L	15.72 mg/L	10:17:07 AM

Mean Data: dose-2.5_pH4-reading1

Analyte	Mean Corrected Intensity	Calib. Conc. Units	Std.Dev.	Sample Conc. Units	Std.Dev.	RSD
Ni 231.604	1118812.6	15.87 mg/L	0.128	15.87 mg/L	0.128	0.80%

=====

Sequence No.: 4
Sample ID: dose-3.0_pH4-reading1
Analyst:
Initial Sample Wt:
Dilution:
Wash Time: 120

Autosampler Location: 11
Date Collected: 3/5/2020 10:19:18 AM
Data Type: Original
Initial Sample Vol:
Sample Prep Vol:
Auto Dilution Factor: 1

Replicate Data: dose-3.0_pH4-reading1

Repl#	Analyte	Net Intensity	Corrected Intensity	Calib. Conc. Units	Sample Conc. Units	Analysis Time
1	Ni 231.604	812861.4	813678.0	11.73 mg/L	11.73 mg/L	10:20:28 AM
2	Ni 231.604	822564.3	823380.9	11.86 mg/L	11.86 mg/L	10:20:30 AM
3	Ni 231.604	784227.1	785043.7	11.34 mg/L	11.34 mg/L	10:20:32 AM

Mean Data: dose-3.0_pH4-reading1

Analyte	Mean Corrected Intensity	Calib. Conc. Units	Std.Dev.	Sample Conc. Units	Std.Dev.	RSD
Ni 231.604	807367.5	11.64 mg/L	0.270	11.64 mg/L	0.270	2.32%

=====

Sequence No.: 5
Sample ID: dose-3.5_pH4-reading1
Analyst:
Initial Sample Wt:
Dilution:
Wash Time: 120

Autosampler Location: 12
Date Collected: 3/5/2020 10:22:44 AM
Data Type: Original
Initial Sample Vol:
Sample Prep Vol:
Auto Dilution Factor: 1

Replicate Data: dose-3.5_pH4-reading1

Repl#	Analyte	Net Intensity	Corrected Intensity	Calib. Conc. Units	Sample Conc. Units	Analysis Time
1	Ni 231.604	885277.1	886093.7	12.71 mg/L	12.71 mg/L	10:23:53 AM
2	Ni 231.604	871002.1	871818.7	12.52 mg/L	12.52 mg/L	10:23:55 AM
3	Ni 231.604	880825.0	881641.6	12.65 mg/L	12.65 mg/L	10:23:57 AM

Mean Data: dose-3.5_pH4-reading1

Analyte	Mean Corrected Intensity	Calib. Conc. Units	Std.Dev.	Sample Conc. Units	Std.Dev.	RSD
Ni 231.604	879851.3	12.62 mg/L	0.099	12.62 mg/L	0.099	0.78%

=====

Sequence No.: 6
Sample ID: dose-4.0_pH4-reading1
Analyst:
Initial Sample Wt:
Dilution:
Wash Time: 120

Autosampler Location: 13
Date Collected: 3/5/2020 10:26:09 AM
Data Type: Original
Initial Sample Vol:
Sample Prep Vol:
Auto Dilution Factor: 1

Replicate Data: dose-4.0_pH4-reading1

Repl#	Analyte	Net		Calib.		Sample		Analysis Time
		Intensity	Corrected Intensity	Conc. Units	Units	Conc. Units	Units	
1	Ni 231.604	361554.4	362371.0	5.604	mg/L	5.604	mg/L	10:27:18 AM
2	Ni 231.604	364954.8	365771.3	5.650	mg/L	5.650	mg/L	10:27:21 AM
3	Ni 231.604	358022.7	358839.3	5.556	mg/L	5.556	mg/L	10:27:25 AM

Mean Data: dose-4.0_pH4-reading1

Analyte	Mean Corrected Intensity	Calib. Conc. Units	Std.Dev.	Sample Conc. Units	Std.Dev.	RSD
Ni 231.604	362327.2	5.604 mg/L	0.0470	5.604 mg/L	0.0470	0.84%

=====

Sequence No.: 7
 Sample ID: dose-2.0_pH5-reading1
 Analyst:
 Initial Sample Wt:
 Dilution:
 Wash Time: 120

Autosampler Location: 14
 Date Collected: 3/5/2020 10:29:37 AM
 Data Type: Original
 Initial Sample Vol:
 Sample Prep Vol:
 Auto Dilution Factor: 1

Replicate Data: dose-2.0_pH5-reading1

Repl#	Analyte	Net		Calib.		Sample		Analysis Time
		Intensity	Corrected Intensity	Conc. Units	Units	Conc. Units	Units	
1	Ni 231.604	684951.0	685767.6	9.992	mg/L	9.992	mg/L	10:30:45 AM
2	Ni 231.604	694407.3	695223.9	10.12	mg/L	10.12	mg/L	10:30:47 AM
3	Ni 231.604	683767.6	684584.2	9.976	mg/L	9.976	mg/L	10:30:49 AM

Mean Data: dose-2.0_pH5-reading1

Analyte	Mean Corrected Intensity	Calib. Conc. Units	Std.Dev.	Sample Conc. Units	Std.Dev.	RSD
Ni 231.604	688525.2	10.03 mg/L	0.079	10.03 mg/L	0.079	0.79%

=====

Sequence No.: 8
 Sample ID: dose-2.5_pH5-reading1
 Analyst:
 Initial Sample Wt:
 Dilution:
 Wash Time: 120

Autosampler Location: 15
 Date Collected: 3/5/2020 10:33:00 AM
 Data Type: Original
 Initial Sample Vol:
 Sample Prep Vol:
 Auto Dilution Factor: 1

Replicate Data: dose-2.5_pH5-reading1

Repl#	Analyte	Net		Calib.		Sample		Analysis Time
		Intensity	Corrected Intensity	Conc. Units	Units	Conc. Units	Units	
1	Ni 231.604	826483.1	827299.6	11.91	mg/L	11.91	mg/L	10:34:08 AM
2	Ni 231.604	839129.4	839945.9	12.08	mg/L	12.08	mg/L	10:34:10 AM
3	Ni 231.604	833471.3	834287.9	12.01	mg/L	12.01	mg/L	10:34:12 AM

Mean Data: dose-2.5_pH5-reading1

Analyte	Mean Corrected Intensity	Calib. Conc. Units	Std.Dev.	Sample Conc. Units	Std.Dev.	RSD
Ni 231.604	833844.5	12.00 mg/L	0.086	12.00 mg/L	0.086	0.72%

=====

Sequence No.: 9
 Sample ID: dose-3.0_pH5-reading1
 Analyst:
 Initial Sample Wt:
 Dilution:
 Wash Time: 120

Autosampler Location: 16
 Date Collected: 3/5/2020 10:36:22 AM
 Data Type: Original
 Initial Sample Vol:
 Sample Prep Vol:
 Auto Dilution Factor: 1

Replicate Data: dose-3.0_pH5-reading1

2	Ni 231.604	361129.3	361945.9	5.599 mg/L	5.599 mg/L	10:47:42 AM
3	Ni 231.604	361324.5	362141.1	5.601 mg/L	5.601 mg/L	10:47:45 AM

Mean Data: dose-2.0_pH7-reading1

Analyte	Mean Corrected Intensity	Calib. Conc. Units	Std.Dev.	Sample Conc. Units	Std.Dev.	RSD
Ni 231.604	361832.7	5.597 mg/L	0.0051	5.597 mg/L	0.0051	0.09%

Sequence No.: 13

Autosampler Location: 20

Sample ID: dose-2.5_pH7-reading1

Date Collected: 3/5/2020 10:49:57 AM

Analyst:

Data Type: Original

Initial Sample Wt:

Initial Sample Vol:

Dilution:

Sample Prep Vol:

Wash Time: 120

Auto Dilution Factor: 1

Replicate Data: dose-2.5_pH7-reading1

Repl#	Analyte	Net Intensity	Corrected Intensity	Calib. Conc. Units	Sample Conc. Units	Analysis Time
1	Ni 231.604	364604.9	365421.5	5.646 mg/L	5.646 mg/L	10:51:05 AM
2	Ni 231.604	360919.0	361735.6	5.596 mg/L	5.596 mg/L	10:51:09 AM
3	Ni 231.604	365214.7	366031.3	5.654 mg/L	5.654 mg/L	10:51:12 AM

Mean Data: dose-2.5_pH7-reading1

Analyte	Mean Corrected Intensity	Calib. Conc. Units	Std.Dev.	Sample Conc. Units	Std.Dev.	RSD
Ni 231.604	364396.1	5.632 mg/L	0.0315	5.632 mg/L	0.0315	0.56%

Sequence No.: 14

Autosampler Location: 21

Sample ID: dose-3.0_pH7-reading1

Date Collected: 3/5/2020 10:53:23 AM

Analyst:

Data Type: Original

Initial Sample Wt:

Initial Sample Vol:

Dilution:

Sample Prep Vol:

Wash Time: 120

Auto Dilution Factor: 1

Replicate Data: dose-3.0_pH7-reading1

Repl#	Analyte	Net Intensity	Corrected Intensity	Calib. Conc. Units	Sample Conc. Units	Analysis Time
1	Ni 231.604	397063.5	397880.1	6.086 mg/L	6.086 mg/L	10:54:31 AM
2	Ni 231.604	408934.0	409750.6	6.247 mg/L	6.247 mg/L	10:54:34 AM
3	Ni 231.604	403740.6	404557.2	6.177 mg/L	6.177 mg/L	10:54:37 AM

Mean Data: dose-3.0_pH7-reading1

Analyte	Mean Corrected Intensity	Calib. Conc. Units	Std.Dev.	Sample Conc. Units	Std.Dev.	RSD
Ni 231.604	404062.6	6.170 mg/L	0.0807	6.170 mg/L	0.0807	1.31%

Sequence No.: 15

Autosampler Location: 22

Sample ID: dose-3.5_pH7-reading1

Date Collected: 3/5/2020 10:56:49 AM

Analyst:

Data Type: Original

Initial Sample Wt:

Initial Sample Vol:

Dilution:

Sample Prep Vol:

Wash Time: 120

Auto Dilution Factor: 1

Replicate Data: dose-3.5_pH7-reading1

Repl#	Analyte	Net Intensity	Corrected Intensity	Calib. Conc. Units	Sample Conc. Units	Analysis Time
1	Ni 231.604	388325.4	389142.0	5.967 mg/L	5.967 mg/L	10:57:58 AM
2	Ni 231.604	387394.6	388211.2	5.955 mg/L	5.955 mg/L	10:58:01 AM
3	Ni 231.604	390157.3	390973.9	5.992 mg/L	5.992 mg/L	10:58:05 AM

Mean Data: dose-3.5_pH7-reading1

Analyte	Mean Corrected Intensity	Calib. Conc. Units	Std.Dev.	Sample Conc. Units	Std.Dev.	RSD
Ni 231.604	389442.4	5.972 mg/L	0.0191	5.972 mg/L	0.0191	0.32%

=====

Sequence No.:	Autosampler Location:
16	23
Sample ID:	Date Collected:
dose-4.0_pH7-reading1	3/5/2020 11:00:17 AM
Analyst:	Data Type:
	Original
Initial Sample Wt:	Initial Sample Vol:
Dilution:	Sample Prep Vol:
Wash Time:	Auto Dilution Factor:
120	1

Replicate Data: dose-4.0_pH7-reading1

Repl#	Analyte	Net Intensity	Corrected Intensity	Calib. Conc. Units	Sample Conc. Units	Analysis Time
1	Ni 231.604	605821.7	606638.3	8.918 mg/L	8.918 mg/L	11:01:26 AM
2	Ni 231.604	602652.4	603469.0	8.875 mg/L	8.875 mg/L	11:01:28 AM
3	Ni 231.604	595955.3	596771.9	8.784 mg/L	8.784 mg/L	11:01:30 AM

Mean Data: dose-4.0_pH7-reading1

Analyte	Mean Corrected Intensity	Calib. Conc. Units	Std.Dev.	Sample Conc. Units	Std.Dev.	RSD
Ni 231.604	602293.1	8.859 mg/L	0.0683	8.859 mg/L	0.0683	0.77%

=====

Sequence No.:	Autosampler Location:
17	24
Sample ID:	Date Collected:
dose-2.0_pH8-reading1	3/5/2020 11:03:42 AM
Analyst:	Data Type:
	Original
Initial Sample Wt:	Initial Sample Vol:
Dilution:	Sample Prep Vol:
Wash Time:	Auto Dilution Factor:
120	1

Replicate Data: dose-2.0_pH8-reading1

Repl#	Analyte	Net Intensity	Corrected Intensity	Calib. Conc. Units	Sample Conc. Units	Analysis Time
1	Ni 231.604	1331410.0	1332226.6	18.76 mg/L	18.76 mg/L	11:04:51 AM
2	Ni 231.604	1340038.5	1340855.1	18.88 mg/L	18.88 mg/L	11:04:53 AM
3	Ni 231.604	1327512.6	1328329.2	18.71 mg/L	18.71 mg/L	11:04:56 AM

Mean Data: dose-2.0_pH8-reading1

Analyte	Mean Corrected Intensity	Calib. Conc. Units	Std.Dev.	Sample Conc. Units	Std.Dev.	RSD
Ni 231.604	1333803.6	18.78 mg/L	0.087	18.78 mg/L	0.087	0.46%

=====

Sequence No.:	Autosampler Location:
18	25
Sample ID:	Date Collected:
dose-2.5_pH8-reading1	3/5/2020 11:07:07 AM
Analyst:	Data Type:
	Original
Initial Sample Wt:	Initial Sample Vol:
Dilution:	Sample Prep Vol:
Wash Time:	Auto Dilution Factor:
120	1

Replicate Data: dose-2.5_pH8-reading1

Repl#	Analyte	Net Intensity	Corrected Intensity	Calib. Conc. Units	Sample Conc. Units	Analysis Time
1	Ni 231.604	1063594.4	1064410.9	15.13 mg/L	15.13 mg/L	11:08:16 AM
2	Ni 231.604	1072288.8	1073105.4	15.25 mg/L	15.25 mg/L	11:08:18 AM
3	Ni 231.604	1055655.8	1056472.4	15.02 mg/L	15.02 mg/L	11:08:21 AM

Mean Data: dose-2.5_pH8-reading1

Analyte	Mean Corrected Intensity	Calib. Conc. Units	Sample Conc. Units
Ni 231.604			

Analyte	Intensity	Conc. Units	Std.Dev.	Conc. Units	Std.Dev.	RSD
Ni 231.604	1064662.9	15.13 mg/L	0.113	15.13 mg/L	0.113	0.75%

Sequence No.: 19

Sample ID: dose-3.0_pH8-reading1

Analyst:

Initial Sample Wt:

Dilution:

Wash Time: 120

Autosampler Location: 26

Date Collected: 3/5/2020 11:10:32 AM

Data Type: Original

Initial Sample Vol:

Sample Prep Vol:

Auto Dilution Factor: 1

Replicate Data: dose-3.0_pH8-reading1

Repl#	Analyte	Net Intensity	Corrected Intensity	Calib. Conc. Units	Sample Conc. Units	Analysis Time
1	Ni 231.604	847458.1	848274.6	12.20 mg/L	12.20 mg/L	11:11:41 AM
2	Ni 231.604	846551.3	847367.9	12.18 mg/L	12.18 mg/L	11:11:43 AM
3	Ni 231.604	818296.2	819112.8	11.80 mg/L	11.80 mg/L	11:11:45 AM

Mean Data: dose-3.0_pH8-reading1

Analyte	Mean Corrected Intensity	Calib. Conc. Units	Std.Dev.	Sample Conc. Units	Std.Dev.	RSD
Ni 231.604	838251.8	12.06 mg/L	0.225	12.06 mg/L	0.225	1.87%

Sequence No.: 20

Sample ID: dose-3.5_pH8-reading1

Analyst:

Initial Sample Wt:

Dilution:

Wash Time: 120

Autosampler Location: 27

Date Collected: 3/5/2020 11:13:56 AM

Data Type: Original

Initial Sample Vol:

Sample Prep Vol:

Auto Dilution Factor: 1

Replicate Data: dose-3.5_pH8-reading1

Repl#	Analyte	Net Intensity	Corrected Intensity	Calib. Conc. Units	Sample Conc. Units	Analysis Time
1	Ni 231.604	733627.2	734443.8	10.65 mg/L	10.65 mg/L	11:15:04 AM
2	Ni 231.604	739016.9	739833.5	10.73 mg/L	10.73 mg/L	11:15:06 AM
3	Ni 231.604	770364.8	771181.3	11.15 mg/L	11.15 mg/L	11:15:08 AM

Mean Data: dose-3.5_pH8-reading1

Analyte	Mean Corrected Intensity	Calib. Conc. Units	Std.Dev.	Sample Conc. Units	Std.Dev.	RSD
Ni 231.604	748486.2	10.84 mg/L	0.269	10.84 mg/L	0.269	2.48%

Sequence No.: 21

Sample ID: dose-4.0_pH8-reading1

Analyst:

Initial Sample Wt:

Dilution:

Wash Time: 120

Autosampler Location: 28

Date Collected: 3/5/2020 11:17:19 AM

Data Type: Original

Initial Sample Vol:

Sample Prep Vol:

Auto Dilution Factor: 1

Replicate Data: dose-4.0_pH8-reading1

Repl#	Analyte	Net Intensity	Corrected Intensity	Calib. Conc. Units	Sample Conc. Units	Analysis Time
1	Ni 231.604	697957.5	698774.1	10.17 mg/L	10.17 mg/L	11:18:27 AM
2	Ni 231.604	691787.0	692603.6	10.08 mg/L	10.08 mg/L	11:18:29 AM
3	Ni 231.604	690289.2	691105.7	10.06 mg/L	10.06 mg/L	11:18:31 AM

Mean Data: dose-4.0_pH8-reading1

Analyte	Mean Corrected Intensity	Calib. Conc. Units	Std.Dev.	Sample Conc. Units	Std.Dev.	RSD
Ni 231.604	694161.2	10.11 mg/L	0.055	10.11 mg/L	0.055	0.55%

=====
Analysis Begun

Start Time: 3/5/2020 11:24:18 AM
 Logged In Analyst: Perkin Elmer
 Spectrometer: Optima 7000

Plasma On Time: 3/5/2020 10:03:30 AM
 Technique: ICP Continuous
 Autosampler: S10

Sample Information File: C:\Documents and Settings\All Users\PerkinElmer\ICP\Data\Sample Information\
 dhivesh, prescreening Ni2.sif

Batch ID:

Results Data Set: ni parameters

Results Library: C:\Documents and Settings\Perkin Elmer\Desktop\student results\2020\dhivesh\
 Results.mdb

Sequence No.: 1

Sample ID: 4g-pH4-reading2

Analyst:

Initial Sample Wt:

Dilution:

Wash Time:

Autosampler Location: 9

Date Collected: 3/5/2020 11:24:18 AM

Data Type: Original

Initial Sample Vol:

Sample Prep Vol:

Replicate Data: 4g-pH4-reading2

Repl#	Analyte	Net Intensity	Corrected Intensity	Calib. Conc. Units	Sample Conc. Units	Analysis Time
1	Ni 231.604	934104.3	934920.9	13.37 mg/L	13.37 mg/L	11:25:28 AM
2	Ni 231.604	908809.7	909626.3	13.03 mg/L	13.03 mg/L	11:25:31 AM
3	Ni 231.604	919636.5	920453.1	13.18 mg/L	13.18 mg/L	11:25:33 AM

Mean Data: 4g-pH4-reading2

Analyte	Mean Corrected Intensity	Calib. Conc. Units	Std.Dev.	Sample Conc. Units	Std.Dev.	RSD
Ni 231.604	921666.8	13.19 mg/L	0.172	13.19 mg/L	0.172	1.31%

Sequence No.: 2

Sample ID: 2.5g-pH6-reading2

Analyst:

Initial Sample Wt:

Dilution:

Wash Time: 120

Autosampler Location: 10

Date Collected: 3/5/2020 11:27:44 AM

Data Type: Original

Initial Sample Vol:

Sample Prep Vol:

Auto Dilution Factor: 1

Replicate Data: 2.5g-pH6-reading2

Repl#	Analyte	Net Intensity	Corrected Intensity	Calib. Conc. Units	Sample Conc. Units	Analysis Time
1	Ni 231.604	807165.7	807982.3	11.65 mg/L	11.65 mg/L	11:28:52 AM
2	Ni 231.604	793513.1	794329.7	11.46 mg/L	11.46 mg/L	11:28:55 AM
3	Ni 231.604	787326.4	788143.0	11.38 mg/L	11.38 mg/L	11:28:57 AM

Mean Data: 2.5g-pH6-reading2

Analyte	Mean Corrected Intensity	Calib. Conc. Units	Std.Dev.	Sample Conc. Units	Std.Dev.	RSD
Ni 231.604	796818.3	11.50 mg/L	0.138	11.50 mg/L	0.138	1.20%

Sequence No.: 3

Sample ID: 4g-pH6-reading1

Analyst:

Initial Sample Wt:

Dilution:

Wash Time: 120

Autosampler Location: 11

Date Collected: 3/5/2020 11:31:08 AM

Data Type: Original

Initial Sample Vol:

Sample Prep Vol:

Auto Dilution Factor: 1

Replicate Data: 4g-pH6-reading1

Repl#	Analyte	Net Intensity	Corrected Intensity	Calib. Conc. Units	Sample Conc. Units	Analysis Time
-------	---------	---------------	---------------------	--------------------	--------------------	---------------

Repl#	Analyte	Intensity	Intensity	Conc. Units	Conc. Units	Time
1	Ni 231.604	514660.1	515476.7	7.681 mg/L	7.681 mg/L	11:32:18 AM
2	Ni 231.604	531414.4	532230.9	7.909 mg/L	7.909 mg/L	11:32:21 AM
3	Ni 231.604	535761.3	536577.9	7.968 mg/L	7.968 mg/L	11:32:23 AM

Mean Data: 4g-pH6-reading1

Analyte	Mean Corrected Intensity	Calib. Conc. Units	Std.Dev.	Sample Conc. Units	Std.Dev.	RSD
Ni 231.604	528095.2	7.853 mg/L	0.1512	7.853 mg/L	0.1512	1.92%

Sequence No.: 5
Sample ID: dose-3.5_pH5-reading2
Analyst:
Initial Sample Wt:
Dilution:
Wash Time: 120

Autosampler Location: 12
Date Collected: 3/13/2020 1:02:57 PM
Data Type: Original
Initial Sample Vol:
Sample Prep Vol:
Auto Dilution Factor: 1

Replicate Data: dose-3.5_pH5-reading2

Repl#	Analyte	Net Intensity	Corrected Intensity	Calib. Conc. Units	Sample Conc. Units	Analysis Time
1	Ni 231.604	-729.9	86.7	0.689 mg/L	0.689 mg/L	1:04:11 PM
2	Ni 231.604	-815.4	1.2	0.688 mg/L	0.688 mg/L	1:04:20 PM
3	Ni 231.604	-791.4	25.1	0.689 mg/L	0.689 mg/L	1:04:29 PM

Mean Data: dose-3.5_pH5-reading2

Analyte	Mean Corrected Intensity	Calib. Conc. Units	Std.Dev.	Sample Conc. Units	Std.Dev.	RSD
Ni 231.604	37.7	0.689 mg/L	0.0006	0.689 mg/L	0.0006	0.09%

Sequence No.: 6
Sample ID: dose-4.0_pH5-reading1
Analyst:
Initial Sample Wt:
Dilution:
Wash Time: 120

Autosampler Location: 13
Date Collected: 3/13/2020 1:06:47 PM
Data Type: Original
Initial Sample Vol:
Sample Prep Vol:
Auto Dilution Factor: 1

Replicate Data: dose-4.0_pH5-reading1

Repl#	Analyte	Net Intensity	Corrected Intensity	Calib. Conc. Units	Sample Conc. Units	Analysis Time
1	Ni 231.604	8701.4	9518.0	0.817 mg/L	0.817 mg/L	1:07:57 PM
2	Ni 231.604	12487.7	13304.3	0.869 mg/L	0.869 mg/L	1:08:06 PM
3	Ni 231.604	6083.7	6900.3	0.782 mg/L	0.782 mg/L	1:08:15 PM

Mean Data: dose-4.0_pH5-reading1

Analyte	Mean Corrected Intensity	Calib. Conc. Units	Std.Dev.	Sample Conc. Units	Std.Dev.	RSD
Ni 231.604	9907.5	0.823 mg/L	0.0437	0.823 mg/L	0.0437	5.31%

Sequence No.: 3
Sample ID: dose-2.0_pH4-reading1
Analyst:
Initial Sample Wt:

Autosampler Location: 9
Date Collected: 3/3/2020 2:44:34 PM
Data Type: Original
Initial Sample Vol:

Replicate Data: dose-2.0_pH4-reading1

Repl#	Analyte	Net Intensity	Corrected Intensity	Calib. Conc. Units	Sample Conc. Units	Analysis Time
1	Ni 231.604	1159652.5	1160469.1	16.43 mg/L	16.43 mg/L	2:45:42 PM
2	Ni 231.604	1211918.9	1212735.5	17.14 mg/L	17.14 mg/L	2:45:45 PM
3	Ni 231.604	1211675.6	1212492.2	17.14 mg/L	17.14 mg/L	2:45:47 PM

Mean Data: dose-2.0_pH4-reading1

Analyte	Mean Corrected Intensity	Calib. Conc. Units	Std.Dev.	Sample Conc. Units	Std.Dev.	RSD
Ni 231.604	1195232.3	16.90 mg/L	0.408	16.90 mg/L	0.408	2.42%

Sequence No.: 4
Sample ID: dose-2.5_pH4-reading1
Analyst:
Initial Sample Wt:
Dilution:
Wash Time: 120

Autosampler Location: 10
Date Collected: 3/3/2020 2:47:58 PM
Data Type: Original
Initial Sample Vol:
Sample Prep Vol:
Auto Dilution Factor: 1

Replicate Data: dose-2.5_pH4-reading1

Repl#	Analyte	Net Intensity	Corrected Intensity	Calib. Conc. Units	Sample Conc. Units	Analysis Time
1	Ni 231.604	957995.5	958812.1	13.70 mg/L	13.70 mg/L	2:49:06 PM
2	Ni 231.604	984563.8	985380.4	14.06 mg/L	14.06 mg/L	2:49:09 PM
3	Ni 231.604	1041475.8	1042292.4	14.83 mg/L	14.83 mg/L	2:49:11 PM

Mean Data: dose-2.5_pH4-reading1

Analyte	Mean Corrected Intensity	Calib. Conc. Units	Std.Dev.	Sample Conc. Units	Std.Dev.	RSD
Ni 231.604	995495.0	14.19 mg/L	0.579	14.19 mg/L	0.579	4.08%

Sequence No.: 6
Sample ID: dose-3.5_pH4-reading1
Analyst:
Initial Sample Wt:
Dilution:
Wash Time: 120

Autosampler Location: 12
Date Collected: 3/3/2020 2:55:13 PM
Data Type: Original
Initial Sample Vol:
Sample Prep Vol:
Auto Dilution Factor: 1

Replicate Data: dose-3.5_pH4-reading1

Repl#	Analyte	Net Intensity	Corrected Intensity	Calib. Conc. Units	Sample Conc. Units	Analysis Time
1	Ni 231.604	4452.1	5268.7	0.760 mg/L	0.760 mg/L	2:56:23 PM
2	Ni 231.604	-6639.7	-5823.2	0.609 mg/L	0.609 mg/L	2:56:34 PM
Saturated outside auto integration window (code 5)						
3	Ni 231.604	-17205.0	-16388.4	0.466 mg/L	0.466 mg/L	2:56:45 PM
Saturated outside auto integration window (code 5)						

Mean Data: dose-3.5_pH4-reading1

Analyte	Mean Corrected Intensity	Calib. Conc. Units	Std.Dev.	Sample Conc. Units	Std.Dev.	RSD
Ni 231.604	-5647.6	0.612 mg/L	0.1469	0.612 mg/L	0.1469	24.02%

Saturated outside auto integration window (code 5)

Sequence No.: 7
Sample ID: dose-2.0_pH5-reading1
Analyst:
Initial Sample Wt:
Dilution:
Wash Time: 120

Autosampler Location: 13
Date Collected: 3/3/2020 2:59:05 PM
Data Type: Original
Initial Sample Vol:
Sample Prep Vol:
Auto Dilution Factor: 1

Replicate Data: dose-2.0_pH5-reading1

Repl#	Analyte	Net Intensity	Corrected Intensity	Calib. Conc. Units	Sample Conc. Units	Analysis Time
1	Ni 231.604	746263.4	747080.0	10.82 mg/L	10.82 mg/L	3:00:14 PM
2	Ni 231.604	753285.2	754101.8	10.92 mg/L	10.92 mg/L	3:00:17 PM
3	Ni 231.604	756042.9	756859.4	10.96 mg/L	10.96 mg/L	3:00:19 PM

Mean Data: dose-2.0_pH5-reading1

Analyte	Mean Corrected Intensity	Calib. Conc. Units	Std.Dev.	Sample Conc. Units	Std.Dev.	RSD
Ni 231.604	752680.4	10.90 mg/L	0.068	10.90 mg/L	0.068	0.63%

Sequence No.: 2

Sample ID: dose_2.0g-pH6

Analyst:

Initial Sample Wt:

Dilution:

Wash Time: 120

Autosampler Location: 9

Date Collected: 2/26/2020 9:31:11 AM

Data Type: Original

Initial Sample Vol:

Sample Prep Vol:

Auto Dilution Factor: 1

Replicate Data: dose_2.0g-pH6

Repl#	Analyte	Net Intensity	Corrected Intensity	Calib. Conc. Units	Sample Conc. Units	Analysis Time
1	Ni 231.604	724904.9	725721.5	10.53 mg/L	10.53 mg/L	9:32:19 AM
2	Ni 231.604	734679.9	735496.5	10.67 mg/L	10.67 mg/L	9:32:23 AM
3	Ni 231.604	747428.6	748245.2	10.84 mg/L	10.84 mg/L	9:32:25 AM

Mean Data: dose_2.0g-pH6

Analyte	Mean Corrected Intensity	Calib. Conc. Units	Std.Dev.	Sample Conc. Units	Std.Dev.	RSD
Ni 231.604	736487.7	10.68 mg/L	0.153	10.68 mg/L	0.153	1.43%

Sequence No.: 3

Sample ID: dose_2.5g-pH6

Analyst:

Initial Sample Wt:

Dilution:

Autosampler Location: 10

Date Collected: 2/26/2020 9:34:36 AM

Data Type: Original

Initial Sample Vol:

Sample Prep Vol:

Sequence No.: 3
Sample ID: dose_2.5g-pH6_reading2
Analyst:
Initial Sample Wt:
Dilution:
Wash Time: 120

Autosampler Location: 10
Date Collected: 2/26/2020 9:52:56 AM
Data Type: Original
Initial Sample Vol:
Sample Prep Vol:
Auto Dilution Factor: 1

Replicate Data: dose_2.5g-pH6_reading2

Repl#	Analyte	Net Intensity	Corrected Intensity	Calib. Conc. Units	Sample Conc. Units	Analysis Time
1	Ni 231.604	850517.2	851333.8	12.24 mg/L	12.24 mg/L	9:54:05 AM
2	Ni 231.604	870025.8	870842.4	12.50 mg/L	12.50 mg/L	9:54:07 AM
3	Ni 231.604	849281.8	850098.4	12.22 mg/L	12.22 mg/L	9:54:09 AM

Mean Data: dose_2.5g-pH6_reading2

Analyte	Mean Corrected Intensity	Calib. Conc. Units	Std.Dev.	Sample Conc. Units	Std.Dev.	RSD
Ni 231.604	857424.9	12.32 mg/L	0.158	12.32 mg/L	0.158	1.28%

Sequence No.: 4
Sample ID: dose_3.0g-pH6
Analyst:
Initial Sample Wt:
Dilution:
Wash Time: 120

Autosampler Location: 11
Date Collected: 2/26/2020 9:38:00 AM
Data Type: Original
Initial Sample Vol:
Sample Prep Vol:
Auto Dilution Factor: 1

Replicate Data: dose_3.0g-pH6

Repl#	Analyte	Net Intensity	Corrected Intensity	Calib. Conc. Units	Sample Conc. Units	Analysis Time
1	Ni 231.604	624210.7	625027.3	9.168 mg/L	9.168 mg/L	9:39:09 AM
2	Ni 231.604	633472.5	634289.1	9.293 mg/L	9.293 mg/L	9:39:11 AM
3	Ni 231.604	627478.2	628294.8	9.212 mg/L	9.212 mg/L	9:39:14 AM

Mean Data: dose_3.0g-pH6

Analyte	Mean Corrected Intensity	Calib. Conc. Units	Std.Dev.	Sample Conc. Units	Std.Dev.	RSD
Ni 231.604	629203.7	9.224 mg/L	0.0637	9.224 mg/L	0.0637	0.69%

Sequence No.: 5
Sample ID: dose_3.5g-pH6
Analyst:
Initial Sample Wt:
Dilution:
Wash Time: 120

Autosampler Location: 12
Date Collected: 2/26/2020 9:41:25 AM
Data Type: Original
Initial Sample Vol:
Sample Prep Vol:
Auto Dilution Factor: 1

Replicate Data: dose_3.5g-pH6

Repl#	Analyte	Net Intensity	Corrected Intensity	Calib. Conc. Units	Sample Conc. Units	Analysis Time
1	Ni 231.604	551398.0	552214.6	8.180 mg/L	8.180 mg/L	9:42:34 AM
2	Ni 231.604	564455.2	565271.8	8.357 mg/L	8.357 mg/L	9:42:38 AM
3	Ni 231.604	566514.4	567331.0	8.385 mg/L	8.385 mg/L	9:42:40 AM

Mean Data: dose_3.5g-pH6

Analyte	Mean Corrected Intensity	Calib. Conc. Units	Std.Dev.	Sample Conc. Units	Std.Dev.	RSD
Ni 231.604	561605.8	8.307 mg/L	0.1112	8.307 mg/L	0.1112	1.34%

=====

Sequence No.: 2

Sample ID: dose_2.0g-pH6_reading2

Analyst:

Initial Sample Wt:

Dilution:

Wash Time: 120

Autosampler Location: 9

Date Collected: 2/26/2020 9:49:32 AM

Data Type: Original

Initial Sample Vol:

Sample Prep Vol:

Auto Dilution Factor: 1

Replicate Data: dose_2.0g-pH6_reading2

Repl#	Analyte	Net Intensity	Corrected Intensity	Calib. Conc. Units	Sample Conc. Units	Analysis Time
1	Ni 231.604	728940.3	729756.9	10.59 mg/L	10.59 mg/L	9:50:40 AM
2	Ni 231.604	718942.1	719758.7	10.45 mg/L	10.45 mg/L	9:50:43 AM
3	Ni 231.604	711392.5	712209.1	10.35 mg/L	10.35 mg/L	9:50:45 AM

Mean Data: dose_2.0g-pH6_reading2

Analyte	Mean Corrected Intensity	Calib. Conc. Units	Std.Dev.	Sample Conc. Units	Std.Dev.	RSD
Ni 231.604	720574.9	10.46 mg/L	0.119	10.46 mg/L	0.119	1.14%

=====

Sequence No.: 3

Sample ID: dose_2.5g-pH6_reading2

Analyst:

Initial Sample Wt:

Dilution:

Wash Time: 120

Autosampler Location: 10

Date Collected: 2/26/2020 9:52:56 AM

Data Type: Original

Initial Sample Vol:

Sample Prep Vol:

Auto Dilution Factor: 1

Replicate Data: dose_2.5g-pH6_reading2

Repl#	Analyte	Net Intensity	Corrected Intensity	Calib. Conc. Units	Sample Conc. Units	Analysis Time
1	Ni 231.604	850517.2	851333.8	12.24 mg/L	12.24 mg/L	9:54:05 AM
2	Ni 231.604	870025.8	870842.4	12.50 mg/L	12.50 mg/L	9:54:07 AM
3	Ni 231.604	849281.8	850098.4	12.22 mg/L	12.22 mg/L	9:54:09 AM

Mean Data: dose_2.5g-pH6_reading2

Analyte	Mean Corrected Intensity	Calib. Conc. Units	Std.Dev.	Sample Conc. Units	Std.Dev.	RSD
Ni 231.604	857424.9	12.32 mg/L	0.158	12.32 mg/L	0.158	1.28%

Sequence No.: 4
Sample ID: dose_3.0g-pH6_reading2
Analyst:
Initial Sample Wt:
Dilution:
Wash Time: 120

Autosampler Location: 11
Date Collected: 2/26/2020 9:56:20 AM
Data Type: Original
Initial Sample Vol:
Sample Prep Vol:
Auto Dilution Factor: 1

Replicate Data: dose_3.0g-pH6_reading2

Repl#	Analyte	Net Intensity	Corrected Intensity	Calib. Conc. Units	Sample Conc. Units	Analysis Time
1	Ni 231.604	617003.3	617819.9	9.070 mg/L	9.070 mg/L	9:57:30 AM
2	Ni 231.604	625560.0	626376.6	9.186 mg/L	9.186 mg/L	9:57:32 AM
3	Ni 231.604	621397.2	622213.8	9.129 mg/L	9.129 mg/L	9:57:34 AM

Mean Data: dose_3.0g-pH6_reading2

Analyte	Mean Corrected Intensity	Calib. Conc. Units	Std.Dev.	Sample Conc. Units	Std.Dev.	RSD
Ni 231.604	622136.8	9.128 mg/L	0.0580	9.128 mg/L	0.0580	0.64%

Sequence No.: 5
Sample ID: dose_3.5g-pH6_reading2
Analyst:
Initial Sample Wt:
Dilution:
Wash Time: 120

Autosampler Location: 12
Date Collected: 2/26/2020 9:59:46 AM
Data Type: Original
Initial Sample Vol:
Sample Prep Vol:
Auto Dilution Factor: 1

Replicate Data: dose_3.5g-pH6_reading2

Repl#	Analyte	Net Intensity	Corrected Intensity	Calib. Conc. Units	Sample Conc. Units	Analysis Time
1	Ni 231.604	547693.3	548509.9	8.130 mg/L	8.130 mg/L	10:00:55 AM
2	Ni 231.604	543930.8	544747.4	8.078 mg/L	8.078 mg/L	10:00:58 AM
3	Ni 231.604	540066.3	540882.9	8.026 mg/L	8.026 mg/L	10:01:00 AM

Mean Data: dose_3.5g-pH6_reading2

Analyte	Mean Corrected Intensity	Calib. Conc. Units	Std.Dev.	Sample Conc. Units	Std.Dev.	RSD
Ni 231.604	544713.4	8.078 mg/L	0.0517	8.078 mg/L	0.0517	0.64%

Sequence No.: 4
Sample ID: dose_3.0g-pH6_reading2
Analyst:
Initial Sample Wt:
Dilution:
Wash Time: 120

Autosampler Location: 11
Date Collected: 2/26/2020 9:56:20 AM
Data Type: Original
Initial Sample Vol:
Sample Prep Vol:
Auto Dilution Factor: 1

Replicate Data: dose_3.0g-pH6_reading2

Repl#	Analyte	Net Intensity	Corrected Intensity	Calib. Conc. Units	Sample Conc. Units	Analysis Time
1	Ni 231.604	617003.3	617819.9	9.070 mg/L	9.070 mg/L	9:57:30 AM
2	Ni 231.604	625560.0	626376.6	9.186 mg/L	9.186 mg/L	9:57:32 AM
3	Ni 231.604	621397.2	622213.8	9.129 mg/L	9.129 mg/L	9:57:34 AM

Mean Data: dose_3.0g-pH6_reading2

Analyte	Mean Corrected Intensity	Calib. Conc. Units	Std.Dev.	Sample Conc. Units	Std.Dev.	RSD
Ni 231.604	622136.8	9.128 mg/L	0.0580	9.128 mg/L	0.0580	0.64%

Sequence No.: 5
Sample ID: dose_3.5g-pH6_reading2
Analyst:
Initial Sample Wt:
Dilution:
Wash Time: 120

Autosampler Location: 12
Date Collected: 2/26/2020 9:59:46 AM
Data Type: Original
Initial Sample Vol:
Sample Prep Vol:
Auto Dilution Factor: 1

Replicate Data: 3g-pH4-reading2

Repl#	Analyte	Net Intensity	Corrected Intensity	Calib. Conc. Units	Sample Conc. Units	Analysis Time
1	Ni 231.604	1238397.2	1239213.8	17.50 mg/L	17.50 mg/L	2:40:03 PM
2	Ni 231.604	1220301.0	1221117.6	17.25 mg/L	17.25 mg/L	2:40:06 PM
3	Ni 231.604	1214705.5	1215522.1	17.18 mg/L	17.18 mg/L	2:40:08 PM

Mean Data: 3g-pH4-reading2

Analyte	Mean Corrected Intensity	Calib. Conc. Units	Std.Dev.	Sample Conc. Units	Std.Dev.	RSD
Ni 231.604	1225284.5	17.31 mg/L	0.168	17.31 mg/L	0.168	0.97%

Sequence No.: 4
Sample ID: 2.5g-pH5-reading2
Analyst:
Initial Sample Wt:
Dilution:
Wash Time: 90

Autosampler Location: 11
Date Collected: 3/17/2020 2:41:49 PM
Data Type: Original
Initial Sample Vol:
Sample Prep Vol:
Auto Dilution Factor: 1

Replicate Data: 2.5g-pH5-reading2

Repl#	Analyte	Net Intensity	Corrected Intensity	Calib. Conc. Units	Sample Conc. Units	Analysis Time
1	Ni 231.604	708816.6	709633.2	10.32 mg/L	10.32 mg/L	2:42:58 PM
2	Ni 231.604	708292.2	709108.8	10.31 mg/L	10.31 mg/L	2:43:00 PM
3	Ni 231.604	715441.0	716257.6	10.41 mg/L	10.41 mg/L	2:43:02 PM

Mean Data: 2.5g-pH5-reading2

Analyte	Mean Corrected Intensity	Calib. Conc. Units	Std.Dev.	Sample Conc. Units	Std.Dev.	RSD
Ni 231.604	711666.5	10.34 mg/L	0.054	10.34 mg/L	0.054	0.52%

=====

Sequence No.: 5

Sample ID: 3g-pH5-reading2

Analyst:

Initial Sample Wt:

Dilution:

Wash Time: 90

Autosampler Location: 12

Date Collected: 3/17/2020 2:44:43 PM

Data Type: Original

Initial Sample Vol:

Sample Prep Vol:

Auto Dilution Factor: 1

Replicate Data: 3g-pH5-reading2

Repl#	Analyte	Net Intensity	Corrected Intensity	Calib. Conc. Units	Sample Conc. Units	Analysis Time
1	Ni 231.604	442178.6	442995.2	6.698 mg/L	6.698 mg/L	2:45:52 PM
2	Ni 231.604	466839.9	467656.5	7.033 mg/L	7.033 mg/L	2:45:56 PM
3	Ni 231.604	476185.7	477002.3	7.159 mg/L	7.159 mg/L	2:45:59 PM

Mean Data: 3g-pH5-reading2

Analyte	Mean Corrected Intensity	Calib. Conc. Units	Std.Dev.	Sample Conc. Units	Std.Dev.	RSD
Ni 231.604	462551.3	6.963 mg/L	0.2383	6.963 mg/L	0.2383	3.42%

=====

Sequence No.: 6

Sample ID: 2.5g-pH6-reading2

Analyst:

Initial Sample Wt:

Dilution:

Wash Time: 90

Autosampler Location: 13

Date Collected: 3/17/2020 2:47:41 PM

Data Type: Original

Initial Sample Vol:

Sample Prep Vol:

Auto Dilution Factor: 1

Replicate Data: 2.5g-pH6-reading2

Repl#	Analyte	Net Intensity	Corrected Intensity	Calib. Conc. Units	Sample Conc. Units	Analysis Time
1	Ni 231.604	358954.4	359771.0	5.569 mg/L	5.569 mg/L	2:48:50 PM
2	Ni 231.604	348411.5	349228.1	5.426 mg/L	5.426 mg/L	2:48:54 PM
3	Ni 231.604	352275.2	353091.7	5.478 mg/L	5.478 mg/L	2:48:58 PM

Mean Data: 2.5g-pH6-reading2

Analyte	Mean Corrected Intensity	Calib. Conc. Units	Std.Dev.	Sample Conc. Units	Std.Dev.	RSD
Ni 231.604	354030.3	5.491 mg/L	0.0724	5.491 mg/L	0.0724	1.32%

Sequence No.: 7

Sample ID: 4g-pH6-reading2

Analyst:

Initial Sample Wt:

Dilution:

Wash Time: 90

Autosampler Location: 14

Date Collected: 3/17/2020 2:50:40 PM

Data Type: Original

Initial Sample Vol:

Sample Prep Vol:

Auto Dilution Factor: 1

Replicate Data: 4g-pH6-reading2

Repl#	Analyte	Net Intensity	Corrected Intensity	Calib. Conc. Units	Sample Conc. Units	Analysis Time
1	Ni 231.604	657404.8	658221.4	9.618 mg/L	9.618 mg/L	2:51:48 PM
2	Ni 231.604	664979.1	665795.7	9.721 mg/L	9.721 mg/L	2:51:50 PM
3	Ni 231.604	674660.0	675476.6	9.852 mg/L	9.852 mg/L	2:51:52 PM

Mean Data: 4g-pH6-reading2

Analyte	Mean Corrected Intensity	Calib. Conc. Units	Std.Dev.	Sample Conc. Units	Std.Dev.	RSD
Ni 231.604	666497.9	9.730 mg/L	0.1173	9.730 mg/L	0.1173	1.21%

Sequence No.: 8

Sample ID: 2g-pH7-reading2

Analyst:

Initial Sample Wt:

Dilution:

Wash Time: 90

Autosampler Location: 15

Date Collected: 3/17/2020 2:53:33 PM

Data Type: Original

Initial Sample Vol:

Sample Prep Vol:

Auto Dilution Factor: 1

Replicate Data: 2g-pH7-reading2

Repl#	Analyte	Net Intensity	Corrected Intensity	Calib. Conc. Units	Sample Conc. Units	Analysis Time
1	Ni 231.604	335857.6	336674.2	5.256 mg/L	5.256 mg/L	2:54:41 PM
2	Ni 231.604	340302.1	341118.7	5.316 mg/L	5.316 mg/L	2:54:44 PM
3	Ni 231.604	340587.5	341404.1	5.320 mg/L	5.320 mg/L	2:54:48 PM

Mean Data: 2g-pH7-reading2

Analyte	Mean Corrected Intensity	Calib. Conc. Units	Std.Dev.	Sample Conc. Units	Std.Dev.	RSD
Ni 231.604	339732.3	5.297 mg/L	0.0360	5.297 mg/L	0.0360	0.68%

Sequence No.: 9
Sample ID: 2.5g-pH7-reading2
Analyst:
Initial Sample Wt:
Dilution:
Wash Time: 90

Autosampler Location: 16
Date Collected: 3/17/2020 2:56:29 PM
Data Type: Original
Initial Sample Vol:
Sample Prep Vol:
Auto Dilution Factor: 1

Replicate Data: 2.5g-pH7-reading2

Repl#	Analyte	Net Intensity	Corrected Intensity	Calib. Conc. Units	Sample Conc. Units	Analysis Time
1	Ni 231.604	340875.5	341692.1	5.324 mg/L	5.324 mg/L	2:57:37 PM
2	Ni 231.604	337030.2	337846.8	5.272 mg/L	5.272 mg/L	2:57:40 PM
3	Ni 231.604	344828.2	345644.7	5.377 mg/L	5.377 mg/L	2:57:43 PM

Mean Data: 2.5g-pH7-reading2

Analyte	Mean Corrected Intensity	Calib. Conc. Units	Std.Dev.	Sample Conc. Units	Std.Dev.	RSD
Ni 231.604	341727.9	5.324 mg/L	0.0529	5.324 mg/L	0.0529	0.99%

Sequence No.: 10
Sample ID: 3g-pH7-reading2
Analyst:
Initial Sample Wt:
Dilution:
Wash Time: 90

Autosampler Location: 17
Date Collected: 3/17/2020 2:59:24 PM
Data Type: Original
Initial Sample Vol:
Sample Prep Vol:
Auto Dilution Factor: 1

Replicate Data: 3g-pH7-reading2

Repl#	Analyte	Net Intensity	Corrected Intensity	Calib. Conc. Units	Sample Conc. Units	Analysis Time
1	Ni 231.604	382918.4	383735.0	5.894 mg/L	5.894 mg/L	3:00:32 PM
2	Ni 231.604	386285.9	387102.4	5.940 mg/L	5.940 mg/L	3:00:35 PM
3	Ni 231.604	385844.1	386660.6	5.934 mg/L	5.934 mg/L	3:00:37 PM

Mean Data: 3g-pH7-reading2

Analyte	Mean Corrected Intensity	Calib. Conc. Units	Std.Dev.	Sample Conc. Units	Std.Dev.	RSD
Ni 231.604	385832.7	5.923 mg/L	0.0248	5.923 mg/L	0.0248	0.42%

Sequence No.: 11

Sample ID: 3.5g-pH7-reading2

Analyst:

Initial Sample Wt:

Dilution:

Wash Time: 90

Autosampler Location: 18

Date Collected: 3/17/2020 3:02:18 PM

Data Type: Original

Initial Sample Vol:

Sample Prep Vol:

Auto Dilution Factor: 1

Replicate Data: 3.5g-pH7-reading2

Repl#	Analyte	Net Intensity	Corrected Intensity	Calib. Conc. Units	Sample Conc. Units	Analysis Time
1	Ni 231.604	368783.1	369599.6	5.702 mg/L	5.702 mg/L	3:03:26 PM
2	Ni 231.604	363301.0	364117.6	5.628 mg/L	5.628 mg/L	3:03:29 PM
3	Ni 231.604	370460.3	371276.9	5.725 mg/L	5.725 mg/L	3:03:32 PM

Mean Data: 3.5g-pH7-reading2

Analyte	Mean Corrected Intensity	Calib. Conc. Units	Std.Dev.	Sample Conc. Units	Std.Dev.	RSD
Ni 231.604	368331.4	5.685 mg/L	0.0508	5.685 mg/L	0.0508	0.89%

Sequence No.: 12

Sample ID: 4g-pH7-reading2

Analyst:

Initial Sample Wt:

Dilution:

Wash Time: 90

Autosampler Location: 19

Date Collected: 3/17/2020 3:05:13 PM

Data Type: Original

Initial Sample Vol:

Sample Prep Vol:

Auto Dilution Factor: 1

Replicate Data: 4g-pH7-reading2

Repl#	Analyte	Net Intensity	Corrected Intensity	Calib. Conc. Units	Sample Conc. Units	Analysis Time
1	Ni 231.604	599964.2	600780.7	8.839 mg/L	8.839 mg/L	3:06:21 PM
2	Ni 231.604	608385.8	609202.4	8.953 mg/L	8.953 mg/L	3:06:24 PM
3	Ni 231.604	606452.7	607269.3	8.927 mg/L	8.927 mg/L	3:06:26 PM

Mean Data: 4g-pH7-reading2

Analyte	Mean Corrected Intensity	Calib. Conc. Units	Std.Dev.	Sample Conc. Units	Std.Dev.	RSD
Ni 231.604	605750.8	8.906 mg/L	0.0598	8.906 mg/L	0.0598	0.67%

Sequence No.: 13
Sample ID: 4g-pH8-reading2
Analyst:
Initial Sample Wt:
Dilution:
Wash Time: 90

Autosampler Location: 20
Date Collected: 3/17/2020 3:08:07 PM
Data Type: Original
Initial Sample Vol:
Sample Prep Vol:
Auto Dilution Factor: 1

Replicate Data: 4g-pH8-reading2

Repl#	Analyte	Net Intensity	Corrected Intensity	Calib. Conc. Units	Sample Conc. Units	Analysis Time
1	Ni 231.604	837591.6	838408.2	12.06 mg/L	12.06 mg/L	3:09:15 PM
2	Ni 231.604	846502.9	847319.5	12.18 mg/L	12.18 mg/L	3:09:17 PM
3	Ni 231.604	855348.4	856164.9	12.30 mg/L	12.30 mg/L	3:09:20 PM

Mean Data: 4g-pH8-reading2

Analyte	Mean Corrected Intensity	Calib. Conc. Units	Std.Dev.	Sample Conc. Units	Std.Dev.	RSD
Ni 231.604	847297.5	12.18 mg/L	0.120	12.18 mg/L	0.120	0.99%

Sequence No.: 14
Sample ID: 3.5g-pH8-reading2
Analyst:
Initial Sample Wt:
Dilution:
Wash Time: 90

Autosampler Location: 21
Date Collected: 3/17/2020 3:11:00 PM
Data Type: Original
Initial Sample Vol:
Sample Prep Vol:
Auto Dilution Factor: 1

Replicate Data: 3.5g-pH8-reading2

Repl#	Analyte	Net Intensity	Corrected Intensity	Calib. Conc. Units	Sample Conc. Units	Analysis Time
1	Ni 231.604	902834.0	903650.6	12.95 mg/L	12.95 mg/L	3:12:08 PM
2	Ni 231.604	878879.9	879696.5	12.62 mg/L	12.62 mg/L	3:12:11 PM
3	Ni 231.604	908187.9	909004.5	13.02 mg/L	13.02 mg/L	3:12:13 PM

Mean Data: 3.5g-pH8-reading2

Analyte	Mean Corrected Intensity	Calib. Conc. Units	Std.Dev.	Sample Conc. Units	Std.Dev.	RSD
Ni 231.604	897450.5	12.86 mg/L	0.212	12.86 mg/L	0.212	1.65%

Sequence No.: 15
Sample ID: 3g-pH8-reading2
Analyst:
Initial Sample Wt:
Dilution:
Wash Time: 90

Autosampler Location: 22
Date Collected: 3/17/2020 3:13:53 PM
Data Type: Original
Initial Sample Vol:
Sample Prep Vol:
Auto Dilution Factor: 1

Replicate Data: 3g-pH8-reading2

Repl#	Analyte	Net Intensity	Corrected Intensity	Calib. Conc. Units	Sample Conc. Units	Analysis Time
1	Ni 231.604	951797.0	952613.6	13.61 mg/L	13.61 mg/L	3:15:02 PM
2	Ni 231.604	991310.7	992127.3	14.15 mg/L	14.15 mg/L	3:15:05 PM
3	Ni 231.604	983998.7	984815.3	14.05 mg/L	14.05 mg/L	3:15:07 PM

Mean Data: 3g-pH8-reading2

Analyte	Mean Corrected Intensity	Calib. Conc. Units	Std.Dev.	Sample Conc. Units	Std.Dev.	RSD
Ni 231.604	976518.7	13.94 mg/L	0.285	13.94 mg/L	0.285	2.05%

Sequence No.: 16

Autosampler Location: 23

Sample ID: 2.5g-pH8-reading2

Date Collected: 3/17/2020 3:16:48 PM

Analyst:

Data Type: Original

Initial Sample Wt:

Initial Sample Vol:

Dilution:

Sample Prep Vol:

Wash Time: 90

Auto Dilution Factor: 1

Replicate Data: 2.5g-pH8-reading2

Repl#	Analyte	Net Intensity	Corrected Intensity	Calib. Conc. Units	Sample Conc. Units	Analysis Time
1	Ni 231.604	1601415.1	1602231.6	22.42 mg/L	22.42 mg/L	3:17:57 PM
2	Ni 231.604	1593807.5	1594624.1	22.32 mg/L	22.32 mg/L	3:17:59 PM
3	Ni 231.604	1642608.4	1643425.0	22.98 mg/L	22.98 mg/L	3:18:01 PM

Mean Data: 2.5g-pH8-reading2

Analyte	Mean Corrected Intensity	Calib. Conc. Units	Std.Dev.	Sample Conc. Units	Std.Dev.	RSD
Ni 231.604	1613426.9	22.58 mg/L	0.356	22.58 mg/L	0.356	1.58%

Sequence No.: 17

Autosampler Location: 24

Sample ID: 2g-pH8-reading2

Date Collected: 3/17/2020 3:19:42 PM

Analyst:

Data Type: Original

Initial Sample Wt:

Initial Sample Vol:

Dilution:

Sample Prep Vol:

Wash Time: 90

Auto Dilution Factor: 1

Replicate Data: 2g-pH8-reading2

Repl#	Analyte	Net Intensity	Corrected Intensity	Calib. Conc. Units	Sample Conc. Units	Analysis Time
1	Ni 231.604	2174200.1	2175016.7	30.20 mg/L	30.20 mg/L	3:20:51 PM
2	Ni 231.604	2224354.3	2225170.9	30.88 mg/L	30.88 mg/L	3:20:53 PM
3	Ni 231.604	2218032.9	2218849.5	30.79 mg/L	30.79 mg/L	3:20:56 PM

Mean Data: 2g-pH8-reading2

Analyte	Mean Corrected Intensity	Calib. Conc. Units	Std.Dev.	Sample Conc. Units	Std.Dev.	RSD
Ni 231.604	2206345.7	30.62 mg/L	0.371	30.62 mg/L	0.371	1.21%

=====
Analysis Begun

Start Time: 1/22/2020 1:58:47 PM

Plasma On Time: 1/22/2020 1:51:38 PM

Logged In Analyst: Perkin Elmer

Technique: ICP Continuous

Spectrometer: Optima 7000

Autosampler: S10

Sample Information File: C:\Documents and Settings\All Users\PerkinElmer\ICP\Data\Sample Information\
dhivesh, prescreening.sif

Batch ID:

Results Data Set: chromium vi

Results Library: C:\Documents and Settings\Perkin Elmer\Desktop\student results\2020\dhivesh\
Results.mdb

Sequence No.: 1

Autosampler Location: 7

Sample ID: blank

Date Collected: 1/22/2020 1:58:47 PM

Analyst:

Data Type: Original

Initial Sample Wt:

Initial Sample Vol:

Dilution:

Sample Prep Vol:

Wash Time:

Replicate Data: blank

Repl#	Analyte	Net Intensity	Corrected Intensity	Calib. Conc. Units	Sample Conc. Units	Analysis Time
1	Cr 267.716	702.4	-147.4	0.089 mg/L	0.089 mg/L	1:59:55 PM
2	Cr 267.716	826.4	-23.4	0.090 mg/L	0.090 mg/L	2:00:04 PM
3	Cr 267.716	819.6	-30.2	0.090 mg/L	0.090 mg/L	2:00:14 PM

Mean Data: blank

Analyte	Mean Corrected Intensity	Calib. Conc. Units	Std.Dev.	Sample Conc. Units	Std.Dev.	RSD
Cr 267.716	-67.0	0.090 mg/L	0.0002	0.090 mg/L	0.0002	0.22%

QC value within limits for Cr 267.716 Recovery = Not calculated

All analyte(s) passed QC.

Sequence No.: 2

Autosampler Location: 9

Sample ID: stock

Date Collected: 1/22/2020 2:02:31 PM

Analyst:

Data Type: Original

Initial Sample Wt:

Initial Sample Vol:

Dilution:

Sample Prep Vol:

Wash Time: 120

Auto Dilution Factor: 1

Replicate Data: stock

Repl#	Analyte	Net Intensity	Corrected Intensity	Calib. Conc. Units	Sample Conc. Units	Analysis Time
1	Cr 267.716	24738828.4	24737978.6	71.07 mg/L	71.07 mg/L	2:03:39 PM
2	Cr 267.716	25106314.8	25105465.0	72.13 mg/L	72.13 mg/L	2:03:44 PM
3	Cr 267.716	24741778.1	24740928.3	71.08 mg/L	71.08 mg/L	2:03:48 PM

Mean Data: stock

Analyte	Mean Corrected Intensity	Calib. Conc. Units	Std.Dev.	Sample Conc. Units	Std.Dev.	RSD
Cr 267.716	24861457.3	71.43 mg/L	0.606	71.43 mg/L	0.606	0.85%

Sequence No.: 3

Autosampler Location: 10

Sample ID: green tea cr

Date Collected: 1/22/2020 2:06:01 PM

Analyst:

Data Type: Original

Initial Sample Wt:

Initial Sample Vol:

Dilution:

Sample Prep Vol:

Wash Time: 120

Auto Dilution Factor: 1

Replicate Data: green tea cr

Repl#	Analyte	Net Intensity	Corrected Intensity	Calib. Conc. Units	Sample Conc. Units	Analysis Time
1	Cr 267.716	2238631.3	2237781.5	6.511 mg/L	6.511 mg/L	2:07:09 PM
2	Cr 267.716	2236288.6	2235438.8	6.504 mg/L	6.504 mg/L	2:07:12 PM
3	Cr 267.716	2169321.4	2168471.6	6.312 mg/L	6.312 mg/L	2:07:14 PM

Mean Data: green tea cr

Analyte	Mean Corrected Intensity	Calib. Conc. Units	Std.Dev.	Sample Conc. Units	Std.Dev.	RSD
Cr 267.716	2213897.3	6.442 mg/L	0.1129	6.442 mg/L	0.1129	1.75%

=====

Sequence No.: 4	Autosampler Location: 11
Sample ID: geinmacha cr	Date Collected: 1/22/2020 2:09:25 PM
Analyst:	Data Type: Original
Initial Sample Wt:	Initial Sample Vol:
Dilution:	Sample Prep Vol:
Wash Time: 120	Auto Dilution Factor: 1

Replicate Data: geinmacha cr

Repl#	Analyte	Net Intensity	Corrected Intensity	Calib. Conc. Units	Sample Conc. Units	Analysis Time
1	Cr 267.716	2981699.8	2980850.0	8.643 mg/L	8.643 mg/L	2:10:34 PM
2	Cr 267.716	2992999.7	2992149.9	8.675 mg/L	8.675 mg/L	2:10:36 PM
3	Cr 267.716	2962227.7	2961377.9	8.587 mg/L	8.587 mg/L	2:10:38 PM

Mean Data: geinmacha cr

Analyte	Mean Corrected Intensity	Calib. Conc. Units	Std.Dev.	Sample Conc. Units	Std.Dev.	RSD
Cr 267.716	2978125.9	8.635 mg/L	0.0447	8.635 mg/L	0.0447	0.52%

=====

Sequence No.: 5	Autosampler Location: 12
Sample ID: salted peanut cr	Date Collected: 1/22/2020 2:12:50 PM
Analyst:	Data Type: Original
Initial Sample Wt:	Initial Sample Vol:
Dilution:	Sample Prep Vol:
Wash Time: 120	Auto Dilution Factor: 1

Replicate Data: salted peanut cr

Repl#	Analyte	Net Intensity	Corrected Intensity	Calib. Conc. Units	Sample Conc. Units	Analysis Time
1	Cr 267.716	4980606.4	4979756.6	14.38 mg/L	14.38 mg/L	2:13:59 PM
2	Cr 267.716	4988277.8	4987428.0	14.40 mg/L	14.40 mg/L	2:14:02 PM
3	Cr 267.716	5049161.3	5048311.5	14.58 mg/L	14.58 mg/L	2:14:04 PM

Mean Data: salted peanut cr

Analyte	Mean Corrected Intensity	Calib. Conc. Units	Std.Dev.	Sample Conc. Units	Std.Dev.	RSD
Cr 267.716	5005165.4	14.45 mg/L	0.108	14.45 mg/L	0.108	0.75%

=====

Sequence No.: 6	Autosampler Location: 13
Sample ID: unsalted peanut cr	Date Collected: 1/22/2020 2:16:16 PM
Analyst:	Data Type: Original
Initial Sample Wt:	Initial Sample Vol:
Dilution:	Sample Prep Vol:
Wash Time: 120	Auto Dilution Factor: 1

Replicate Data: unsalted peanut cr

Repl#	Analyte	Net Intensity	Corrected Intensity	Calib. Conc. Units	Sample Conc. Units	Analysis Time
-------	---------	---------------	---------------------	--------------------	--------------------	---------------

Repl#	Analyte	Intensity	Intensity	Conc. Units	Conc. Units	Time
1	Cr 267.716	12067679.8	12066830.0	34.71 mg/L	34.71 mg/L	2:17:25 PM
2	Cr 267.716	12219250.4	12218400.6	35.15 mg/L	35.15 mg/L	2:17:29 PM
3	Cr 267.716	12202991.5	12202141.7	35.10 mg/L	35.10 mg/L	2:17:32 PM

Mean Data: unsalted peanut cr

Analyte	Mean Corrected Intensity	Calib. Conc. Units	Std.Dev.	Sample Conc. Units	Std.Dev.	RSD
Cr 267.716	12162457.4	34.99 mg/L	0.239	34.99 mg/L	0.239	0.68%

=====

Sequence No.: 7

Sample ID: 60ppm

Analyst:

Initial Sample Wt:

Dilution:

Wash Time: 120

User canceled analysis.

Autosampler Location: 8

Date Collected: 1/22/2020 2:19:44 PM

Data Type: Original

Initial Sample Vol:

Sample Prep Vol:

Auto Dilution Factor: 1

Sequence No.: 2
Sample ID: dose_2.5g-pH2_reading1
Analyst:
Initial Sample Wt:
Dilution:
Wash Time: 120

Autosampler Location: 9
Date Collected: 2/26/2020 10:24:03 AM
Data Type: Original
Initial Sample Vol:
Sample Prep Vol:
Auto Dilution Factor: 1

Replicate Data: dose_2.5g-pH2_reading1

Repl#	Analyte	Net Intensity	Corrected Intensity	Calib. Conc. Units	Sample Conc. Units	Analysis Time
1	Cr 267.716	9300794.0	9299944.2	26.77 mg/L	26.77 mg/L	10:25:12 AM
2	Cr 267.716	9347782.8	9346933.0	26.91 mg/L	26.91 mg/L	10:25:15 AM
3	Cr 267.716	9360972.0	9360122.2	26.95 mg/L	26.95 mg/L	10:25:18 AM

Mean Data: dose_2.5g-pH2_reading1

Analyte	Mean Corrected Intensity	Calib. Conc. Units	Std.Dev.	Sample Conc. Units	Std.Dev.	RSD
Cr 267.716	9335666.5	26.88 mg/L	0.091	26.88 mg/L	0.091	0.34%

Sequence No.: 3
Sample ID: dose_3g-pH2_reading1
Analyst:
Initial Sample Wt:
Dilution:

Autosampler Location: 10
Date Collected: 2/26/2020 10:27:31 AM
Data Type: Original
Initial Sample Vol:
Sample Prep Vol:

Wash Time: 120

Auto Dilution Factor: 1

Replicate Data: dose_3g-pH2_reading1

Repl#	Analyte	Net Intensity	Corrected Intensity	Calib. Conc. Units	Sample Conc. Units	Analysis Time
1	Cr 267.716	5609983.3	5609133.5	16.18 mg/L	16.18 mg/L	10:28:40 AM
2	Cr 267.716	5587330.7	5586480.9	16.12 mg/L	16.12 mg/L	10:28:42 AM
3	Cr 267.716	5634153.7	5633303.9	16.25 mg/L	16.25 mg/L	10:28:45 AM

Mean Data: dose_3g-pH2_reading1

Analyte	Mean Corrected Intensity	Calib. Conc. Units	Std.Dev.	Sample Conc. Units	Std.Dev.	RSD
Cr 267.716	5609639.5	16.19 mg/L	0.067	16.19 mg/L	0.067	0.42%

Sequence No.: 4
Sample ID: dose_3.5g-pH2_reading1
Analyst:
Initial Sample Wt:
Dilution:
Wash Time: 120

Autosampler Location: 11
Date Collected: 2/26/2020 10:30:56 AM
Data Type: Original
Initial Sample Vol:
Sample Prep Vol:
Auto Dilution Factor: 1

Replicate Data: dose_3.5g-pH2_reading1

Repl#	Analyte	Net Intensity	Corrected Intensity	Calib. Conc. Units	Sample Conc. Units	Analysis Time
1	Cr 267.716	3024090.2	3023240.4	8.765 mg/L	8.765 mg/L	10:32:05 AM
2	Cr 267.716	3133867.0	3133017.1	9.080 mg/L	9.080 mg/L	10:32:07 AM
3	Cr 267.716	3120648.8	3119799.0	9.042 mg/L	9.042 mg/L	10:32:09 AM

Mean Data: dose_3.5g-pH2_reading1

Analyte	Mean Corrected Intensity	Calib. Conc. Units	Std.Dev.	Sample Conc. Units	Std.Dev.	RSD
Cr 267.716	3092018.8	8.962 mg/L	0.1720	8.962 mg/L	0.1720	1.92%

Sequence No.: 5

Sample ID: dose_2.5g-pH3_reading1

Analyst:

Initial Sample Wt:

Dilution:

Wash Time: 120

Autosampler Location: 12

Date Collected: 2/26/2020 10:34:21 AM

Data Type: Original

Initial Sample Vol:

Sample Prep Vol:

Auto Dilution Factor: 1

Replicate Data: dose_2.5g-pH3_reading1

Repl#	Analyte	Net Intensity	Corrected Intensity	Calib. Conc. Units	Sample Conc. Units	Analysis Time
1	Cr 267.716	2717428.8	2716579.0	7.885 mg/L	7.885 mg/L	10:35:31 AM
2	Cr 267.716	2681128.2	2680278.4	7.781 mg/L	7.781 mg/L	10:35:33 AM
3	Cr 267.716	2701371.3	2700521.5	7.839 mg/L	7.839 mg/L	10:35:36 AM

Mean Data: dose_2.5g-pH3_reading1

Analyte	Mean Corrected Intensity	Calib. Conc. Units	Std.Dev.	Sample Conc. Units	Std.Dev.	RSD
Cr 267.716	2699126.3	7.835 mg/L	0.0522	7.835 mg/L	0.0522	0.67%

Sequence No.: 6

Sample ID: dose_3g-pH3_reading1

Analyst:

Initial Sample Wt:

Dilution:

Wash Time: 120

Autosampler Location: 13

Date Collected: 2/26/2020 10:37:47 AM

Data Type: Original

Initial Sample Vol:

Sample Prep Vol:

Auto Dilution Factor: 1

Sequence No.: 6

Sample ID: dose_3g-pH3_reading1

Analyst:

Initial Sample Wt:

Dilution:

Wash Time: 120

Autosampler Location: 13

Date Collected: 2/26/2020 10:37:47 AM

Data Type: Original

Initial Sample Vol:

Sample Prep Vol:

Auto Dilution Factor: 1

Replicate Data: dose_3g-pH3_reading1

Repl#	Analyte	Net Intensity	Corrected Intensity	Calib. Conc. Units	Sample Conc. Units	Analysis Time
1	Cr 267.716	2018342.8	2017493.0	5.879 mg/L	5.879 mg/L	10:38:56 AM
2	Cr 267.716	2058973.8	2058124.0	5.995 mg/L	5.995 mg/L	10:38:58 AM
3	Cr 267.716	2045774.7	2044924.9	5.957 mg/L	5.957 mg/L	10:39:01 AM

Mean Data: dose_3g-pH3_reading1

Analyte	Mean Corrected Intensity	Calib. Conc. Units	Std.Dev.	Sample Conc. Units	Std.Dev.	RSD
Cr 267.716	2040180.6	5.944 mg/L	0.0595	5.944 mg/L	0.0595	1.00%

Sequence No.: 7
Sample ID: dose_3.5g-pH3_reading1
Analyst:
Initial Sample Wt:
Dilution:
Wash Time: 120

Autosampler Location: 14
Date Collected: 2/26/2020 10:41:12 AM
Data Type: Original
Initial Sample Vol:
Sample Prep Vol:
Auto Dilution Factor: 1

Replicate Data: dose_3.5g-pH3_reading1

Repl#	Analyte	Net Intensity	Corrected Intensity	Calib. Conc. Units	Sample Conc. Units	Analysis Time
1	Cr 267.716	1288669.7	1287819.9	3.785 mg/L	3.785 mg/L	10:42:21 AM
2	Cr 267.716	1259559.6	1258709.8	3.702 mg/L	3.702 mg/L	10:42:23 AM
3	Cr 267.716	1265443.1	1264593.3	3.718 mg/L	3.718 mg/L	10:42:25 AM

Mean Data: dose_3.5g-pH3_reading1

Analyte	Mean Corrected Intensity	Calib. Conc. Units	Std.Dev.	Sample Conc. Units	Std.Dev.	RSD
Cr 267.716	1270374.3	3.735 mg/L	0.0442	3.735 mg/L	0.0442	1.18%

Sequence No.: 11
Sample ID: dose_2.5g-pH5_reading1
Analyst:
Initial Sample Wt:
Dilution:
Wash Time: 120

Autosampler Location: 18
Date Collected: 2/26/2020 10:54:51 AM
Data Type: Original
Initial Sample Vol:
Sample Prep Vol:
Auto Dilution Factor: 1

Replicate Data: dose_2.5g-pH5_reading1

Repl#	Analyte	Net Intensity	Corrected Intensity	Calib. Conc. Units	Sample Conc. Units	Analysis Time
1	Cr 267.716	1384393.5	1383543.7	4.060 mg/L	4.060 mg/L	10:55:59 AM
2	Cr 267.716	1367804.1	1366954.3	4.012 mg/L	4.012 mg/L	10:56:02 AM
3	Cr 267.716	1387088.4	1386238.6	4.067 mg/L	4.067 mg/L	10:56:04 AM

Mean Data: dose_2.5g-pH5_reading1

Analyte	Mean Corrected Intensity	Calib. Conc. Units	Std.Dev.	Sample Conc. Units	Std.Dev.	RSD
Cr 267.716	1378912.2	4.046 mg/L	0.0300	4.046 mg/L	0.0300	0.74%

Sequence No.: 12
Sample ID: dose_3g-pH5_reading1
Analyst:
Initial Sample Wt:
Dilution:
Wash Time: 120

Autosampler Location: 19
Date Collected: 2/26/2020 10:58:14 AM
Data Type: Original
Initial Sample Vol:
Sample Prep Vol:
Auto Dilution Factor: 1

Replicate Data: dose_3g-pH5_reading1

Repl#	Analyte	Net Intensity	Corrected Intensity	Calib. Conc. Units	Sample Conc. Units	Analysis Time
1	Cr 267.716	1796145.4	1795295.6	5.241 mg/L	5.241 mg/L	10:59:22 AM
2	Cr 267.716	1772318.5	1771468.7	5.173 mg/L	5.173 mg/L	10:59:24 AM
3	Cr 267.716	1765401.7	1764551.9	5.153 mg/L	5.153 mg/L	10:59:26 AM

Mean Data: dose_3g-pH5_reading1

Analyte	Mean Corrected Intensity	Calib. Conc. Units	Std.Dev.	Sample Conc. Units	Std.Dev.	RSD
Cr 267.716	1777105.4	5.189 mg/L	0.0463	5.189 mg/L	0.0463	0.89%

Sequence No.: 15

Sample ID: dose_2.5g-pH6_reading1

Analyst:

Initial Sample Wt:

Dilution:

Wash Time: 120

Autosampler Location: 22

Date Collected: 2/26/2020 11:08:28 AM

Data Type: Original

Initial Sample Vol:

Sample Prep Vol:

Auto Dilution Factor: 1

Replicate Data: dose_2.5g-pH6_reading1

Repl#	Analyte	Net Intensity	Corrected Intensity	Calib. Conc. Units	Sample Conc. Units	Analysis Time
1	Cr 267.716	2081087.6	2080237.8	6.059 mg/L	6.059 mg/L	11:09:38 AM
2	Cr 267.716	2056218.1	2055368.3	5.987 mg/L	5.987 mg/L	11:09:40 AM
3	Cr 267.716	2058613.9	2057764.1	5.994 mg/L	5.994 mg/L	11:09:42 AM

Mean Data: dose_2.5g-pH6_reading1

Analyte	Mean Corrected Intensity	Calib. Conc. Units	Std.Dev.	Sample Conc. Units	Std.Dev.	RSD
Cr 267.716	2064456.7	6.014 mg/L	0.0394	6.014 mg/L	0.0394	0.65%

Sequence No.: 16

Sample ID: dose_3g-pH6_reading1

Analyst:

Initial Sample Wt:

Dilution:

Wash Time: 120

Autosampler Location: 23

Date Collected: 2/26/2020 11:11:53 AM

Data Type: Original

Initial Sample Vol:

Sample Prep Vol:

Auto Dilution Factor: 1

Replicate Data: dose_3g-pH6_reading1

Repl#	Analyte	Net Intensity	Corrected Intensity	Calib. Conc. Units	Sample Conc. Units	Analysis Time
1	Cr 267.716	2354718.4	2353868.6	6.844 mg/L	6.844 mg/L	11:13:02 AM
2	Cr 267.716	2383937.5	2383087.7	6.928 mg/L	6.928 mg/L	11:13:04 AM
3	Cr 267.716	2321154.3	2320304.5	6.748 mg/L	6.748 mg/L	11:13:06 AM

Mean Data: dose_3g-pH6_reading1

Analyte	Mean Corrected Intensity	Calib. Conc. Units	Std.Dev.	Sample Conc. Units	Std.Dev.	RSD
Cr 267.716	2352420.3	6.840 mg/L	0.0901	6.840 mg/L	0.0901	1.32%

Initial Sample Wt:
Dilution:
Wash Time: 120

Initial Sample Vol:
Sample Prep Vol:
Auto Dilution Factor: 1

Replicate Data: 4g-pH2-reading1

Repl#	Analyte	Net Intensity	Corrected Intensity	Calib. Conc. Units	Sample Conc. Units	Analysis Time
1	Cr 267.716	Saturated3	Saturated3			9:26:54 AM
	Saturated in preshot (code 3)					
2	Cr 267.716	-54865.5	-55715.3	-0.070 mg/L	-0.070 mg/L	9:27:04 AM
	Saturated within auto integration window (code 4)					
3	Cr 267.716	-54970.5	-55820.3	-0.070 mg/L	-0.070 mg/L	9:27:14 AM
	Saturated within auto integration window (code 4)					

Mean Data: 4g-pH2-reading1

Analyte	Mean Corrected Intensity	Calib. Conc. Units	Std.Dev.	Sample Conc. Units	Std.Dev.	RSD
Cr 267.716	Saturated4	-0.070 mg/L	0.0002	-0.070 mg/L	0.0002	0.30%

Sequence No.: 3

Sample ID: 4g-pH3-reading1

Analyst:

Initial Sample Wt:

Dilution:

Wash Time: 120

Autosampler Location: 10

Date Collected: 3/10/2020 9:29:32 AM

Data Type: Original

Initial Sample Vol:

Sample Prep Vol:

Auto Dilution Factor: 1

Replicate Data: 4g-pH3-reading1

Repl#	Analyte	Net Intensity	Corrected Intensity	Calib. Conc. Units	Sample Conc. Units	Analysis Time
1	Cr 267.716	Saturated3	Saturated3			9:30:11 AM
	Saturated in preshot (code 3)					
2	Cr 267.716	-46354.5	-47204.3	-0.046 mg/L	-0.046 mg/L	9:30:21 AM
	Saturated within auto integration window (code 4)					
3	Cr 267.716	-46373.8	-47223.6	-0.046 mg/L	-0.046 mg/L	9:30:31 AM
	Saturated within auto integration window (code 4)					

Mean Data: 4g-pH3-reading1

Analyte	Mean Corrected Intensity	Calib. Conc. Units	Std.Dev.	Sample Conc. Units	Std.Dev.	RSD
Cr 267.716	Saturated4	-0.046 mg/L	0.0000	-0.046 mg/L	0.0000	0.09%

Replicate Data: 4g-pH4-reading1

Repl#	Analyte	Net Intensity	Corrected Intensity	Calib. Conc. Units	Sample Conc. Units	Analysis Time
1	Cr 267.716	Saturated3	Saturated3			9:33:56 AM
Saturated in preshot (code 3)						
2	Cr 267.716	-28159.2	-29009.0	0.007 mg/L	0.007 mg/L	9:34:06 AM
Saturated outside auto integration window (code 5)						
3	Cr 267.716	-28213.4	-29063.2	0.007 mg/L	0.007 mg/L	9:34:15 AM
Saturated within auto integration window (code 4)						

Mean Data: 4g-pH4-reading1

Analyte	Mean Corrected Intensity	Calib. Conc. Units	Std.Dev.	Sample Conc. Units	Std.Dev.	RSD
Cr 267.716	Saturated4	0.007 mg/L	0.0001	0.007 mg/L	0.0001	1.67%

Sequence No.: 5

Sample ID: 4g-pH5-reading1

Analyst:

Initial Sample Wt:

Dilution:

Wash Time: 120

Autosampler Location: 12

Date Collected: 3/10/2020 9:36:34 AM

Data Type: Original

Initial Sample Vol:

Sample Prep Vol:

Auto Dilution Factor: 1

Replicate Data: 4g-pH5-reading1

Repl#	Analyte	Net Intensity	Corrected Intensity	Calib. Conc. Units	Sample Conc. Units	Analysis Time
1	Cr 267.716	1386.9	537.1	0.091 mg/L	0.091 mg/L	9:37:13 AM
2	Cr 267.716	7786.6	6936.8	0.110 mg/L	0.110 mg/L	9:37:23 AM
Saturated outside auto integration window (code 5)						
3	Cr 267.716	9663.0	8813.2	0.115 mg/L	0.115 mg/L	9:37:32 AM
Saturated outside auto integration window (code 5)						

Mean Data: 4g-pH5-reading1

Analyte	Mean Corrected Intensity	Calib. Conc. Units	Std.Dev.	Sample Conc. Units	Std.Dev.	RSD
Cr 267.716	5429.0	0.105 mg/L	0.0125	0.105 mg/L	0.0125	11.80%

Sequence No.: 6
Sample ID: 4g-pH6-reading1
Analyst:
Initial Sample Wt:
Dilution:
Wash Time: 120

Autosampler Location: 13
Date Collected: 3/10/2020 9:39:51 AM
Data Type: Original
Initial Sample Vol:
Sample Prep Vol:
Auto Dilution Factor: 1

Replicate Data: 4g-pH6-reading1

Repl#	Analyte	Net Intensity	Corrected Intensity	Calib. Conc. Units	Sample Conc. Units	Analysis Time
1	Cr 267.716	1574.4	724.6	0.092 mg/L	0.092 mg/L	9:40:30 AM
2	Cr 267.716	4291.2	3441.4	0.100 mg/L	0.100 mg/L	9:40:39 AM
Saturated outside auto integration window (code 5)						
3	Cr 267.716	8481.4	7631.6	0.112 mg/L	0.112 mg/L	9:40:48 AM
Saturated outside auto integration window (code 5)						

Mean Data: 4g-pH6-reading1

Analyte	Mean Corrected Intensity	Calib. Conc. Units	Std.Dev.	Sample Conc. Units	Std.Dev.	RSD
Cr 267.716	3932.5	0.101 mg/L	0.0100	0.101 mg/L	0.0100	9.87%
Saturated outside auto integration window (code 5)						

Sequence No.: 7
Sample ID: 2g-pH2-reading1

Autosampler Location: 14
Date Collected: 3/10/2020 9:43:07 AM

Sequence No.: 9
Sample ID: 2g-pH4-reading1
Analyst:
Initial Sample Wt:
Dilution:
Wash Time: 120

Autosampler Location: 16
Date Collected: 3/10/2020 9:49:33 AM
Data Type: Original
Initial Sample Vol:
Sample Prep Vol:
Auto Dilution Factor: 1

Replicate Data: 2g-pH4-reading1

Repl#	Analyte	Net Intensity	Corrected Intensity	Calib. Conc. Units	Sample Conc. Units	Analysis Time
1	Cr 267.716	2398.9	1549.1	0.094 mg/L	0.094 mg/L	9:50:11 AM
2	Cr 267.716	-18406.8	-19256.6	0.035 mg/L	0.035 mg/L	9:50:19 AM
Saturated outside auto integration window (code 5)						
3	Cr 267.716	-18957.3	-19807.1	0.033 mg/L	0.033 mg/L	9:50:28 AM
Saturated outside auto integration window (code 5)						

Mean Data: 2g-pH4-reading1

Analyte	Mean Corrected Intensity	Calib. Conc. Units	Std.Dev.	Sample Conc. Units	Std.Dev.	RSD
Cr 267.716	-12504.9	0.054 mg/L	0.0349	0.054 mg/L	0.0349	64.67%
Saturated outside auto integration window (code 5)						

Sequence No.: 1
Sample ID: 3.5g pH 4
Analyst:
Initial Sample Wt:
Dilution:
Wash Time:

Autosampler Location: 9
Date Collected: 2/18/2020 3:25:31 PM
Data Type: Original
Initial Sample Vol:
Sample Prep Vol:

Replicate Data: 3.5g pH 4

Repl#	Analyte	Net Intensity	Corrected Intensity	Calib. Conc. Units	Sample Conc. Units	Analysis Time
1	Cr 267.716	391940.4	391090.6	1.212 mg/L	1.212 mg/L	3:26:43 PM
2	Cr 267.716	385194.4	384344.6	1.193 mg/L	1.193 mg/L	3:26:46 PM
3	Cr 267.716	395292.4	394442.6	1.222 mg/L	1.222 mg/L	3:26:49 PM

Mean Data: 3.5g pH 4

Analyte	Mean Corrected Intensity	Calib. Conc. Units	Std.Dev.	Sample Conc. Units	Std.Dev.	RSD
Cr 267.716	389959.2	1.209 mg/L	0.0148	1.209 mg/L	0.0148	1.22%

Sequence No.: 2
Sample ID: 3.5g pH 5
Analyst:
Initial Sample Wt:
Dilution:
Wash Time: 120

Autosampler Location: 10
Date Collected: 2/18/2020 3:29:01 PM
Data Type: Original
Initial Sample Vol:
Sample Prep Vol:
Auto Dilution Factor: 1

Replicate Data: 3.5g pH 5

Repl#	Analyte	Net Intensity	Corrected Intensity	Calib. Conc. Units	Sample Conc. Units	Analysis Time
1	Cr 267.716	361461.1	360611.3	1.125 mg/L	1.125 mg/L	3:30:09 PM
2	Cr 267.716	365720.8	364871.0	1.137 mg/L	1.137 mg/L	3:30:13 PM
3	Cr 267.716	361926.2	361076.4	1.126 mg/L	1.126 mg/L	3:30:16 PM

Mean Data: 3.5g pH 5

Analyte	Mean Corrected Intensity	Calib. Conc. Units	Std.Dev.	Sample Conc. Units	Std.Dev.	RSD
Cr 267.716	362186.2	1.129 mg/L	0.0067	1.129 mg/L	0.0067	0.59%

Sequence No.: 3
Sample ID: 3.5g pH 6
Analyst:
Initial Sample Wt:
Dilution:

Autosampler Location: 11
Date Collected: 2/18/2020 3:32:28 PM
Data Type: Original
Initial Sample Vol:
Sample Prep Vol:

Replicate Data: 3.5g pH 6

Repl#	Analyte	Net Intensity	Corrected Intensity	Calib. Conc. Units	Sample Conc. Units	Analysis Time
1	Cr 267.716	550359.6	549509.8	1.667 mg/L	1.667 mg/L	3:33:37 PM
2	Cr 267.716	558070.6	557220.8	1.689 mg/L	1.689 mg/L	3:33:39 PM
3	Cr 267.716	556974.6	556124.8	1.686 mg/L	1.686 mg/L	3:33:42 PM

Mean Data: 3.5g pH 6

Analyte	Mean Corrected Intensity	Calib. Conc. Units	Std.Dev.	Sample Conc. Units	Std.Dev.	RSD
Cr 267.716	554285.1	1.680 mg/L	0.0120	1.680 mg/L	0.0120	0.71%

=====

Sequence No.: 4

Sample ID: 3g pH 4

Analyst:

Initial Sample Wt:

Dilution:

Wash Time: 120

Autosampler Location: 12

Date Collected: 2/18/2020 3:35:53 PM

Data Type: Original

Initial Sample Vol:

Sample Prep Vol:

Auto Dilution Factor: 1

Replicate Data: 3g pH 4

Repl#	Analyte	Net Intensity	Corrected Intensity	Calib. Conc. Units	Sample Conc. Units	Analysis Time
1	Cr 267.716	441734.2	440884.4	1.355 mg/L	1.355 mg/L	3:37:02 PM
2	Cr 267.716	433020.6	432170.8	1.330 mg/L	1.330 mg/L	3:37:06 PM
3	Cr 267.716	439408.2	438558.4	1.348 mg/L	1.348 mg/L	3:37:09 PM

Mean Data: 3g pH 4

Analyte	Mean Corrected Intensity	Calib. Conc. Units	Std.Dev.	Sample Conc. Units	Std.Dev.	RSD
Cr 267.716	437204.6	1.344 mg/L	0.0129	1.344 mg/L	0.0129	0.96%

=====

Sequence No.: 5

Sample ID: 2.5g pH 4

Analyst:

Initial Sample Wt:

Dilution:

Wash Time: 120

Autosampler Location: 13

Date Collected: 2/18/2020 3:39:21 PM

Data Type: Original

Initial Sample Vol:

Sample Prep Vol:

Auto Dilution Factor: 1

Replicate Data: 2.5g pH 4

Repl#	Analyte	Net Intensity	Corrected Intensity	Calib. Conc. Units	Sample Conc. Units	Analysis Time
1	Cr 267.716	498620.5	497770.7	1.518 mg/L	1.518 mg/L	3:40:30 PM
2	Cr 267.716	508481.0	507631.2	1.546 mg/L	1.546 mg/L	3:40:33 PM
3	Cr 267.716	507867.6	507017.8	1.545 mg/L	1.545 mg/L	3:40:35 PM

Mean Data: 2.5g pH 4

Analyte	Mean Corrected Intensity	Calib. Conc. Units	Std.Dev.	Sample Conc. Units	Std.Dev.	RSD
Cr 267.716	504139.9	1.536 mg/L	0.0159	1.536 mg/L	0.0159	1.03%

Sequence No.: 6
Sample ID: 2g pH 6
Analyst:
Initial Sample Wt:
Dilution:
Wash Time: 120

Autosampler Location: 14
Date Collected: 2/18/2020 3:42:47 PM
Data Type: Original
Initial Sample Vol:
Sample Prep Vol:
Auto Dilution Factor: 1

Replicate Data: 2g pH 6

Repl#	Analyte	Net Intensity	Corrected Intensity	Calib. Conc. Units	Sample Conc. Units	Analysis Time
1	Cr 267.716	690669.5	689819.7	2.069 mg/L	2.069 mg/L	3:43:55 PM
2	Cr 267.716	685947.4	685097.6	2.056 mg/L	2.056 mg/L	3:43:57 PM
3	Cr 267.716	690408.3	689558.5	2.068 mg/L	2.068 mg/L	3:43:59 PM

Mean Data: 2g pH 6

Analyte	Mean Corrected Intensity	Calib. Conc. Units	Std.Dev.	Sample Conc. Units	Std.Dev.	RSD
Cr 267.716	688158.6	2.064 mg/L	0.0076	2.064 mg/L	0.0076	0.37%

Sequence No.: 2
Sample ID: 2g-pH2-reading2
Analyst:
Initial Sample Wt:
Dilution:
Wash Time: 120

Autosampler Location: 9
Date Collected: 3/13/2020 12:10:26 PM
Data Type: Original
Initial Sample Vol:
Sample Prep Vol:
Auto Dilution Factor: 1

Replicate Data: 2g-pH2-reading2

Repl#	Analyte	Net Intensity	Corrected Intensity	Calib. Conc. Units	Sample Conc. Units	Analysis Time
1	Cr 267.716	717.8	-132.0	0.090 mg/L	0.090 mg/L	12:11:04 PM
2	Cr 267.716	-932.2	-1782.0	0.085 mg/L	0.085 mg/L	12:11:14 PM
Saturated within auto integration window (code 4)						
3	Cr 267.716	-21541.5	-22391.3	0.026 mg/L	0.026 mg/L	12:11:24 PM
Saturated outside auto integration window (code 5)						

Mean Data: 2g-pH2-reading2

Analyte	Mean Corrected Intensity	Calib. Conc. Units	Std.Dev.	Sample Conc. Units	Std.Dev.	RSD
Cr 267.716	-8101.8	0.067 mg/L	0.0356	0.067 mg/L	0.0356	53.39%

Mean Data: 2g-pH2-reading2

Analyte	Mean Corrected Intensity	Calib. Conc. Units	Std.Dev.	Sample Conc. Units	Std.Dev.	RSD
Cr 267.716	-8101.8	0.067 mg/L	0.0356	0.067 mg/L	0.0356	53.39%
Saturated outside auto integration window (code 5)						

Sequence No.: 3

Autosampler Location: 10

Sample ID: 2g-pH3-reading1

Date Collected: 3/13/2020 12:13:43 PM

Analyst:

Data Type: Original

Initial Sample Wt:

Initial Sample Vol:

Dilution:

Sample Prep Vol:

Wash Time: 120

Auto Dilution Factor: 1

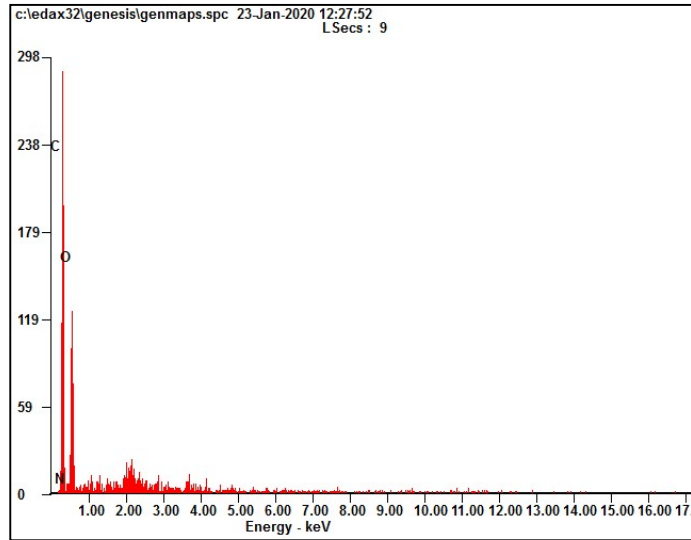
Replicate Data: 2g-pH3-reading1

Repl#	Analyte	Net Intensity	Corrected Intensity	Calib. Conc. Units	Sample Conc. Units	Analysis Time
1	Cr 267.716	1286.9	437.1	0.091 mg/L	0.091 mg/L	12:14:22 PM
2	Cr 267.716	-1350.5	-2200.3	0.084 mg/L	0.084 mg/L	12:14:31 PM
	Saturated within auto integration window (code 4)					
3	Cr 267.716	358.1	-491.7	0.088 mg/L	0.088 mg/L	12:14:41 PM
	Saturated within auto integration window (code 4)					

Mean Data: 2g-pH3-reading1

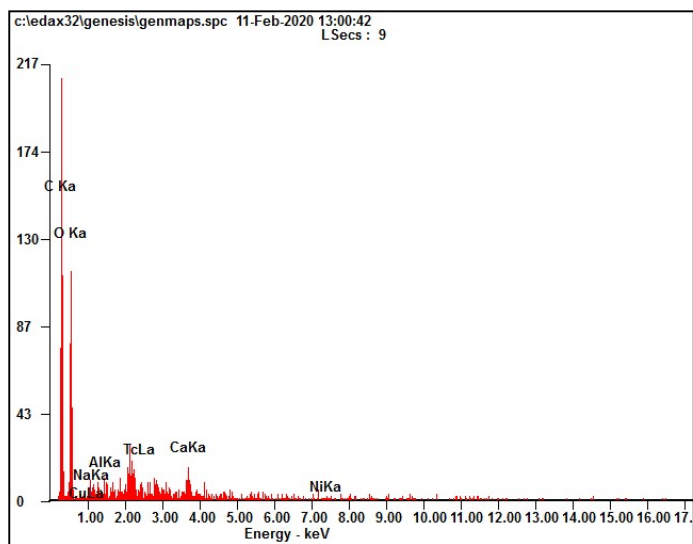
Analyte	Mean Corrected Intensity	Calib. Conc. Units	Std.Dev.	Sample Conc. Units	Std.Dev.	RSD
Cr 267.716	-751.7	0.088 mg/L	0.0038	0.088 mg/L	0.0038	4.37%

Appendix H: EDX Results



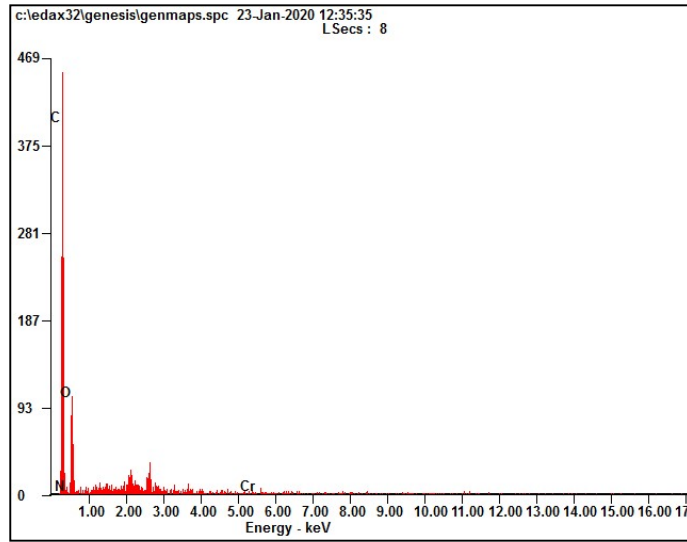
<i>Element</i>	<i>Wt%</i>	<i>At%</i>
<i>CK</i>	50.50	57.21
<i>NK</i>	05.78	05.62
<i>OK</i>	43.71	37.17
<i>Matrix</i>	Correction	ZAF

Figure H-1: EDX Results of Virgin Jasmine Green Tea Leaves



<i>Element</i>	<i>Wt%</i>	<i>At%</i>
<i>CK</i>	41.68	54.13
<i>OK</i>	40.60	39.58
<i>NK</i>	02.04	01.38
<i>NiK</i>	02.02	00.54
<i>Matrix</i>	Correction	ZAF

Figure H-2: EDX Results of Ni (II) Loaded Jasmine Green Tea Leaves



<i>Element</i>	<i>Wt%</i>	<i>At%</i>
<i>CK</i>	62.44	68.64
<i>NK</i>	04.84	04.56
<i>OK</i>	32.37	26.71
<i>CrK</i>	00.35	00.09
<i>Matrix</i>	Correction	ZAF

Figure H-3: EDX Results of Cr (VI) Loaded Jasmine Green Tea Leaves

Appendix I: XRD Raw Data

*** Basic Data Process ***

Group : DrSim
 Data : DHIVESH_GREEN-TEA

Strongest 3 peaks

no.	peak no.	2Theta (deg)	d (A)	I/I1	FWHM (deg)	Intensity (Counts)	Integrated Int (Counts)
1	9	21.3400	4.16036	100	4.00000	165	22832
2	8	20.0200	4.43159	82	0.00000	135	0
3	7	18.9800	4.67201	63	0.00000	104	0

Peak Data List

peak no.	2Theta (deg)	d (A)	I/I1	FWHM (deg)	Intensity (Counts)	Integrated Int (Counts)
1	11.3800	7.76934	3	0.32000	5	159
2	13.5600	6.52479	5	0.28000	8	204
3	14.9400	5.92506	26	1.22660	43	2616
4	15.6200	5.66862	24	0.00000	40	0
5	17.0800	5.18721	33	0.00000	55	0
6	18.4800	4.79728	56	0.00000	92	0
7	18.9800	4.67201	63	0.00000	104	0
8	20.0200	4.43159	82	0.00000	135	0
9	21.3400	4.16036	100	4.00000	165	22832
10	24.0800	3.69281	42	1.42000	70	4465
11	25.2600	3.52291	18	1.20000	29	1748
12	26.5600	3.35336	10	0.44000	16	441
13	27.4100	3.25127	5	0.30000	8	281
14	29.9300	2.98301	8	0.68000	13	467
15	30.6600	2.91363	4	0.16000	7	127
16	32.0800	2.78783	4	0.36000	7	188
17	34.5800	2.59179	7	0.52000	12	455
18	35.8050	2.50587	8	0.67000	14	593
19	38.2550	2.35083	17	0.69000	28	1078
20	39.6350	2.27210	3	0.13000	5	83
21	43.3800	2.08423	5	0.32000	8	205
22	44.4800	2.03521	7	0.60000	11	452
23	64.4960	1.44363	37	0.59200	61	1900

*** Basic Data Process ***

Data Information

Group : DrSim
Data : DHIVESH_GREEN-TEA
Sample Name : DHIVESH_GREEN-TEA
Comment :
Date & Time : 02-12-20 11:07:48

Measurement Condition

X-ray tube
target : Cu
voltage : 40.0 (kV)
current : 30.0 (mA)

Slits
Auto Slit : not Used
divergence slit : 1.00000 (deg)
scatter slit : 1.00000 (deg)
receiving slit : 0.30000 (mm)

Scanning
drive axis : Theta-2Theta
scan range : 10.0000 - 70.0000 (deg)
scan mode : Continuous Scan
scan speed : 2.0000 (deg/min)
sampling pitch : 0.0200 (deg)
preset time : 0.60 (sec)

Data Process Condition

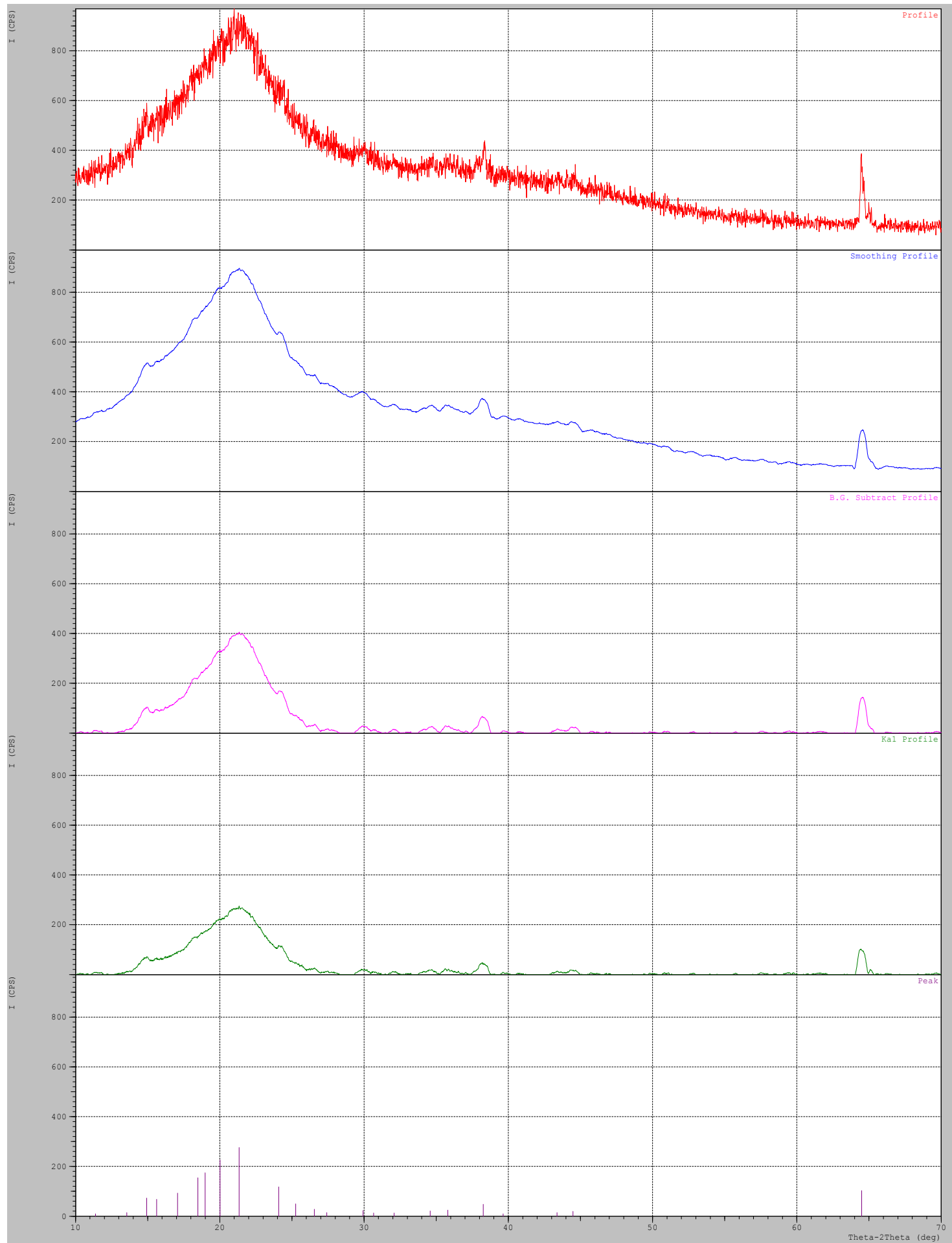
Smoothing [AUTO]
smoothing points : 51

B.G.Subtraction [AUTO]
sampling points : 51
repeat times : 30

Ka1-a2 Separate [MANUAL]
Ka1 a2 ratio : 50 (%)

Peak Search [AUTO]
differential points : 51
FWHM threshold : 0.050 (deg)
intensity threshold : 30 (par mil)
FWHM ratio (n-1)/n : 2

System error Correction [NO]
Precise peak Correction [NO]



*** Basic Data Process ***

Group : DrSim
 Data : DHIVESH_GREEN-CHROMIUM

Strongest 3 peaks

no.	peak no.	2Theta (deg)	d (A)	I/I1	FWHM (deg)	Intensity (Counts)	Integrated Int (Counts)
1	10	21.5400	4.12218	100	0.00000	151	0
2	27	64.6382	1.44080	95	0.60360	143	4630
3	9	19.8800	4.46249	75	0.00000	113	0

Peak Data List

peak no.	2Theta (deg)	d (A)	I/I1	FWHM (deg)	Intensity (Counts)	Integrated Int (Counts)
1	11.6500	7.58988	3	0.10000	5	59
2	13.4200	6.59255	4	0.28000	6	108
3	13.7200	6.44906	5	0.08000	7	31
4	14.0400	6.30279	6	0.44000	9	225
5	15.0600	5.87812	17	0.90660	26	2788
6	16.6200	5.32973	26	0.00000	40	0
7	17.8000	4.97898	39	0.00000	59	0
8	18.7200	4.73631	58	0.00000	88	0
9	19.8800	4.46249	75	0.00000	113	0
10	21.5400	4.12218	100	0.00000	151	0
11	23.3800	3.80177	57	0.00000	86	0
12	24.1400	3.68377	42	1.66000	63	5740
13	25.7400	3.45830	14	0.00000	21	0
14	26.4000	3.37332	9	0.00000	14	0
15	26.5600	3.35336	10	0.92000	15	502
16	27.4308	3.24885	6	0.28830	9	252
17	28.3700	3.14339	5	0.14000	7	137
18	29.8550	2.99033	6	0.25000	9	181
19	34.7800	2.57734	10	0.68000	15	706
20	35.9366	2.49700	5	0.55330	8	247
21	36.9800	2.42890	4	0.24000	6	102
22	38.1000	2.36004	32	0.80000	48	1871
23	39.9266	2.25618	5	0.37330	7	205
24	41.3000	2.18427	3	0.08000	5	50
25	42.2750	2.13612	3	0.11000	5	50
26	44.2650	2.04459	19	0.63000	29	1088
27	64.6382	1.44080	95	0.60360	143	4630

*** Basic Data Process ***

Data Information

Group : DrSim
Data : DHIVESH_GREEN-CHROMIUM
Sample Nmae : DHIVESH_GREEN-CHROMIUM
Comment :
Date & Time : 02-12-20 12:15:02

Measurement Condition

X-ray tube
target : Cu
voltage : 40.0 (kV)
current : 30.0 (mA)

Slits
Auto Slit : not Used
divergence slit : 1.00000 (deg)
scatter slit : 1.00000 (deg)
receiving slit : 0.30000 (mm)

Scanning
drive axis : Theta-2Theta
scan range : 10.0000 - 70.0000 (deg)
scan mode : Continuous Scan
scan speed : 2.0000 (deg/min)
sampling pitch : 0.0200 (deg)
preset time : 0.60 (sec)

Data Process Condition

Smoothing [AUTO]
smoothing points : 51

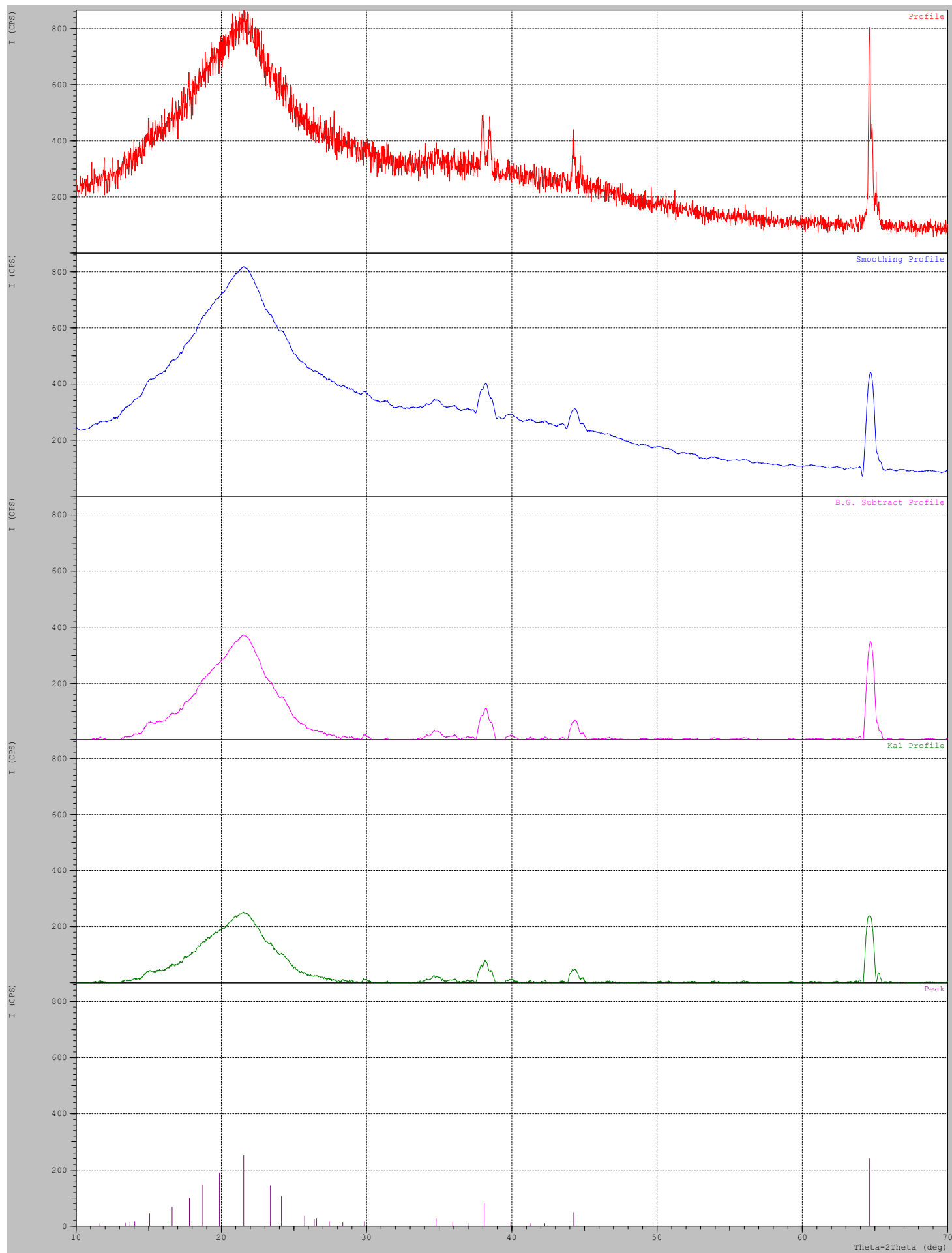
B.G.Subtruction [AUTO]
sampling points : 51
repeat times : 30

Ka1-a2 Separate [MANUAL]
Ka1 a2 ratio : 50 (%)

Peak Search [AUTO]
differential points : 51
FWHM threhold : 0.050 (deg)
intensity threhold : 30 (par mil)
FWHM ratio (n-1)/n : 2

System error Correction [NO]
Precise peak Correction [NO]

< Group: DrSim Data: DHIVESH_GREEN-CHROMIUM >



*** Basic Data Process ***

Group : DrSim
 Data : DHIVESH_GREEN-TEA-NICKEL

Strongest 3 peaks

no.	peak no.	2Theta (deg)	d (A)	I/I1	FWHM (deg)	Intensity (Counts)	Integrated Int (Counts)
1	9	21.6800	4.09588	100	0.00000	140	0
2	33	64.6312	1.44094	91	0.59350	128	3884
3	10	22.6200	3.92775	89	0.00000	125	0

Peak Data List

peak no.	2Theta (deg)	d (A)	I/I1	FWHM (deg)	Intensity (Counts)	Integrated Int (Counts)
1	11.6150	7.61267	4	0.07000	6	45
2	12.7750	6.92391	4	0.27000	6	124
3	13.7400	6.43972	6	0.32000	8	210
4	15.3000	5.78645	23	0.78000	32	2821
5	16.7600	5.28552	23	0.00000	32	0
6	17.8600	4.96239	36	0.00000	50	0
7	19.6600	4.51192	66	0.00000	92	0
8	20.8800	4.25097	86	0.00000	120	0
9	21.6800	4.09588	100	0.00000	140	0
10	22.6200	3.92775	89	0.00000	125	0
11	23.3000	3.81464	68	0.00000	95	0
12	24.1200	3.68678	52	2.18000	73	7441
13	26.0200	3.42171	16	0.00000	22	0
14	26.8800	3.31416	12	1.00000	17	1449
15	30.3450	2.94315	9	0.63000	13	443
16	31.4550	2.84178	4	0.09000	6	56
17	32.6850	2.73759	4	0.05000	5	28
18	34.1800	2.62120	4	0.04000	5	31
19	34.7400	2.58021	8	0.40000	11	567
20	35.6600	2.51573	7	0.00000	10	0
21	35.8200	2.50486	9	1.16000	12	488
22	38.2100	2.35350	25	1.10000	35	1763
23	40.2800	2.23719	5	0.16000	7	162
24	42.5650	2.12223	4	0.09000	6	48
25	44.2575	2.04492	17	0.78500	24	1018
26	46.1600	1.96497	5	0.56000	7	266
27	47.1750	1.92503	6	0.27000	8	153
28	49.6650	1.83419	4	0.19000	5	106
29	53.5483	1.70997	4	0.12330	5	89
30	55.3950	1.65726	4	0.19000	5	95
31	55.5700	1.65245	3	0.14000	4	63
32	63.5800	1.46220	3	0.05340	4	19
33	64.6312	1.44094	91	0.59350	128	3884

*** Basic Data Process ***

Data Information

Group : DrSim
Data : DHIVESH_GREEN-TEA-NICKEL
Sample Nmae : DHIVESH_GREEN-TEA-NI
Comment :
Date & Time : 02-12-20 11:41:35

Measurement Condition

X-ray tube
target : Cu
voltage : 40.0 (kV)
current : 30.0 (mA)

Slits
Auto Slit : not Used
divergence slit : 1.00000 (deg)
scatter slit : 1.00000 (deg)
receiving slit : 0.30000 (mm)

Scanning
drive axis : Theta-2Theta
scan range : 10.0000 - 70.0000 (deg)
scan mode : Continuous Scan
scan speed : 2.0000 (deg/min)
sampling pitch : 0.0200 (deg)
preset time : 0.60 (sec)

Data Process Condition

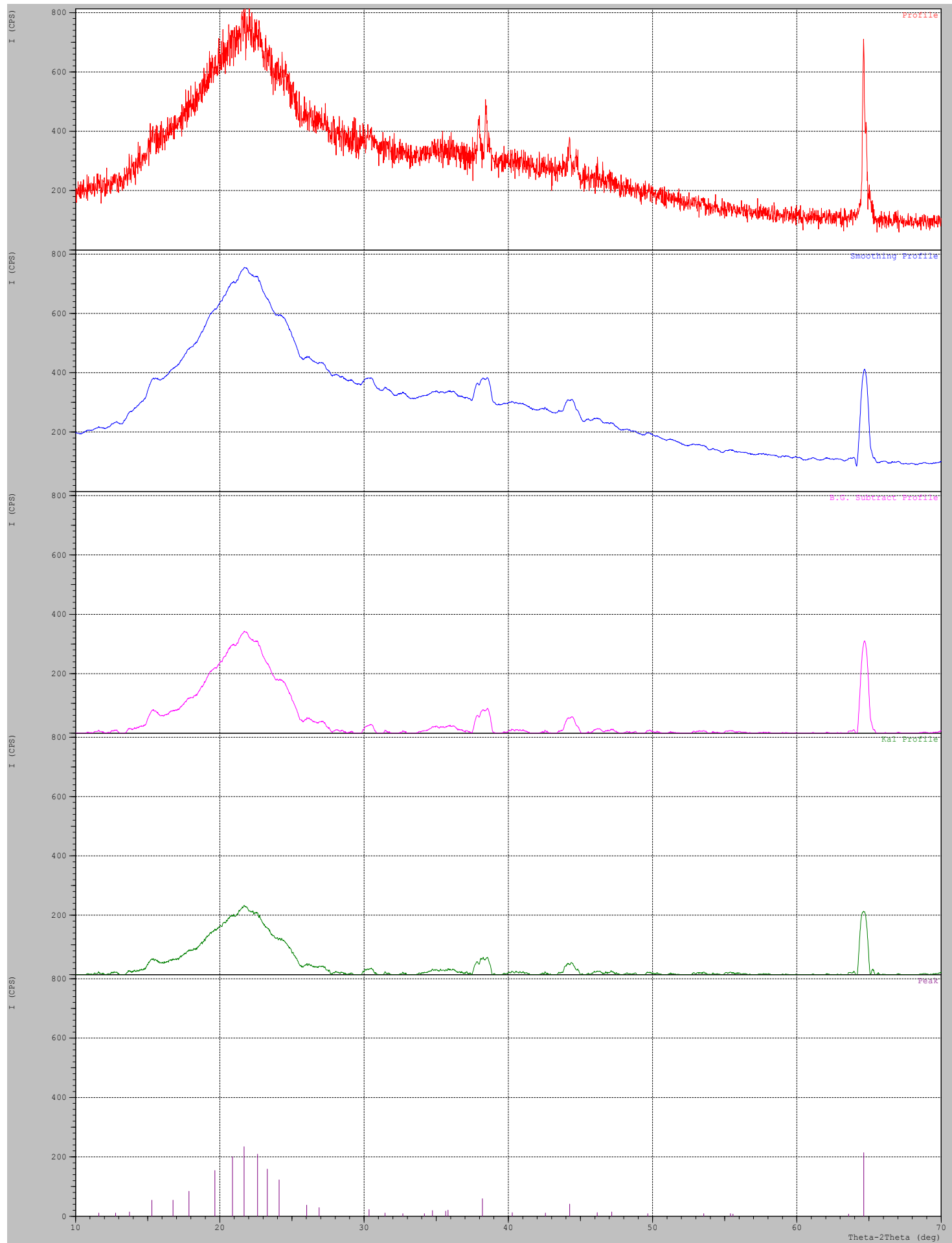
Smoothing [AUTO]
smoothing points : 51

B.G.Subtruction [AUTO]
sampling points : 51
repeat times : 30

Ka1-a2 Separate [MANUAL]
Ka1 a2 ratio : 50 (%)

Peak Search [AUTO]
differential points : 51
FWHM threshold : 0.050 (deg)
intensity threshold : 30 (par mil)
FWHM ratio (n-1)/n : 2

System error Correction [NO]
Precise peak Correction [NO]



APPENDIX J: Sample Calculation of Crystallite Size, d_x (nm)

The calculation of crystallite size from the XRD raw data can be obtained with the use of Debye Scherrer's equation is shown below.

$$d_x = \frac{0.94 \lambda}{FWHM \cdot \cos \theta}$$

where,

d_x = Crystallite size, nm

λ = X-ray wavelength (CuK α) = 0.15406 nm

FWHM = Full Width Half Maximum, rad

θ = Bragg's angle, rad

According to the XRD raw data of virgin jasmine green tea leaves, the information below is obtained:

2 Theta, 2θ (deg) = 21.24 °

Full Width Half Maximum, FWHM (deg) = 4 °

Unit Conversion from degrees to radians

$$2 \text{ Theta, } 2\theta = 21.24^\circ \times \frac{\pi}{180^\circ}$$

$$2 \text{ Theta, } 2\theta = 0.3707 \text{ rad}$$

$$\text{Full Width Half Maximum, FWHM} = 4^\circ \times \frac{\pi}{180^\circ}$$

$$\text{Full Width Half Maximum, FWHM} = 0.0698$$

Calculation of Crystallite Size, d_x (nm)

$$\text{Crystallite size, } d_x (\text{nm}) = \frac{0.94 (0.15406 \text{ nm})}{0.0698 \cdot \cos\left(\frac{0.3707}{2}\right)}$$

$$\text{Crystallite size, } d_x (\text{nm}) = 2.1109 \text{ nm}$$